FINITE ELEMENT BASED THERMOMECHANICAL FATIGUE ANALYSIS OF SOLDER JOINTS IN ELECTRONIC PACKAGES

A THESIS SUBMITTED TO
THE GRADUATE SCHOOL OF NATURAL AND APPLIED SCIENCES
OF
MIDDLE EAST TECHNICAL UNIVERSITY

BY

HASAN SAĞDIÇ

IN PARTIAL FULFILLMENT OF THE REQUIREMENTS
FOR
THE DEGREE OF MASTER OF SCIENCE
IN
MECHANICAL ENGINEERING

JUNE 2024

Approval of the thesis:

submitted by **HASAN SAĞDIÇ** in partial fulfillment of the requirements for the degree of **Master of Science** i**n Mechanical Engineering, Middle East Technical University** by,

Prof. Dr. Naci Emre Altun
Dean, **Graduate School of Natural and Applied Sciences**

Prof. Dr. Mehmet Ali Sahir Arıkan
Head of the Department, **Mechanical Engineering**

Prof. Dr. Suat Kadıoğlu
Supervisor, **Mechanical Engineering, METU**

Examining Committee Members:

Prof. Dr. Haluk Darendeliler
Mechanical Engineering, METU

Prof. Dr. Fevzi Suat Kadıoğlu
Mechanical Engineering, METU

Assist. Prof. Dr. Orkun Özşahin
Mechanical Engineering, METU

Assist. Prof. Dr. Gökhan Osman Özgen
Mechanical Engineering, METU

Assoc. Prof. Dr. Hamit Tekin
Mechanical Engineering, UTAA

Date: 07.06.2024

I hereby declare that all information in this document has been obtained and presented in accordance with academic rules and ethical conduct. I also declare that, as required by these rules and conduct, I have fully cited and referenced all material and results that are not original to this work.

Name Last Name: Hasan Sağdıç

Signature:

ABSTRACT

FINITE ELEMENT BASED THERMOMECHANICAL FATIGUE ANALYSIS OF SOLDER JOINTS IN ELECTRONIC PACKAGES

Sağdıç, Hasan
Master of Science, Mechanical Engineering
Supervisor: Prof. Dr. Suat Kadıoğlu

June 2024, 109 pages

Due to the materials with different thermal expansion coefficients in electronic packages, failures occur with temperature changes. The location of the failure is observed in the solder balls used as joining materials for different components and failure type is crack formation. In this study, thermomechanical simulation and fatigue lifetime calculations of a 144-connection ball grid array (BGA) electronic package made of Sn3.0Ag0.5Cu (SAC305) were performed. For lifetime prediction model Engelmair modified Coffin-Manson method was used. In order to find the geometric configuration of the electronic package with the longest lifetime, a response surface optimization study was performed, including parameters such as under bump metallization (UBM) thicknesses, solder ball diameter and height. Two separate optimization studies were performed, one using the Anand viscoplastic (AV) material model for SAC305 and the other using the Elastoplastic (EP) material model. As a result of the optimization study with the AV material model, a geometric configuration with a 140% increase in lifetime value compared to the original geometry was found, and a configuration with a 163% increase was found with the EP material model. Finally, when the lifetime results of the best configurations from each material model are compared, it is found that the AV material model produces more conservative lifetime results than EP.

Keywords: TMF, Solder ball, RSO

ÖZ

ELEKTRONIK PAKETLERDE BULUNAN LEHİM TOPÇUKLARININ SONLU ELEMANLAR YÖNTEMİ İLE YORULMA ANALİZLERİ

Sağdıç, Hasan
Yüksek Lisans, Makina Mühendisliği
Tez Yöneticisi: Prof. Dr. Suat Kadıoğlu

Haziran 2024, 109 sayfa

Farklı termal genleşme katsayılarına sahip olan malzemelerden oluşan elektronik paketlerde sıcaklık değişikliklerine bağlı olarak hasar durumları gözükmektedir. Hasar, birleştirici malzeme olarak kullanılan lehim topçuklarında sıcaklık çevrimlerine bağlı olarak çatlak oluşumu olarak görülmektedir. Bu çalışmada Sn3.0Ag0.5Cu (SAC305) malzemeden oluşan 144 bağlantılı BGA ye sahip elektronik paketin termomekanik yorulma simulasyonları yapılmış ve ömür hesapları gerçekleştirilmiştir. Ömür hesaplarında Engelmair Coffin-Manson metodu kullanılmıştır. Elektronik paketin en uzun ömre sahip geometrik konfigürasyonunu bulmak için içerisinde lehim topçuk altı kalınlıklarının, lehim topçuk çap ve yükselik gibi parametrelerinin de olduğu yanıt yüzey optimizasyon çalışması gerçekleştirilmiştir. İki ayrı optimizasyon çalışması gerçekleştirilmiş, birinde SAC305 için Anand viscoplastic (AV) malzeme modeli diğerinde ise Elastoplastik (EP) malzeme modeli kullanılmıştır. AV malzeme modeli ile yapılan optimizasyon çalışması sonucu orijinal geometriye göre ömür değeri %140 artan bir geometrik konfigürasyon, EP malzeme modeli yapılan da ise ömür değeri %163 artan bir konfigürasyon bulunmuştur. Son olarak, en iyi konfigürasyonların ömür sonuçları karşılaştırıldığında AV malzeme modelinin EP ye göre daha düşük ömür sonuçları ürettiği görülmüştür.

Anahtar Kelimeler: TMF, Solder Ball, RSO

To my dear mom and brother

ACKNOWLEDGMENTS

The author wishes to express his deepest gratitude to his supervisor Prof. Dr. Suat Kadıoğlu for his guidance, advice, criticism, encouragements and insight throughout the research.

.

TABLE OF CONTENTS

CHAPTERS

LIST OF TABLES

TABLES

LIST OF FIGURES

FIGURES

LIST OF ABBREVIATIONS

ABBREVIATIONS

Abbreviation	Definition
BGA	Ball Grid Array
PBGA	Plastic Ball Grid Array
SAC	Sn-Ag-Cu
SAC305	Sn3.0Ag0.5Cu
UBM	Under Bump Metallization
IC	Integrated Circuit
SMT	Surface Mount Technology
PWB	Printed Wiring Board
CTE	Coefficient of Thermal Expansion
TMF	Thermomechanical Fatigue
PCB	Printed Circuit Board
FPC	Flexible Printed Circuit Board
FE	Finite Element
FEA	Finite Element Analysis
AV	Anand Viscoplastic
EP	Elasto-Plastic
EPC	Elasto-Plastic Creep
CM	Coffin-Manson
ECM	Engelmair modified Coffin-Manson
EPS	Equivalent Plastic Strain
LCF	Low Cycle Fatigue
LPM	Life Prediction Models
CAD	Computer Aided Design
VM	Von-Misses

DOE	Design of Experiment
RS	Response Surface
RSO	Response Surface Optimization
OSF	Optimal Space Filling
NPR	Non-parametric Regression
MOGA	Multi-Objective Genetic Algorithm
WB	Workbench

LIST OF SYMBOLS

SYMBOLS

Symbol	Definition
MPa	Mega Pascal
GPa	Giga Pascal
K	Kelvin
s	Second
ppm	Particle per Million
°C	Degree Celsius
J	Joule
Si	Silicon
Mo	Molybdenum
Cu	Copper
Ti	Titanium
Ni	Nickel
Pd	Palladium
Cr	Chromium
W	Tungsten
Au	Gold
µm	Micrometer
mm	Millimeter

CHAPTER 1

INTRODUCTION

1.1 Electronic Packages

Electronic devices are used in defense, aerospace and everyday commercial products. In order for these devices to fulfill their tasks, they contain electronic packages to perform logical operations. Fig. 1 shows an example of a cross-sectional drawing of an electronic package. Electronic packages generally consist of the following components

- Integrated circuit chip to perform logical calculations
- The substrate that carries the chip and other components and is used to integrate them into an upper system
- Element to provide electronic and mechanical connection between chip and substrate
- And components that thermally, mechanically, electronically and chemically improve the efficiency of the package (underfill, under bump metallization, solder mask etc.)

Over the years, there has been a need for electronic packages to be smaller, lighter and denser systems. For this reason, surface mount technology has been adopted and widely used in the construction of electronic packages. In SMT structure, the chip is joined to the substrate component in the electronic package using one of its surfaces entirely. This ensures a uniform contact area on the entire surface and reduces the planar dimensions of the electronic package since no external lead is needed.

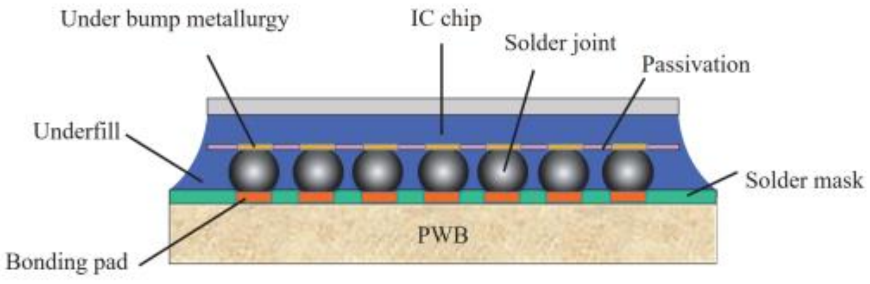

Figure 1. Generic image of electronic package with BGA connection [1]

One type of junction used in SMT is the ball grid array. In this type, solder balls are used as an array between the IC chip and the substrate material (Fig. 1). This type of junction is widely used and as a result of developments, it appears to be advantageous to use. Advantages include the following [1]

- Efficient use of the surface of the substrate
- Improvement in electronic and thermal performance. Solder balls have low electronic resistance and high thermal conductivity and good heat dissipation due to the large number of connection paths
- Manufacturing yield increases as a result of improved solderability. BGAs provide a better level of solderability as well as wide spacing between joints
- Low total package thickness
- Excellent reworkability with larger pad sizes

In July 2006, the Restriction of Hazardous Substances directive restricted the use of lead-containing soldering materials. This has opened research and application areas for lead-free solder materials. When lead-free solder materials are examined, it is seen that Sn-Ag-Cu based materials have promising characteristics to replace lead-based materials [2].

In its simplest form, the solder bump interconnection in electronic packages consists of a multi-layer UBM, solder bump and metallic bond pads [3]. Fig. 2 shows a representative drawing of this form. It shows where the UBM layers, bond pads and solder ball are located in relation to each other.

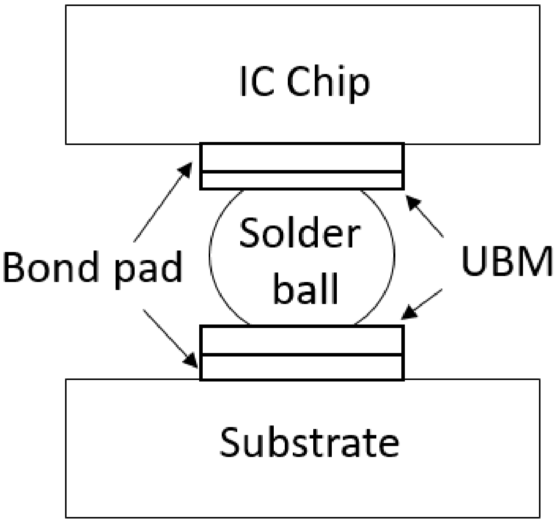

Figure 2. Representative drawing of one solder ball BGA electronic package

The main purpose of the UBM layer is to join metal bond pads, solder bumps and metallic materials. In addition to electrical and mechanical connection, UBM solder provides wettable characteristics, diffusion resistance and the ability to join different metallic materials. Table 1 shows briefly the materials used in UBM and their functions.

Table 1. Functions of UBM and associated used metal types

UBM Layer	**Function**	**Metals Used**
Adhesion & diffusion barrier	Joining of bond pad metal with passivation layer Prevent diffusion interactions of bond pad and solder materials	Cr, Ti, TiW, Ni, Pd, Mo
Solder wettable layer	Improves ability of melted solder to create a reliable joint	Cu, Ni, Pd
Oxidation barrier layer	Prevents UBM structure from oxidation	Au

1.2 Thermal Problem with Operation of Electronic Packages

Electronic packages are exposed to temperature changes due to their usage environment and this creates problems in the reliability of the packages. Each component of the electronic package has a different coefficient of thermal expansion value. With temperature changes, each component expands at different levels and this creates stresses in each component.

Solder balls are subjected to stress as they are the layer that connects components with these different expansion coefficients (Fig. 1,2). When the temperature change is cyclic, crack formation and propagation in solder balls is observed. Fig. 3 shows the formation and propagation of cracks in the solder ball due to temperature cycles as shown in scanning electron microscopy images [4]. These results show that thermomechanical fatigue studies are important in improving the reliability of solder balls.

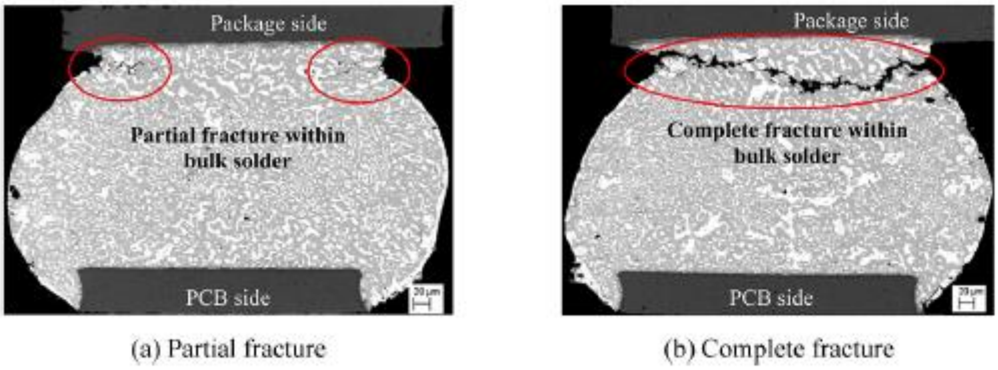

(a) Partial fracture

(b) Complete fracture

Figure 3. Result of thermal cycles (a) Formation of crack and (b) propagation of crack causing failure in the solder ball [4]

1.3 Scope of This Thesis

It is known that temperature is the effect that most shortens the life of solder balls in electronic packages. However, it is often not possible to change the operating temperature of electronic packages to eliminate this effect. Therefore, if it is desired to increase the lifetime of the solder balls, one of the solutions is to adjust the dimensions of the components in the electronic package to reduce the stress/strain accumulation on it.

In this thesis, a life prediction and life improvement study of an electronic package with 144 connection 12x12 BGA (Fig. 15,16) was performed. The optimization study was performed using 9 different parameters including values of UBM thicknesses and solder ball diameter and height. It was aimed to find a geometric configuration that improves the lifetime compared to the original size structure. The response surface optimization module in ANSYS was used as the optimization tool.

In the thesis, the finite element method was used as the basic progress tool and TMF analysis of the structure of interest was performed in ANSYS 2023R2 program. SAC305 is used as the solder material. Preliminary analysis showed that the components with the lowest lifetime appeared to be the solder balls. Therefore, the main objective of the optimization was to extend the life of the most critical solder ball.

Within the scope of the thesis study, two different optimization studies were carried out. For SAC305 material, AV material model was used in the first one and EP material model was used in the second one.

Finally, it was observed that there is no such optimization study in the literature for the dimensions and material combination of the electronic package of interest. Therefore, this study is considered to be original and contributes to the literature.

1.4 Structure of This Thesis

This thesis contains 6 chapters. Chapter 1 presents the purpose and general scope of the study.

Chapter 2 presents the results of the literature survey related to the thesis topic. The historical development of the tools and models used in the thesis is presented and the reasons why they are used are explained.

In Chapter 3, in order to verify the capabilities of finite element simulation, a similar study in the literature was repeated and a benchmark study was performed.

In Chapter 4, the finite element model studies using the AV material model for SAC305 are presented. As a result of the response surface optimization, the geometric configuration with the highest solder ball lifetime was found.

Chapter 5 contains the repetition of the work done in Chapter 4. Here the EP material model was used for SAC305.

In Chapter 6, the results of the studies and the level of success achieved are presented. A dimensional comparison of the best geometric configurations obtained in Chapter 4 and Chapter 5 is presented and it is seen how much life improvement is achieved by optimization with each material model.

CHAPTER 2

LITERATURE REVIEW

With the developments in microelectronics, solder balls started to take place in electronic packages. After practical applications and observations, it was realized that the temperature excursions create problems on solder balls. Within the scope of this thesis, a literature survey on the problems caused by temperature excursions and proposed solutions has been conducted and presented.

2.1 Observed Problems in Solder Balls due to Temperature Effect

Electronic packages are structures that experience temperature changes in the components inside them due to their nature of generating heat while operating and the ambient temperatures at which they must operate.

Since the components that make up the electronic package have different CTEs, the components tend to experience different amounts of elongation with temperature changes. Due to the non-uniformity of these elongations, significant stresses arise at the interfaces between the components. In [5], stress generation on solder layers with temperature variations in multi-layer electronic packages consisting of different components was demonstrated. FE simulations were used to find the stress values. The related study is useful in terms of showing that the stresses which occur due to temperature changes are not specific to solder ball type connections, it affects all type of connections.

Repeated cycles of the stress generated due to temperature changes are the most damaging conditions for the reliability of the packages. Qiang Guo et. al. [6] showed that the main cause of failure among different types of loading in electronic packages is the temperature effect with 55%.

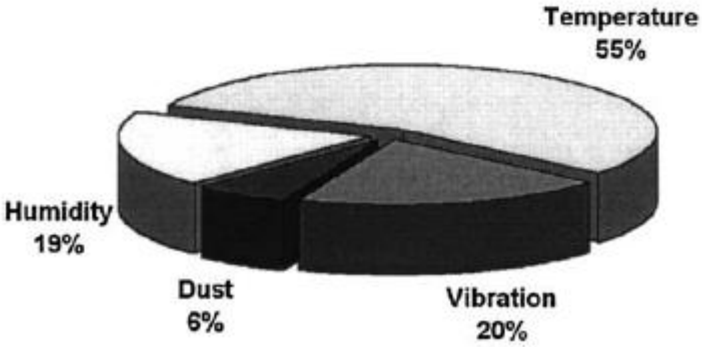

Figure 4. Main cause for failure of electronic packages [6]

Temperature cycles cause crack formation and propagation due to thermomechanical stress at solder interfaces. H. Xiao et al. [7] conducted a test study with different materials and SAC interface solders and demonstrated the crack formation and propagation in the solder material with the application of temperature cycles to the structure.

Similarly, in electronic packages with the type of joints using solder balls, it is seen that the solder interface is the component that receives the most critical damage and fails in the earliest with temperature cycles. C. Huang [8] performed thermal cycling tests on an electronic package using Sn3.0Ag0.5Cu solder balls. Thermal cycles were applied to electronic packages which were pre-applied different aging processes. Experimentally, a study was carried out to show if and where cracks would occur for different aging and temperature cycle times. In addition, F.X. Che and John H.L. [9] showed in an experimental study that the first failure occurs in the solder balls due to temperature cycles. In the study supported by experimental findings and FE simulation, no major problems were observed in the other components of the structure, while cracks formed in the solder balls. They propagated and caused the structure to fail. Similarly, H. Tohmyoh et. Al [10] performed thermal cycling tests of electronic packages consisting of Si chip, printed circuit board and solder balls with SAC305 material in between. In his tests, he used different Si chip thicknesses and temperature ranges and showed that the solder balls failed in each test. Table 2 summarizes the fatigue life of the solder ball test specimens. Cracks formed in the solder balls with temperature cycles, propagated and caused the structure to become inoperable (Fig. 5).

Table 2. Thermomechanical fatigue life of the test specimens in cycles [10]

Chip Thickness (mm)	Applied Temperature Range (℃)		
	140	165	190
4	1920 ± 225	890 ± 98	420 ± 24
6	-	565 ± 75	-
7	787 ± 99	375 ± 45	229 ± 32

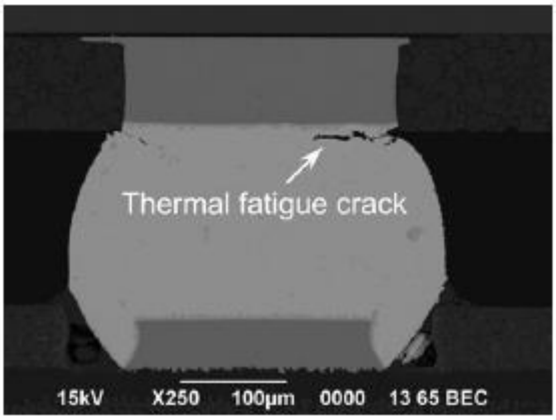

Figure 5. A failure site in a Pb-free solder bump joint after the thermal test [10]

2.2 Finite Element Analysis as a Proposed Improvement Tool

Engineers and researchers have studied the problems of solder balls in electronic packages caused by temperature cycling. The center and goal of those investigations have been to predict the lifetime of solder balls in each configuration. FE analysis and experimental methods have been used to estimate the lifetime information of solder balls.

Simple or complex structures can be modeled using the FE method and results can be obtained on the components with appropriate adjustments. In the literature, many studies have used FE analysis simulations to find the damage parameter values on solder balls. The relevant damage parameter values are then used in the life prediction models and the thermal cycle life information of the solder balls can be extracted.

Studies have shown that SAC and soft metal (In, Pb, etc.) solder materials in electronic packages undergo plastic deformation with temperature cycles. These cycles generally have approximately 120-180°C temperature ranges and under these conditions solder balls have low lives ($<10^5$ cycles). It is therefore understood that solder balls exhibit low cycle fatigue behavior [11-14]. Therefore, the material models used for solder balls in FEA simulations are important.

2.3 Material Models in Thermomechanical Analysis of Solder Balls

Different material models have been used in different studies to find the lifetime of solder balls exposed to thermal cycling. It is seen that the damage parameter values on solder balls are extracted with FE simulations according to these material models.

When the literature is reviewed, it is seen that the Elasto-Plastic material model is used in some FE simulations. S.C. Yang et. al. [15] conducted an optimization study to find a different type of geometry for the joint as an alternative to the traditional solder ball geometry in order to increase the number of thermal cycle life. The author used the EP material model in his model. He validated the FE model with reference experiments and then performed the optimization study. In the optimization, the equivalent plastic strain value accumulated on the solder balls was used as the performance output parameter. After the optimization study, the solder geometry with the lowest EPS value in thermal cycles was determined. This study [15] is valuable in showing that experimental results can be captured, and optimization work can be done using the EP model.

In the literature, Elasto-Plastic Creep and AV material models are also used. F.X. Che and John H.L. [9] compared the life outputs of FE simulations using EP, EPC and AV material models with experimental data. The characteristic lifetime of the electronic package was deduced from the experiments. It is shown that the FE simulation using the AV material model gives the closest lifetime result to the characteristic lifetime.

T. Hayashi et. al. [16] compared EPC and AV material models in his study. Tensile and stress relaxation tests were performed on a test clipping made of solder material. Then, both tests were modeled and simulated using FE method. The results of the FE simulations using both material models were compared with the test results. The results of the FE simulation using the AV material model were found to be consistent with the results of the tensile and stress relaxation tests in both transition and stationary regions. The EPC material model agreed with the stress relaxation test results in both transition and stationary regions in the FE simulation, but agreed with the tensile test results only in the transition region in the FE simulation. The author stated that the AV material model is a successful model in capturing the experimental results.

J-B. Libot et. al. [17] conducted an experimental and FE simulation study of an electronic package consisting of PCB and electronic components assembled with SAC305 solder balls. In the study, the solder balls in the electronic package were first tested with 4 different temperature profiles and the maximum shear stress-strain hysteresis loops were extracted. Then, FE simulations of the tests with AV material model were performed and 4 different shear stress-strain hysteresis loops were extracted. When the results are compared, it is observed that the simulation and test results were close for all 4 applications.

G.Z. Wang et. al. [18] compared the steady state creep test results of different solder materials found in the literature with the FE simulation results of the same test using the AV material model. After the comparison, the author stated that the results were close, and the AV material model can be used to find the stress and strain results of solder materials accurately.

In addition, different material models than those used above (Creep, Chaboche, Wiesse, etc.) are available in the literature [11,12,19]. However, these material models are seen in a limited number of studies and there is not enough data for their verification with experimental studies.

As a result of the literature survey, it is concluded that the AV and EP material models can successfully extract the results of TMF analysis studies of solder components in electronic packages. In addition, it is noteworthy that the number of studies in the literature with AV [4,9,12,14,16,17,18,20-27] and EP material models [9,10,28-31] are much more than the other material models. In the next topics, AV and EP material models are explained physically and mathematically.

2.3.1 Anand Viscoplastic Material Model

AV material model is firstly proposed by Anand and Brown [32] to describe the deformation behaviors of conventional metals which are formed under elevated temperatures. Researches have shown that AV model can be used for materials whose deformation characteristics are sensitive and susceptible to strain rate, temperature and strain hardening and softening.

AV model contains set of constitutive equations that includes flow and evolution equations to fully describe the plastic flow of the material. The plastic flow includes both rate-dependent creep and rate-independent plastic deformations. Additionally, the model uses an internal state variable which is named deformation resistance to represent material's isotropic resistance to large plastic flows. This internal variable is denoted by s, and has the same dimension with stress. There is also one basic feature for this model; it needs no explicit yielding condition so that loading and unloading criterion is not needed. The plastic flow is assumed to take place at any non-zero stress values, although the inelastic strain values are very small at low stress values.

As stated earlier, the internal state variable s represents averaged isotropic deformation resistance to macroscopic plastic flow of materials. This variable characterizes the isotropic strengthening mechanisms such as dislocation density, solid solution strengthening, sub grain and grain size effects, etc. In AV model, variable s is proportional to the equivalent stress σ_e.That is [18].

$$\sigma_e = c \cdot s;\ c < 1 \tag{2.3.1}$$

Equivalent stress σ_e is defined as

$$\sigma_e = \sqrt{\frac{1}{2}[(\sigma_{11} - \sigma_{22})^2 + (\sigma_{22} - \sigma_{33})^2 + (\sigma_{33} - \sigma_{11})^2 + 6({\sigma_{23}}^2 + {\sigma_{31}}^2 + {\sigma_{12}}^2)]} \tag{2.3.2}$$

where σ_{ij} ($i, j = 1,2,3$), are the stress components of Cauchy stress tensor σ.

And, c is material parameter and function of strain rate and temperature, which is defined as

$$c = \frac{1}{\xi} \sin h^{-1} \left[\left(\frac{\dot{\epsilon}_p}{A} e^{Q/RT} \right)^m \right] \tag{2.3.3}$$

where $\dot{\epsilon}_p$ is the inelastic strain rate in 1/s, Q is the activation energy in kJ/mol, T is absolute temperature in K, R is the universal gas constant in J/(K·mol), A is the pre-exponential factor in 1/s , m is the strain rate sensitivity and ξ is the stress multiplier.

The Anand model employs following functional form of flow equation to accommodate the strain rate dependence on the stress. Combining the Eq. (2.3.1) and (2.3.2), flow equation can be found as

$$\dot{\varepsilon}_p = Aexp\left(-\frac{Q}{RT}\right) \left[\sinh\left(\xi \frac{\sigma_e}{s}\right)\right]^{1/m} \tag{2.3.4}$$

Observe that deformation resistance variable enters the flow equation only as a ratio with equivalent stress. Also, temperature effect on the inelastic strain rate is incorporated via Arrhenius term. To fully use the flow equation to capture the inelastic strain rate under constant stress, internal variable s needs to be determined.

The evolution equation for the internal variable s is assumed to be of the form as

$$\dot{s} = h(\sigma, s, T)\dot{\varepsilon}_p \tag{2.3.5}$$

where function $h(\sigma, s, T)$ is associated with and incorporate the effects of dynamic recovery and strain hardening. Anand has given a simple form of evolution equation of Eq. (2.3.5) as follows:

$$\dot{s} = \left\{h_0 \left|1 - \frac{s}{s^*}\right|^a \cdot sign\left(1 - \frac{s}{s^*}\right)\right\} \cdot \dot{\varepsilon}_p;\ a > 1 \tag{2.3.6}$$

where

$$s^* = \hat{s}\left[\frac{\dot{\varepsilon}_p}{A} exp\left(\frac{Q}{RT}\right)\right]^n \tag{2.3.7}$$

In Eq. (2.3.7), the value of s^* represents a saturation value of s associated with a set of applied temperature and strain rate. $\hat{s}$ is a coefficient in MPa, h_0 is the hardening/softening coefficient in MPa, n is the strain rate sensitivity for the saturation value of deformation resistance, a is the strain rate sensitivity of hardening/softening, respectively.

2.3.2 Elasto-Plastic Material Model

In the Elasto-Plastic material model, the loaded material is modeled not only where it shows elastic deformation but also where it shows plastic deformation. In this model, the amount of deformation does not depend on the rate of loading but only on the amount of loading.

As an example, Fig. 6 shows the stress-strain graph of a material with elastoplastic behavior under loading. Here, the material shows plastic behavior after the stress on the material exceeds the elastic limit (yield point). At the point where it shows plastic behavior, the material has both elastic and plastic strain. In the plastic region, the elastic strain is recovered when the load on the material is released, but the plastic strain is permanent. Total strain can be defined as follows

$$\varepsilon = \varepsilon_e + \varepsilon_p \tag{2.3.8}$$

$$\varepsilon_e = \frac{\sigma}{E} \tag{2.3.9}$$

$$\varepsilon_p = \varepsilon - \varepsilon_e \tag{2.3.10}$$

where ε_e is elastic strain, ε_p is plastic strain and E is the elastic modulus.

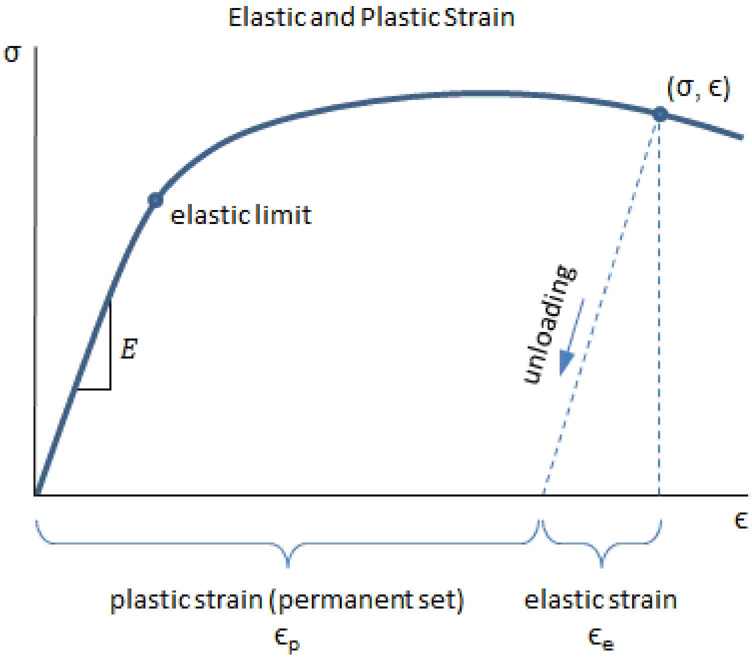

Figure 6. Typical stress strain curve for materials which shows Elasto-Plastic material behavior [33]

In this model, it is also necessary to define a criterion that shows how much the materials will yield under how much loading amount. Two different criteria can be used here. The first one is Von-Misses yield criterion and the second one is Tresca yield criterion.

According to Von-Misses yield criterion; yield occurs when the equivalent stress value (σ_e) specified in Eq. 2.3.2 is greater than or equal to the yield stress of the material in uniaxial tension (Y).

Tresca yield criterion is also called maximum shear stress theory. According to this criterion Eq. 2.3.11 condition is met, the material yields.

$$\max(|\sigma_1 - \sigma_2|, |\sigma_2 - \sigma_3|, |\sigma_3 - \sigma_1|) = Y \tag{2.3.11}$$

where σ_i $(i = 1,2,3)$ principal stress components of Cauchy stress tensor σ.

In the Elasto-Plastic material model, it is also necessary to define the evolution of the yield surface due to deformation in the plastic region, these are called strain hardening laws. There are three different strain hardening laws. These are listed below.

- Isotropic Hardening
- Kinematic Hardening
- Mixed Hardening

In this thesis Von Mises Yield criterion and kinematic hardening is used.

2.4 Life Prediction Models

Another tool that should be used for life prediction of solder ball components due to thermomechanical loading is life prediction models [34]. Life prediction models are tools that extract life cycle information about solder materials using the material properties and the damage parameters resulting from calculations, e.g. plastic strain range, shear strain range etc.

X. Xu et. al. [23] performed a life prediction study based on FE simulation using accurate material and life prediction model. The system was modeled in FE environment and the solution was performed using AV material model for solder material. With the solution, the plastic strain range was found in the solder ball. Then, with the Engelmaier modified Coffin-Manson model used as a life prediction model, the life cycle prediction results of the most critical ball were calculated and revealed.

Following the literature review, it is noticeable that CM [10-14,21,29,30] and ECM [11,12,13,23,25] lifetime prediction models are the most commonly used tools for life estimation of solder balls due to thermomechanical loading. It is stated that ECM is the preferred model as it includes the temperature range and frequency of the applied temperature cycle in the lifetime calculations [12]. In the next section, ECM is explained.

2.4.1 Engelmaier Modified Coffin-Manson Life Prediction Model

The Engelmaier modified Coffin-Manson equation used in the determination of the life of solder balls due to temperature cycles is as follows [35]

$$N_f = \frac{1}{2}\left(\frac{\Delta\gamma}{2\epsilon'_f}\right)^{\frac{1}{c}} \tag{2.4.1}$$

Where N_f is the number of cycles to failure, ϵ'_f is the fatigue ductility coefficient which is a material parameter and $\Delta\gamma$ is the shear strain range which is calculated by Eq. (2.4.2)

$$\Delta\gamma = \sqrt{3}\Delta\varepsilon \tag{2.4.2}$$

Where $\Delta\varepsilon$ is equivalent strain range, which can be found from cyclic stress-strain hysteresis loops of solder balls and c is fatigue ductility exponent which can be calculated by Eq. (2.4.3)

$$c = -0.442 - 6 \times 10^{-4} T_m + 1.74 \times 10^{-2} \ln(1 + f) \tag{2.4.3}$$

where T_m is the mean temperature of the applied cyclic temperature range and f is the frequency of applied temperature profile.

ECM model can be considered as an extension of the CM model. It includes the average temperature in the temperature profile applied to the solder balls and frequency effects in the lifetime calculation. Basically, the damage parameter it uses is the strain range, so this is a strain-based method. In Fig. 7, generic hysteresis curve for viscoplastic materials under thermomechanical loading is illustrated [36] and representative total and plastic strain ranges could be seen.

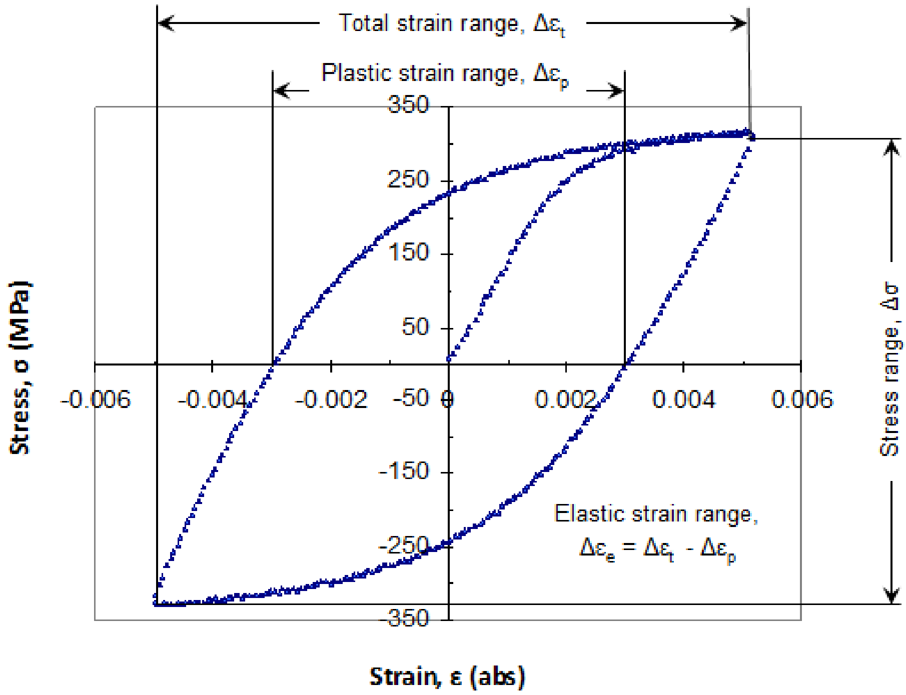

Figure 7. Typical stress-strain hysteresis loop of viscoplastic materials and total and plastic strain ranges [35]

2.5 Global-Local Modelling Approach for Finite Element Analysis

Within the scope of this thesis, the FE analysis of solder balls was evaluated with a global-local approach. Therefore, the existence and suitability of such a study was investigated in the literature.

Basically, global-local modeling approach in FE analysis is technique that helps analyzing relevant portion (local) of a larger model (global) with refined mesh and hence acquiring more accurate and detailed results within this portion of interest.

Global model is solved first with a coarser mesh to acquire displacement or temperature results. Afterwards, these results are mapped to local model at the cut boundary faces to analyze the response of the portion with denser mesh. It is most useful for obtaining accurate results while keeping the computation time as low as possible.

C. Chen et. al. [27] investigated the relationship of the global-local approach in the analysis of solder balls in FE environment. They performed their analysis according to the output value of inelastic strain energy density in solder balls. It is shown that the global-local analysis result changes only by 2.4% compared to the global model result with the same settings, but the analysis solution time is reduced by 75 times.

In addition, they stated that the aspect ratios of the solder ball and UBM structures, which are small compared to the global model dimensions, are close to 25 during mesh creation in the global model, while this value decreases to 5 in the local model. This would be useful to improve the accuracy of solutions with the local model.

In the literature, there are also optimization studies with the global-local approach. A. Deshpande [37] performed an optimization study to determine the optimal solder ball dimensions in terms of lifetime in a structure consisting of PCB, electronic package, and solder balls. In the study using global-local approach, the global model was solved and then the most critical solder ball was found and then that region was modeled locally. With the optimization in the local model, the dimensions that will have the lowest strain energy density under temperature variation were determined.

CHAPTER 3

FINITE ELEMENT MODEL VALIDATION

Within the scope of this thesis, TMF life prediction of solder balls in a specially designed electronic package has been carried out by FE simulations. Before starting the studies, the path was followed according to the conclusions learned from the literature survey.

Following the literature survey, conclusions given below were drawn:

- FE simulations is going to be used to find the lifetime of solder balls.
- In FE simulations, both AV and EP models will be used as material model of solder balls to extract the stress & strain results.
- Engelmair modified Coffin-Manson fatigue life prediction model will be used to generate lifetime results.

When producing an electronics package, laying down the solder balls, post-processing and assembling the structures in the package are costly activities. Along with this consideration, [23] X. Xu et. al. stated the difficulty of doing experimental work in life determination studies of solder balls that are subjected to thermomechanical loading. For this reason, the optimization and finding the best solder ball geometry is carried out by FE simulations in this thesis.

Before simulating and optimizing the structure of interest, a benchmark study is required to validate our FE modeling and solution capabilities. When the literature is examined, it is seen that there is no experimental study that will include all the details necessary to make the mentioned verification. The missing details include some of the dimensions of the test sample, the material type information of some components, etc. It seems that the literature is incomplete in this respect.

Like the experimental studies, FE simulation-based studies also seem to lack sufficient information to validate our own model. For example, the material type and dimensions of the components in the FE model is missing in [12,20].

Although all the necessary information is not fully provided, information in [21] is nearly complete for benchmarking at a certain level. This study has been attempted to be repeated with the data provided and the lifetime on the most critical solder ball has been extracted.

3.1 Benchmark Study

H. Chunyue [21] performed the lifetime analysis of solder balls in a 144-Pin plastic ball grid array structure integrated on printed circuit board with two different solder ball materials (63Sn37Pb, 96.5Sn3.5Ag). In this FE simulation-based study, AV was used as the material model and ECM was used as the life prediction model. Material properties for both materials are given in the related article. The boundary condition and applied temperature profile information required for the repetition of the simulations were defined, but the geometric dimensions of the modeled components were not fully defined. The missing dimensions were estimated by considering the figures and images in the article.

Separate reruns have been carried out for two different material types found in the related study. For this, an FE model was tried to be constructed and then the analysis results were obtained by changing the material assignment of the solder balls. These analysis results were then used in ECM to obtain the life results and compared with the values in the paper.

ANSYS 2023R2 has been used in FE simulations. The program has the AV material model in its embedded library. With the convenience provided by this program, there is no need to write a material model again and it can be directly applied to the solder balls in the analysis.

Hereafter, studied model in the article [21] and the constructed model are going to be called as Model A and Model B, respectively. Fig. 8 shows the computer aided design images of Model A and Model B.

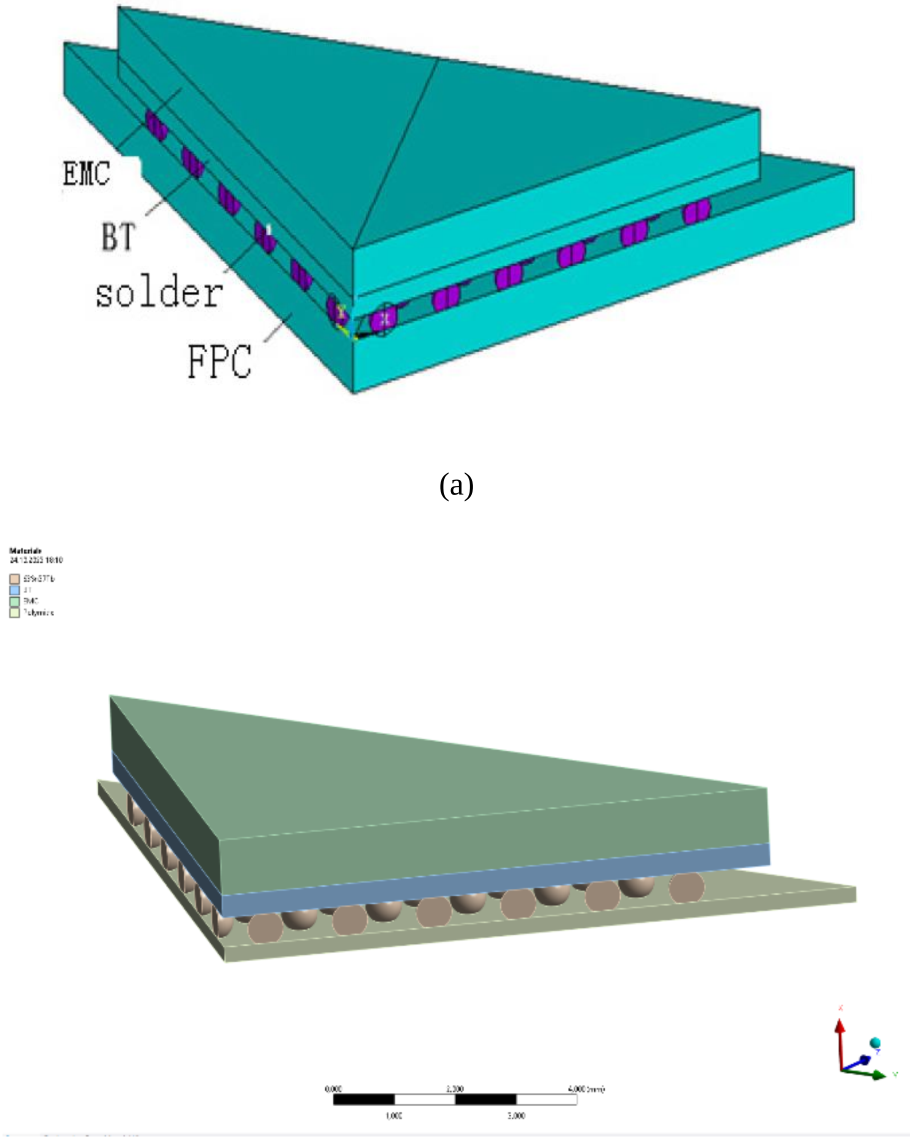

(a)

(b)

Figure 8. Quarter model CAD images of Model A [21] (a) and Model B (current study) (b)

The Model B was first generated in accordance with Model A's given physical dimensions and then evolved into a quarter model to form the symmetry surfaces specified in the article. In Table 3, original dimension comparison of the models can be seen. Some of the dimension in the Model A is not available (N/A), thus they are guessed according to given images in the article.

Table 3. Original dimensions of the Model A and Model B.

Dimension Name	**Dimension Value (mm)**	
	Model A	Model B
EMC thickness	N/A	0.95
EMC planar	13x13	13x13
BT thickness	N/A	0.38
BT planar	13x13	13x13
EMC+BT thickness	1.33	1.33
Solder ball diameter	0.6	0.6
Solder ball height	0.5	0.5
Solder ball pitch	1	1
FPC thickness	N/A	0.27
FPC planar	N/A	15x15

Fig. 9 shows the FE models of Model A and Model B. In Table 4, FE model property comparison can be seen. For simulations of Model A, ANSYS V11.0 is used [21].

Table 4. Finite element properties of the Model A and Model B.

	Model A	**Model B**
Element type for solder balls	VISCO107	SOLID 186
Element type for rest of the model	SOLID45	SOLID186 & SOLID 187
Total number of elements	253652	222148

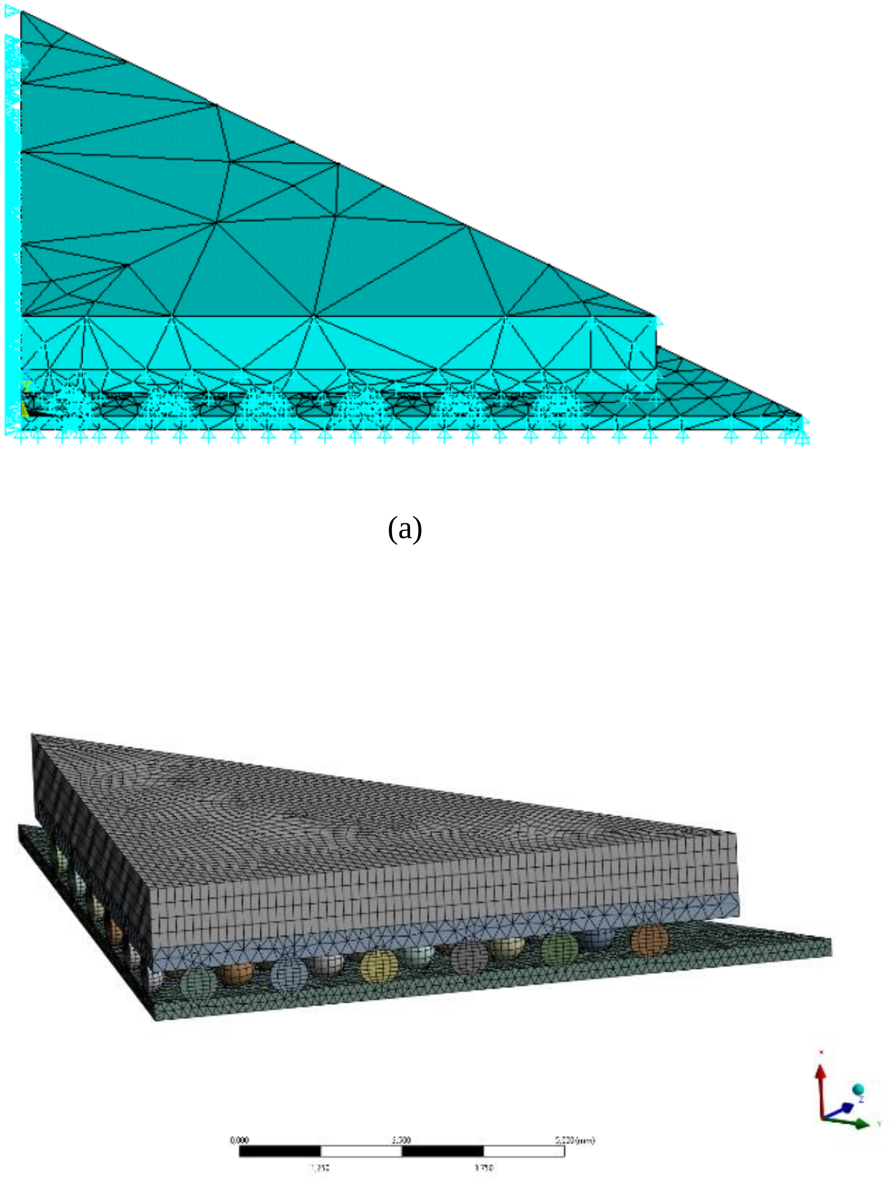

(a)

(b)

Figure 9. Quarter finite element model of Model A (a) and Model B (b)

Contact and mesh interaction information of Model A are not given. Also, there is no image or figure to demonstrate mesh and contact configuration of the solder balls closely. In Model B, conformal mesh is used between components. Fig. 10 shows the conformal mesh transition.

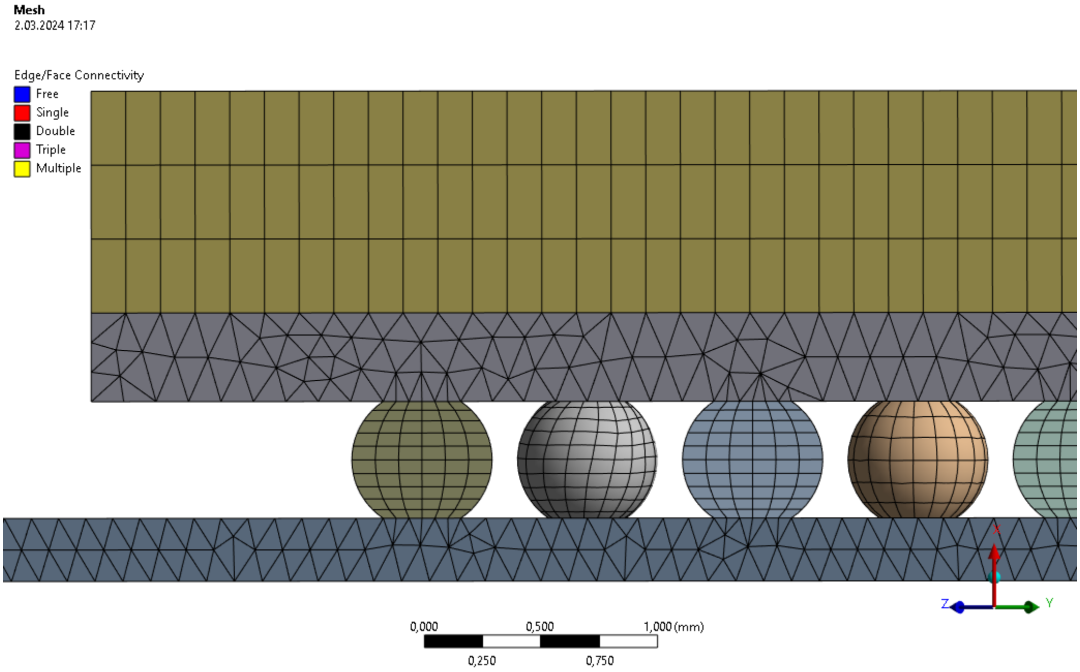

Figure 10. Side view of Model B's mesh model, the transition of mesh

Fig. 11 shows the applied temperature profile in both models A and B. They are exactly the same. Temperature profile has higher extreme at 125 °C and lower extreme at -55 °C. Initial temperature for the bodies are selected as 125 °C for Model A and B so they are in stress-free state initially.

In [21] and other studies in the literature, it is seen that the material behavior reaches steady state after the first 3 cycles and there is no further change in the hysteresis loops and strain ranges [7,17,20] in the subsequent cycles. For this reason, 3 cycles are selected in the temperature applications to find the strain range values to be used in ECM. This approach saves a long numerical solution time.

Additionally, material properties specified in Model A is used exactly at Model B’s simulations. In Model A, only solder balls are modeled with AV, other components are assumed to behave linear isotropic. In Tables 5 and 6, material properties of the components used in Model A [21] can be seen. Term *t* is temperature in °C.

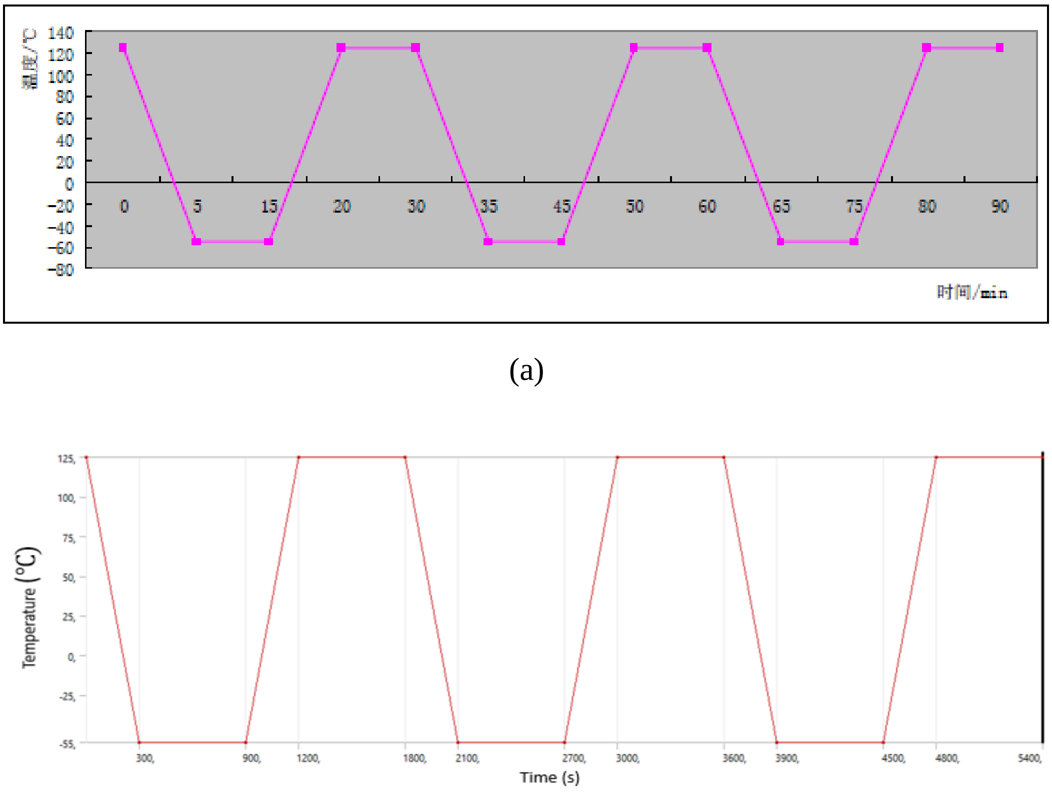

(a)

(b)

Figure 11. Applied temperature cycle profiles of (a) Model A and (b) Model B

Table 5. Elastic and thermophysical material properties of Model A components

Material	**Elastic Modulus (GPa)**	**Poisson’s Ratio**	**Coefficient of Thermal Expansion (ppm/°C)**
EMC	15.435	0.250	15.0
BT	17.8	0.390	15.0
FPC	3.724	0.335	15.0
67Sn37Pb	(34474-152*t*)/1000	0.35	21.0
96.5Sn3.5Ag	(52708-67.14*t*-0.0587*t*2)/1000	0.4	21.85+0.02039*t*

Then, the FE simulation settings specified in the article [21] were similarly adjusted

- Symmetry planes are constrained with “frictionless support” which only allows them to make in-plane motions
- Stress free state is selected at 125 °C, it is starting temperature point of the simulations

and the calculations were performed. The relevant results were extracted from the solder ball that showed maximum strain throughout the cycles as stated in the article. Then, the maximum output values in this solder ball were again compared with the results of Model A. First, the solder ball material was chosen as 63Sn37Pb to compare the results.

Table 6. Anand viscoplasticity material properties for two different solder materials

Parameters	**Solder Material**	
	67Sn37Pb	96.5Sn3.5Ag
s_0 (MPa)	12.41	39.09
Q/R (K)	9400	8900
A (1/s)	4.0E6	2.23E4
ξ	1.5	6
m	0.303	0.182
h_0 (MPa)	1378.95	3321.15
$\hat{s}$ (MPa)	13.79	73.81
n	0.07	0.018
a	1.3	1.82

As a reminder, Model A’s results are gathered from article [21]. Model B is constructed model and its results are generated.

In Fig. 12, location of critical solder ball of the Model B is shown. Red label with name Max in Fig. 11 shows the most critical point of Model B through the temperature cycles. Unfortunately, the most critical point in Model A is not shown in the article.

In Fig. 13 the time-dependent Von-Misses equivalent stress result at the most critical point is extracted and compared with the curve in the article. Fig. 13a and Fig. 13b show the results of Model A and Model B, respectively. It is seen that in Model A, maximum stress is around 44 MPa and in Model B, the maximum stress is around 41 MPa through the cycles. For both results, maximum stress is increasing with each cycle.

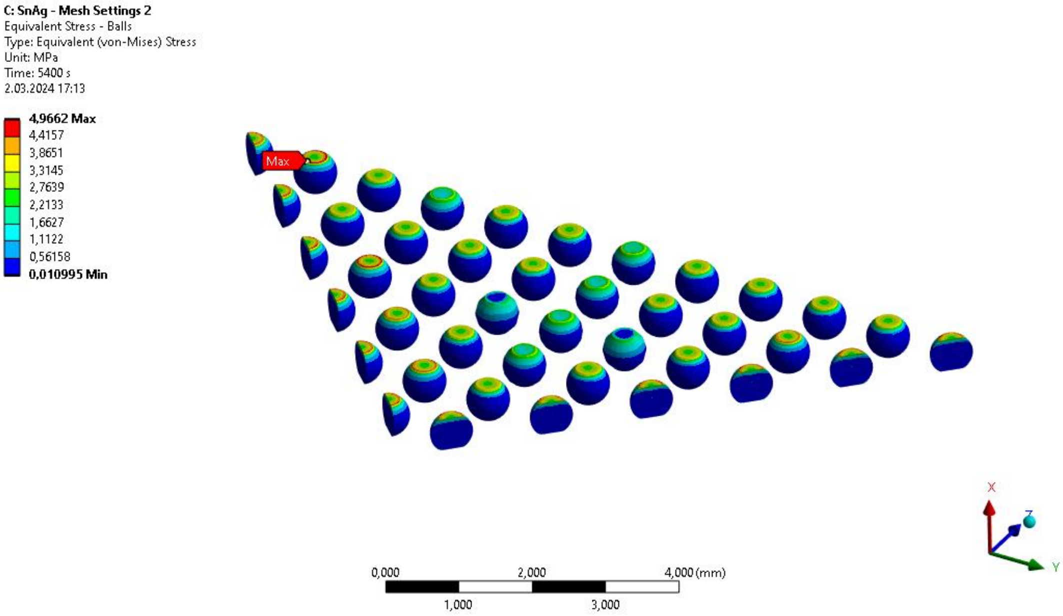

Figure 12. Critical solder ball location of Model B throughout the analysis

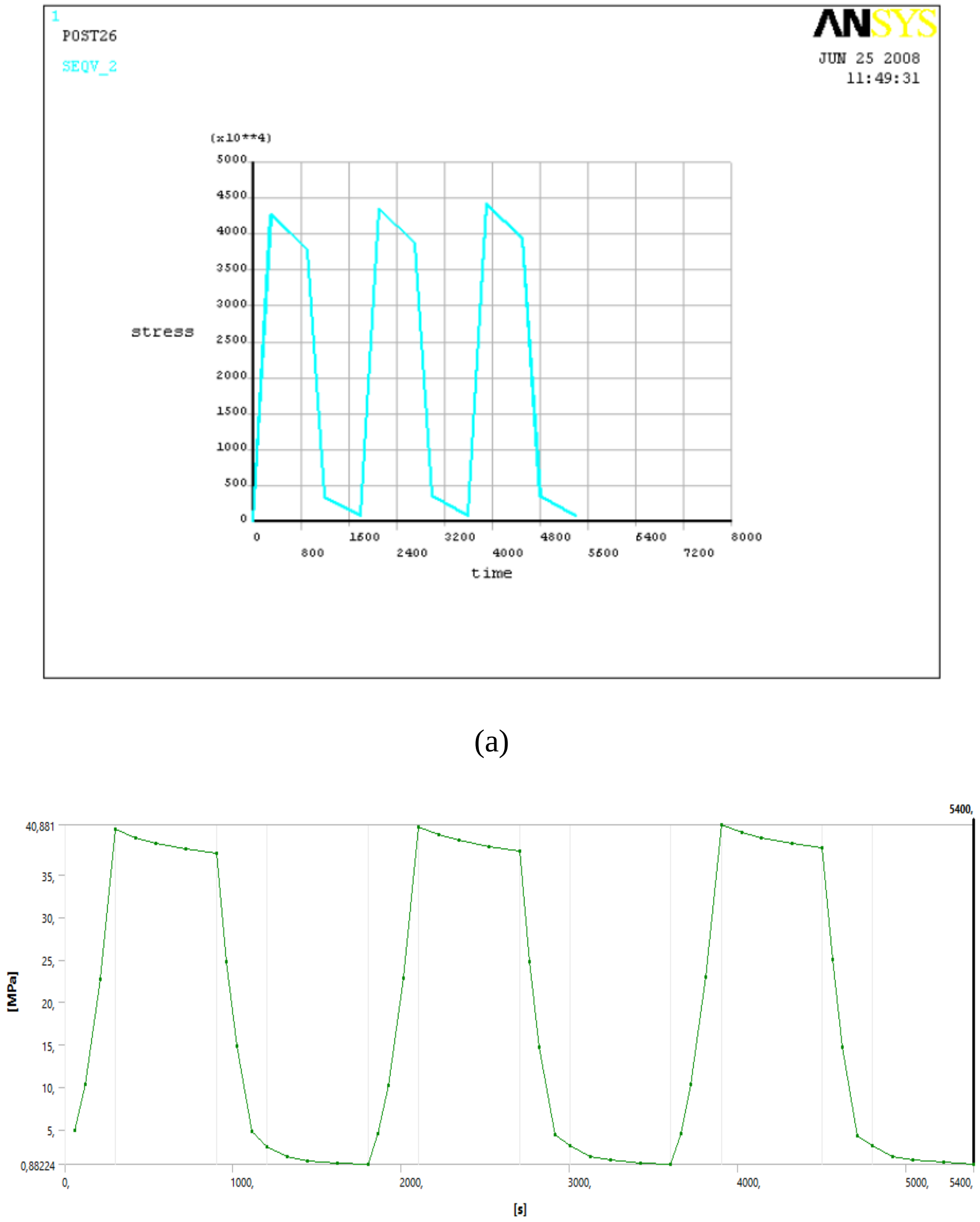

(a)

(b)

Figure 13. Equivalent stress at the critical point throughout the temperature cycles (63Sn37Pb); (a) Model A [21], (b) Model B

In Fig. 14, the time-dependent VM equivalent plastic strain result at the same critical point was extracted and compared with the curve in the article. Fig. 14a and Fig. 14b show the results of Model A and Model B, respectively. Maximum strains are 1.35E-

03 for Model A and 1.25E-03 for Model B. For Model A, maximum strain is decreasing for each cycle, however for Model B maximum strain is increasing.

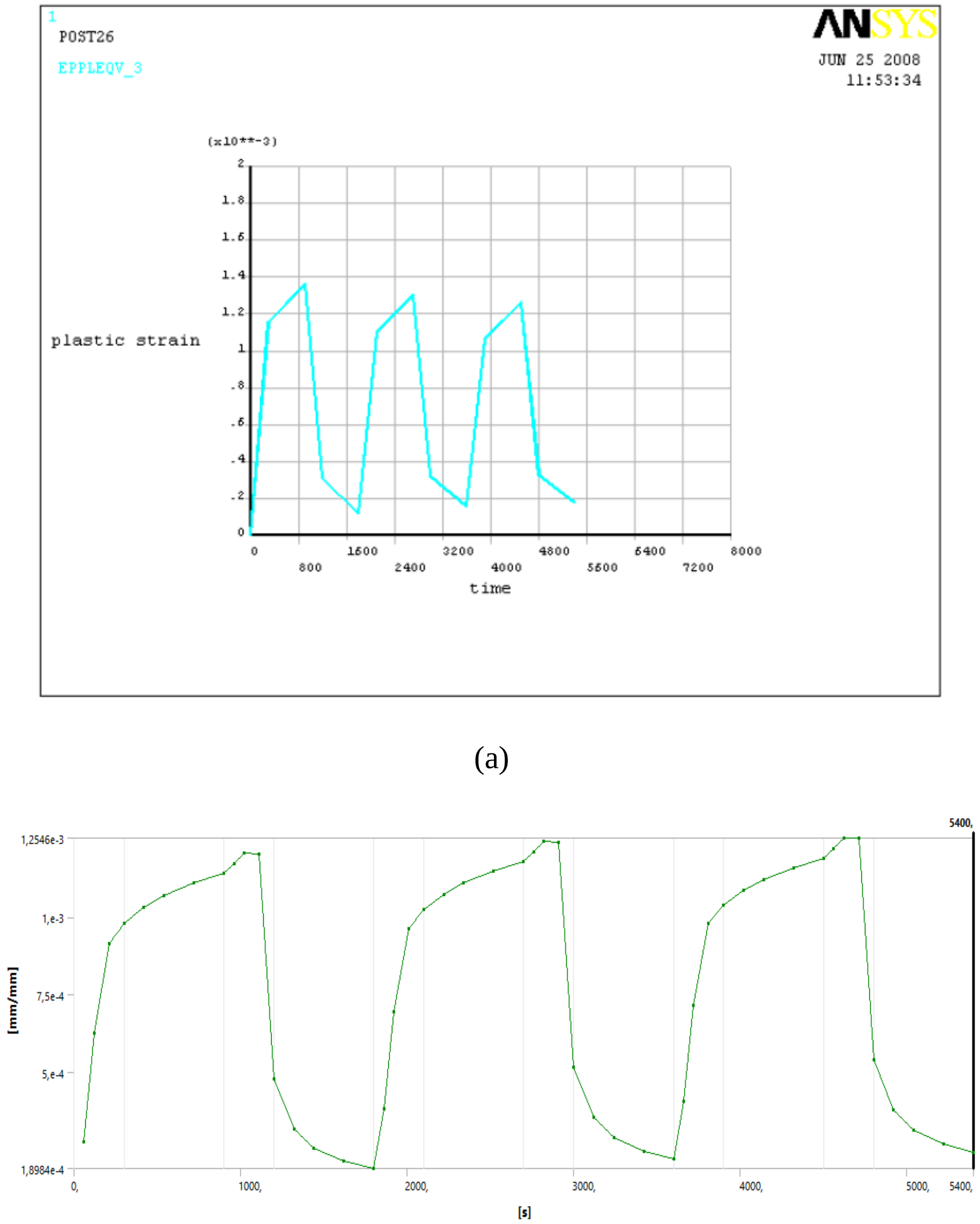

(a)

(b)

Figure 14. Equivalent strain at the critical point throughout the temperature cycles (63Sn37Pb); (a) Model A, (b) Model B

For material 63Sn37Pb after analyzing the results Fig. 13 and Fig. 14, it can be concluded that at low temperature dwell times, solder ball exhibits both creep and stress relaxation behavior. Stress is decreasing and plastic strain is increasing. However, for high temperature dwell times it only exhibits stress relaxation. Stress is decreasing and strain is also decreasing.

In Fig. 15, the stress-strain hysteresis loop at the same critical point was extracted and compared with the curve in the article. Fig. 15a and Fig 15b show the results of Model A and Model B, respectively. There is a shape difference between curve results of the Model A and Model B. Possible causes of this difference are explained later in this chapter.

Secondly, 96.5Sn3.5Ag material was chosen for the solder balls to compare the results. Similar to the 63Sn37Pb material type, the stress and strain values in the most critical solder ball were plotted and compared with the corresponding curves in the article [21].

Fig. 16, the time-dependent VM equivalent stress result at the most critical point was extracted and compared with the curve in the paper. Fig. 16a and Fig. 16b show the results of Model A and Model B, respectively.

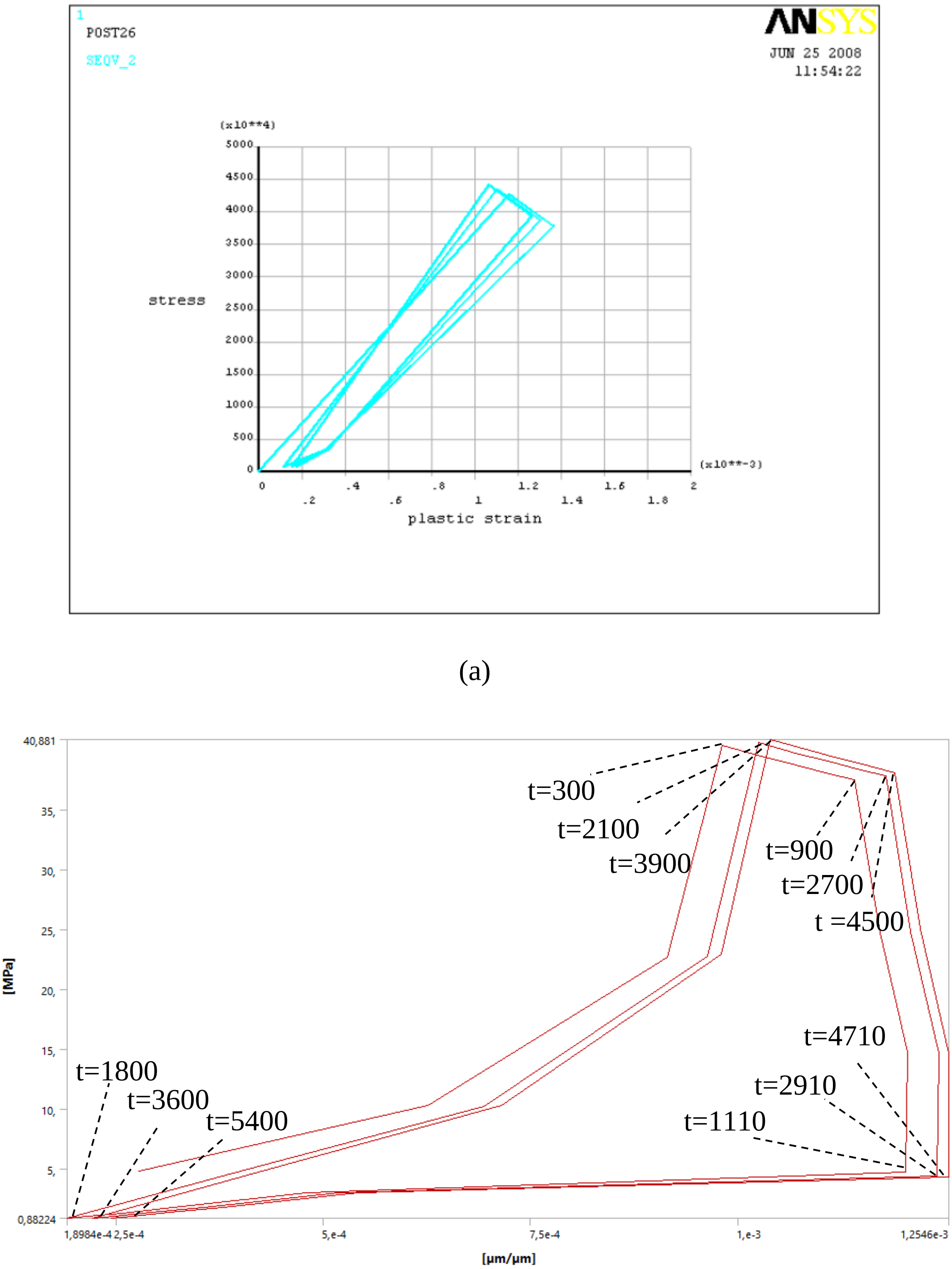

(a)

(b)

Figure 15. Equivalent stress vs equivalent strain hysteresis loop (63Sn37Pb); (a) Model A, (b) Model B

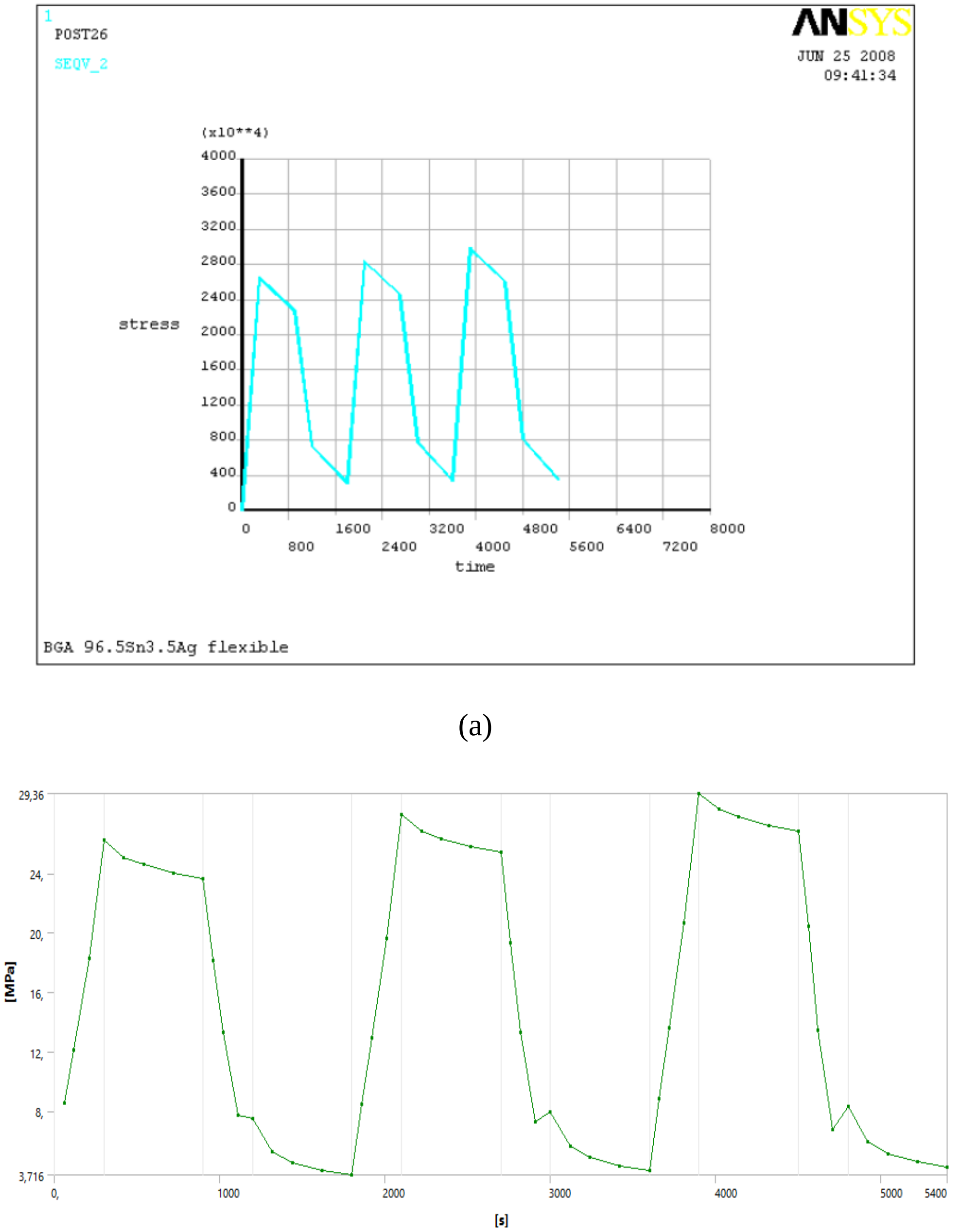

(a)

(b)

Figure 16. Equivalent stress at the critical point throughout the temperature cycles (96.5Sn3.5Ag); (a) Model A, (b) Model B

In Fig. 17, the time-dependent equivalent plastic strain result at the same critical point was extracted and compared with the curve in the article. Fig. 17a and Fig. 17b show the results of Model A and Model B, respectively.

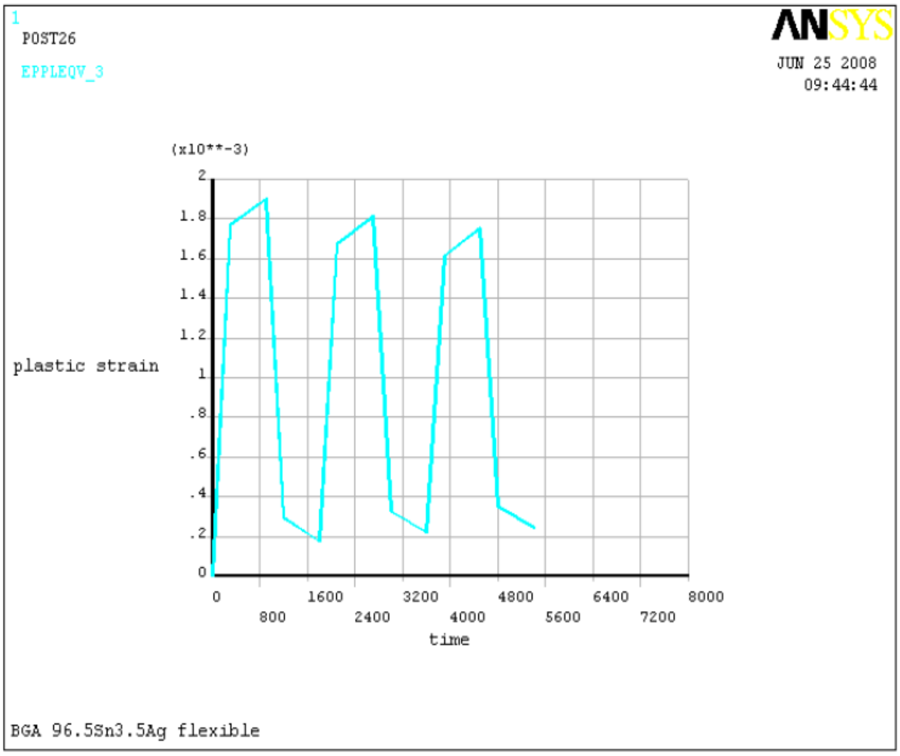

(a)

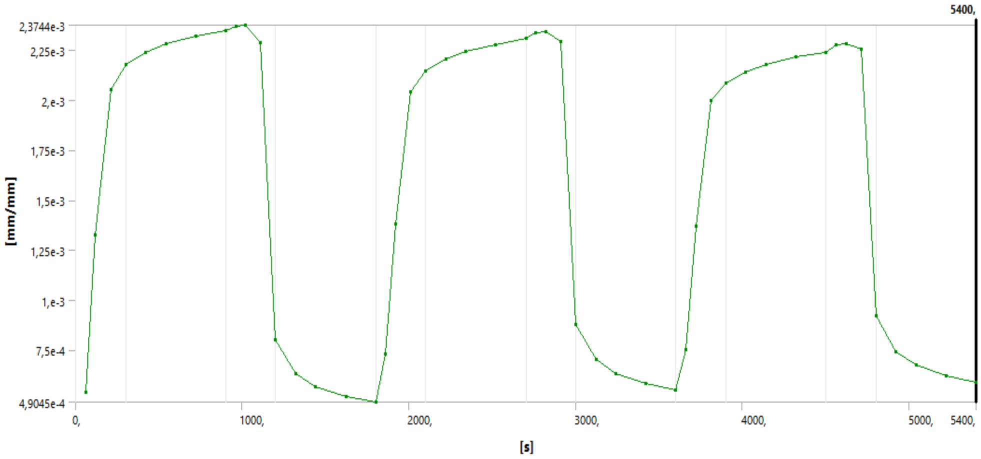

(b)

Figure 17. Equivalent strain at the critical point throughout the temperature cycles (96.5Sn3.5Ag); (a) Model A, (b) Model B

For material 96.5Sn3.5Ag after analyzing the results Fig. 16 and Fig. 17, it can be concluded that at low temperature dwell times, solder ball exhibits both creep and stress relaxation behavior. Stress is decreasing and plastic strain is increasing. However, for high temperature dwell times it only exhibits stress relaxation. Stress is decreasing and strain is also decreasing.

In Fig. 18, the stress-strain hysteresis loop at the same critical point was extracted and compared with the curve in the article. Fig. 18a and Fig. 18b show the results of Model A and Model B, respectively.

The hysteresis loops extracted for both material types were used to find the strain range values (Fig. 15b, 18b). These strain range values were then used in the ECM life prediction model (Eq. 2.4.1) as mentioned in the article. In the ECM equation the ϵ_f' value is taken the same as in the paper [21] (Table 7).

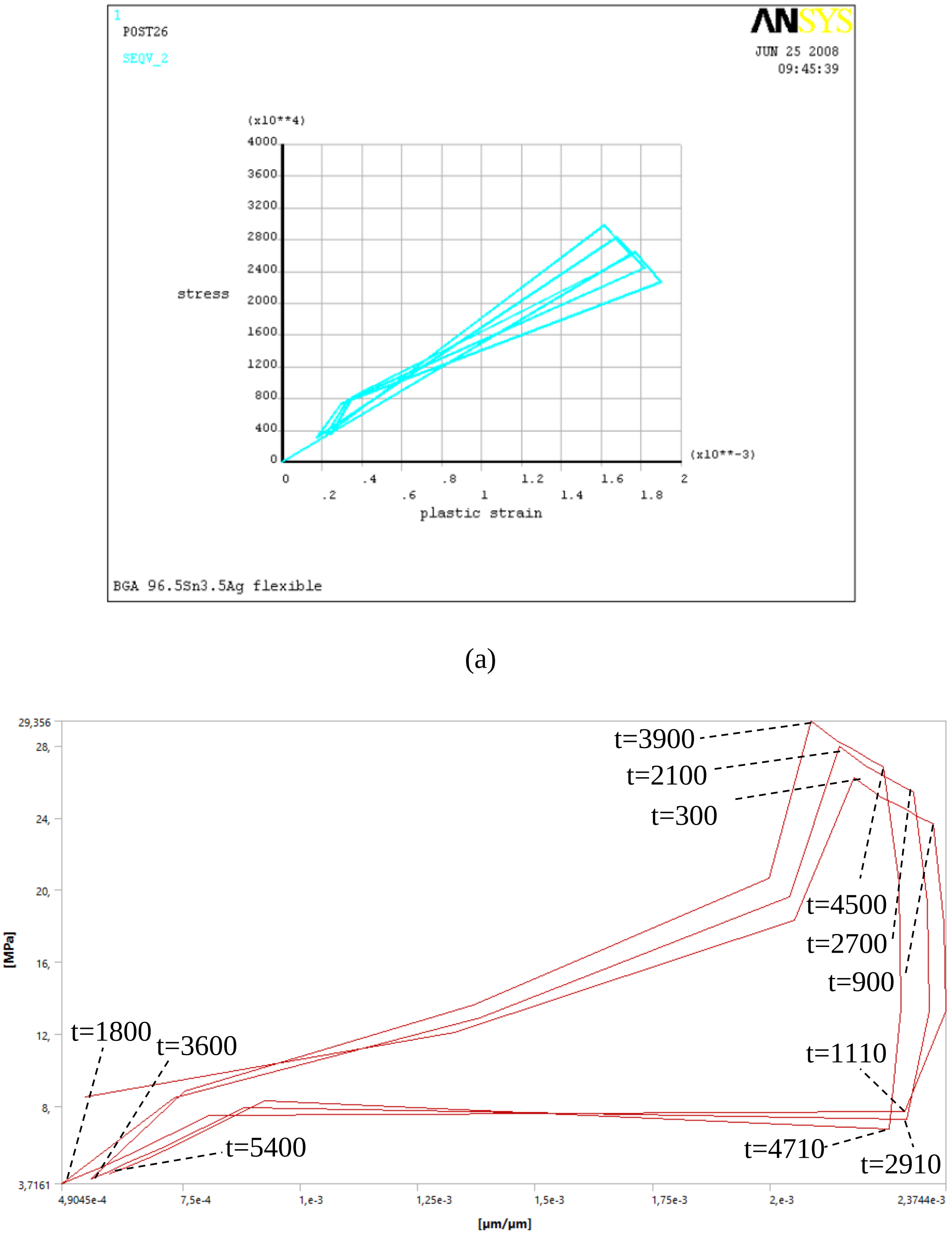

(a)

(b)

Figure 18. Equivalent stress vs equivalent strain hysteresis loop (96.5Sn3.5Ag); (a) Model A, (b) Model B

Table 7. Solder material type and associated fatigue ductility coefficient

Material Type	**Parameter ϵ_f'**
63Sn37Pb	0.323608
96.5Sn3.5Ag	0.323643

To find life cycles values of solder balls, Eq. 2.4.1 with Eq. 2.4.3 and material property ϵ_f' are used. For example, life calculation of critical solder ball with material 63Sn37Pb was made as follows. And the calculation for the other material was done in the same way.

Starting with Eq.2.4.3 to find value c.

$$c = -0.442 - 6 \times 10^{-4} T_m + 1.74 \times 10^{-2} \ln(1 + f) \qquad (2.4.3)$$

$$T_m = \frac{T_{max} + T_{min}}{2} \qquad (3.1.1)$$

$$T_m = \frac{125 - 55}{2} = 35 \qquad (3.1.2)$$

Where T_m is the average of the temperature profile extreme values and f is the frequency of the temperature profile, $f = 48\ (\frac{cycles}{day})$, thus $c = -0.395$.

And using equation $\Delta\gamma = \sqrt{3}\Delta\varepsilon$ to find plastic shear strain range to use in Eq.2.4.2.

$$\Delta\gamma = \sqrt{3}\Delta\varepsilon = \sqrt{3} * 1.01 * 10^{-3} = 1{,}75 * 10^{-3} \qquad (3.1.3)$$

And finally substituting all the generated and found values into Eq.2.4.1.

$$N_f = \frac{1}{2}\left(\frac{\Delta\gamma}{2\epsilon_f'}\right)^{\frac{1}{c}} = \frac{1}{2}\left(\frac{1.75*10^{-3}}{2*0.323608}\right)^{\frac{1}{-0.395}} = 1.58 * 10^{6}\ cycles \qquad (3.1.4)$$

The strain range and life values specified for both material types in [21] are given in Table 7. At the same time, the values obtained from calculations in the current model are also added to the table.

Table 8. Comparison of values between Model A and Model B

Simulation	Solder Material	**Strain Range ($\Delta\varepsilon$)**		**Life (Cycles)**		
		Model A	Model B	Model A	Model B	Difference (%)
1	63Sn37Pb	9.11E-04	1.01E-03	2.06E+06	1.58E+06	**23.3**
2	96.5Sn3.5Ag	1.53E-03	1.69E-03	5.50E+05	4.32E+05	**21.5**

From the results, it seems that the lifetimes for different solder ball materials are not very different from each other. For example, in simulations using 96.5Sn3.5Ag material, the life difference between our calculation and the one in the paper is 21.5%. Potential reasons for these differences are listed below:

- Planar dimensions of FPC component are not given, they are guessed,
- Thickness values of the components are not given, they are guessed,
- Mesh model quality and solver settings may be different, solver settings of Model A are not known.

As a result of this validation study, FE modeling and simulation capabilities were thought to be confirmed and further studies could be confidently undertaken.

In addition, when the hysteresis loop is examined after the solution was made with the Model B, it is seen that those result curves are similar to the results in a study in the literature [18] (Fig.19). With this referenced study [18], it is accepted that the curves similar to the hysteresis loop in the [21] did not appear, but the strain range values were close. Those shape differences were possibly taking place due to the three reasons mentioned above.

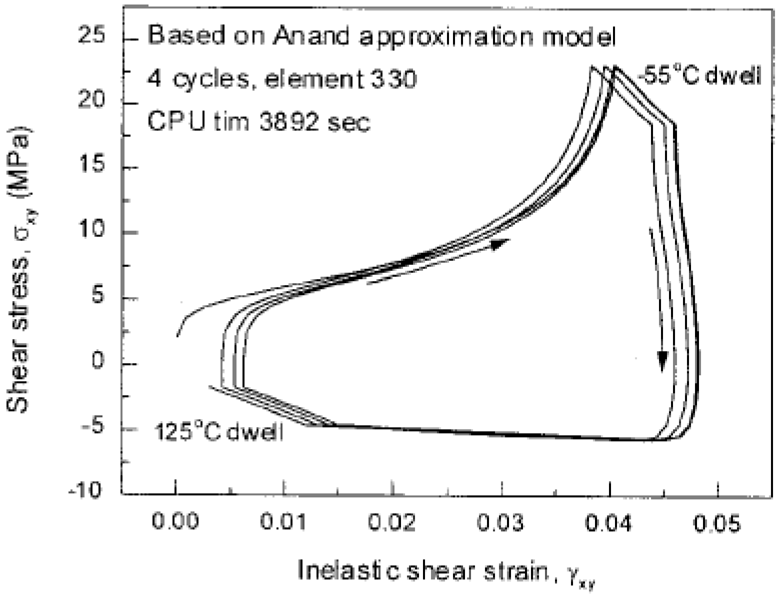

Figure 19. Stress vs strain hysteresis loop result using Anand viscoplastic model in [18].

CHAPTER 4

FINITE ELEMENT SIMULATION AND OPTIMIZATION WITH AV MATERIAL MODEL

After the completion of benchmark study and no major problems were observed in comparison between results of Model A and Model B, similar type of simulation and optimization study of the structure under consideration have been carried out by using AV material model.

The structure studied is an electronic package with 144 connection BGA (12x12). The CAD image of the related structure is shown in Fig. 20. Fig. 21a shows a cross-sectional view of the structure with the vertical plane passing through the center of one row of solder balls, Fig. 21b shows a close-up cross-sectional view of the solder ball and UBM components. The names of the components are indicated with arrows in Fig. 20 and Fig. 21b. The CAD of the structure was made in PTC Creo 9.0 program.

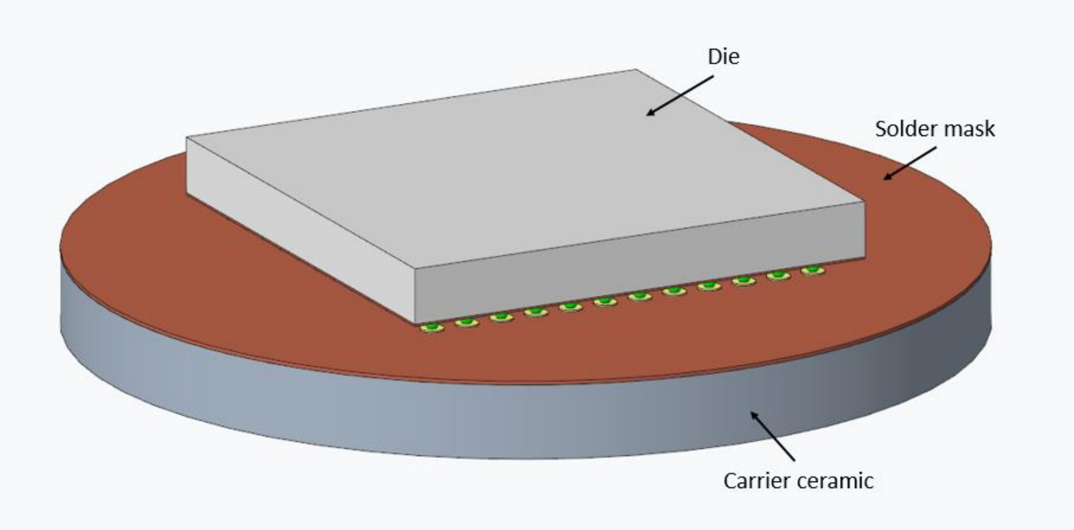

Figure 20. CAD image of electronic package with 144 connection BGA with names of components indicated.

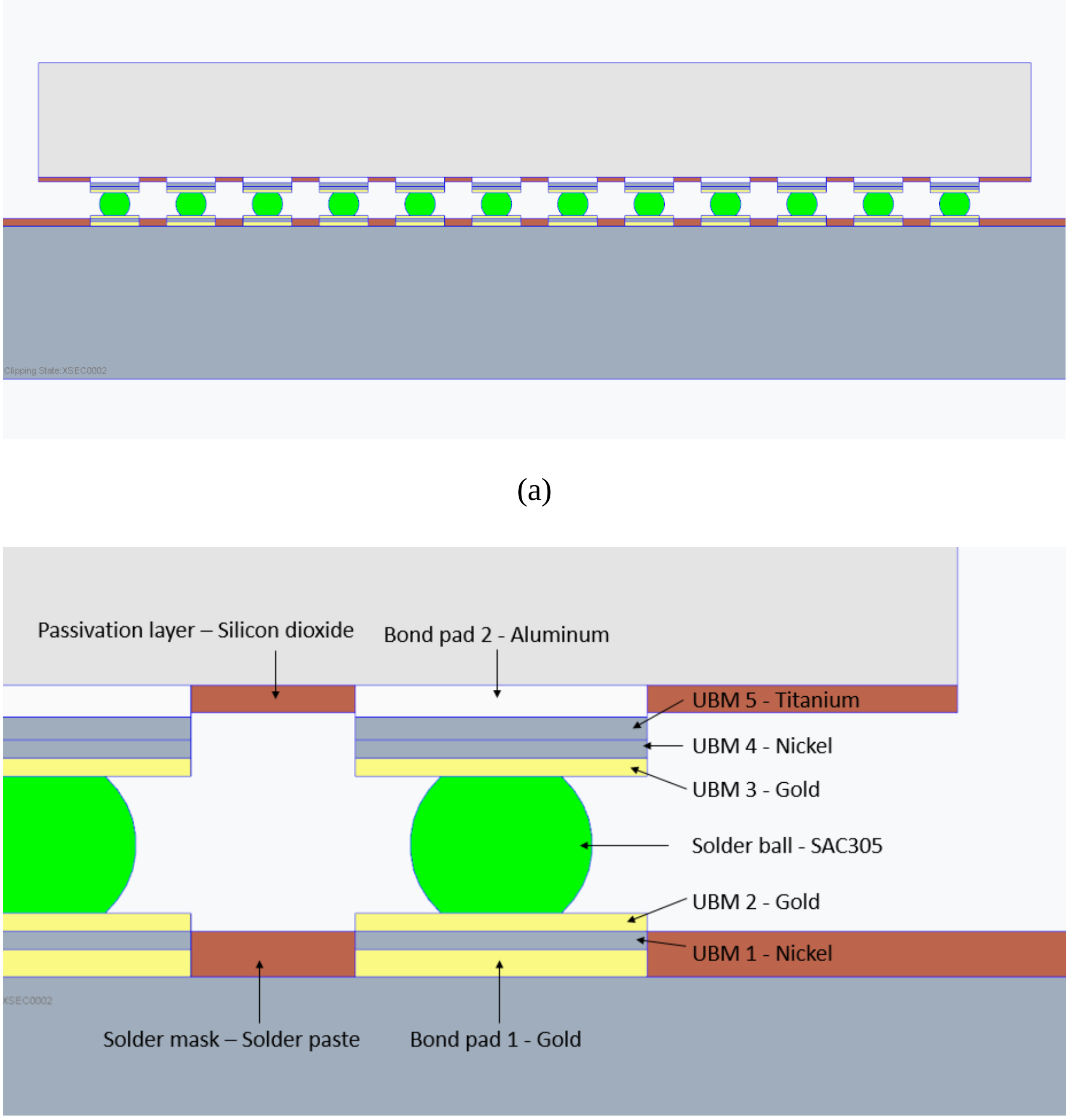

(a)

(b)

Figure 21. (a) Cross-sectional view of structure under consideration, (b) close-up cross-sectional view of solder ball and UBM with names of components indicated

The name and associated material of the components that make up the structure are shown in Table 9.

Table 9. Names of the components in the interested structure and their associated materials

Component Name	**Material**
Carrier ceramic	Alumina (Al_2O_3)
Bond pad 1	Gold
UBM 1	Nickel
UBM 2	Gold
Solder mask	Solder paste
Solder ball	SAC305
UBM 3	Gold
UBM 4	Nickel
UBM 5	Titanium
Bond pad 2	Aluminum
Passivation layer	Silicon dioxide
Die	Silicon

Firstly, AV material model was used for solder balls during the simulations. The other components were found to demonstrate linear elastic behavior by pre-analysis and only linear elastic material properties were defined for these components. The linear elastic and CTE properties of the materials are given in Table 10 and the AV material properties of SAC305 are given in Table 11.

Table 10. Elastic and thermophysical properties of used materials

Material	**Elastic Modulus (GPa)**	**Poisson's Ratio**	**Coefficient of Thermal Expansion (ppm/°C)**
Alumina [17]	310	0.27	5.5
Gold [38]	80	0.3	14
Nickel [39]	207	0.31	13.1
Solder paste [27]	3.1	0.3	16.3
SAC305 [12]	51	0.4	23.5

Table 10 (continued). Elastic and thermophysical properties of used materials

Material	**Elastic Modulus (GPa)**	**Poisson's Ratio**	**Coefficient of Thermal Expansion (ppm/°C)**
Titanium [39]	116	0.34	8.9
Aluminum [39]	68	0.36	24
Silicon dioxide [40]	70	0.16	6
Silicon [12]	110	0.24	2.6

Table 11. AV material model properties of SAC305 material

Anand Parameters	**SAC305 [12]**
s_0 (MPa)	45.9
Q/R (K)	7460
A (1/s)	5.86E06
ξ	2
m	0.0942
h_0 (MPa)	9350
$\hat{s}$ (MPa)	58.3
n	0.015
a	1.5

Within the scope of this thesis, an optimization study was carried out according to the input parameters

- Solder ball diameter and height
- UBM thicknesses
- Bond pad thicknesses

and the design configuration with the highest lifetime was tried to be found. As it is known from the Eq. 2.4.1, lower strain range means higher lifetimes.

Dimension values of the components which are used in original electronic package are shown in Table 12 and 13. In Table 12, dimensions whose values will remain constant during optimization are shown. And in Table 13, dimensions whose values will be optimized are shown.

Table 12. Dimensions of the components whose values will remain constant during optimizations.

Component	**Dimensions (mm)**
Carrier ceramic	R6x1
Solder paste	R6x1
Solder ball pitch	0.5
Passivation layer	6.5x6.5x0.03
Die	6.5x6.5x0.03

Table 13. Original dimensions of the components whose values will be optimized

Dimension	**Value (µm)**
Bond pad 1 thickness	12.5
UBM 1 thickness	12.5
UBM 2 thickness	4
Solder ball radius	130
Solder ball height	140
UBM 3 thickness	4
UBM 4 thickness	12.5
UBM 5 thickness	10
Bond pad 2 thickness	17.5

A global-local FE model approach was applied in the optimization study. In the global model, the mesh quality metrics appears to be low due to the small sizes of the UBM parts and bond pads compared to the other components and their high diameter-to-thickness ratios. When it is desired to increase the mesh quality for these parts, the total number of elements increases very much. This causes longer solution times and makes the optimization study inefficient. For this reason, it was decided that the optimization study could not be done with the global model, and it was decided to create a local model using the results from the global model.

4.1 Global Model Simulation

Before proceeding to the local model, the solution was obtained in the global model. The original structure was converted into a quarter model (Fig. 22) and then the mesh model was generated for numerical calculations (Fig. 23). Meshing is done with conformal mesh type for global and local models, thus contact application was not needed. The total number of elements becomes 329395. Table 14 shows the mesh element types used in the global model.

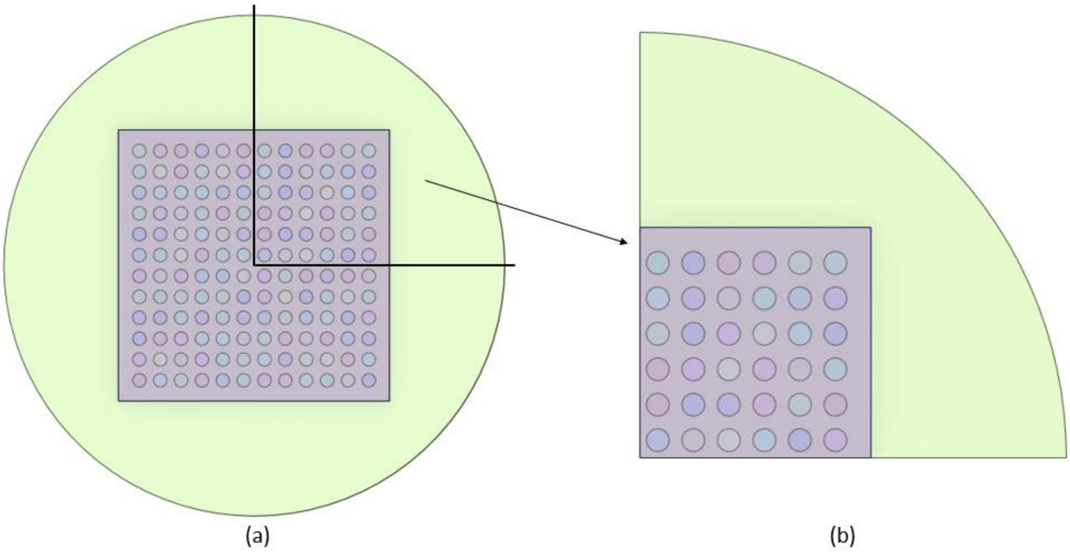

Figure 22. Converting original structure to quarter model to form global model (Die is transparent to show to solder balls), (a) original model (b) quarter model

Table 14. Element types used in the global model.

Element Type	**Applied Components**
SOLID186	UBM1-5, bond pad 1-2, solder ball, solder mask, passivation layer
SOLID187	Carrier ceramic, die

In simulation setup:

- MIL-STD-883 standard [41] was selected as the applied temperature profile (Fig. 11).
- Temperature profile are applied for all the bodies which means all the nodes in the global model has the same temperature value at the same time step.
- Symmetry surfaces are bounded with "frictionless support" boundary condition that allows them to move only in those surface planes (Fig. 24).
- In order to reduce the degree of freedom of the model in space, the lower intersection point of the symmetry surfaces is fixed with "fix support" boundary condition to fix that point in space (Fig. 24).
- The material properties of the components have been defined in accordance with the values in Tables 10 and 11.

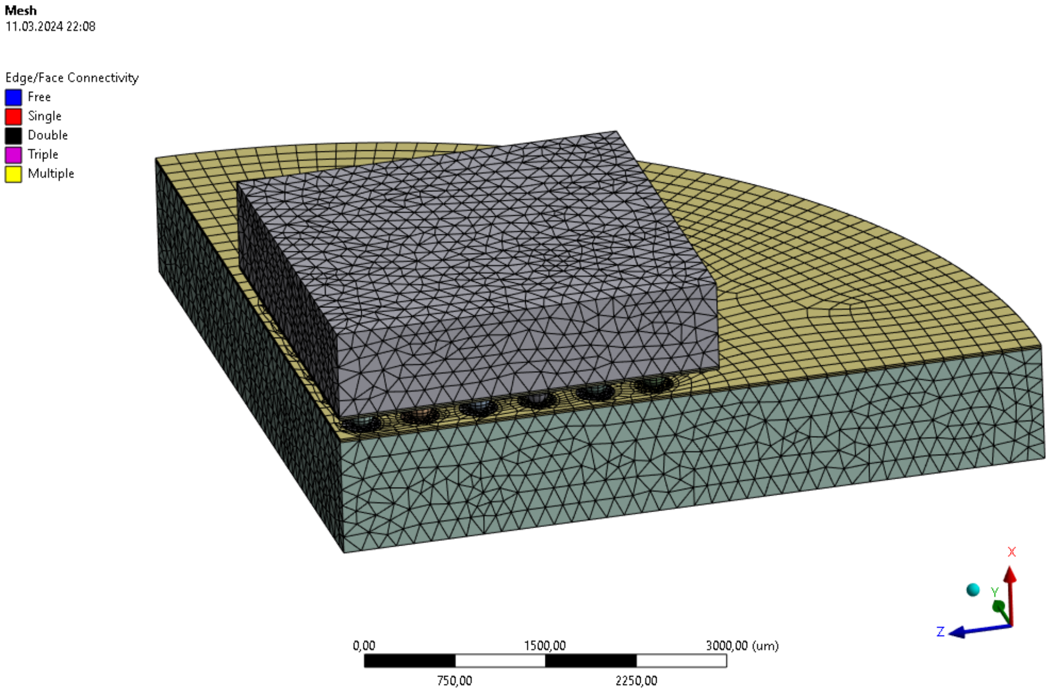

Figure 23. Mesh structure of the global model

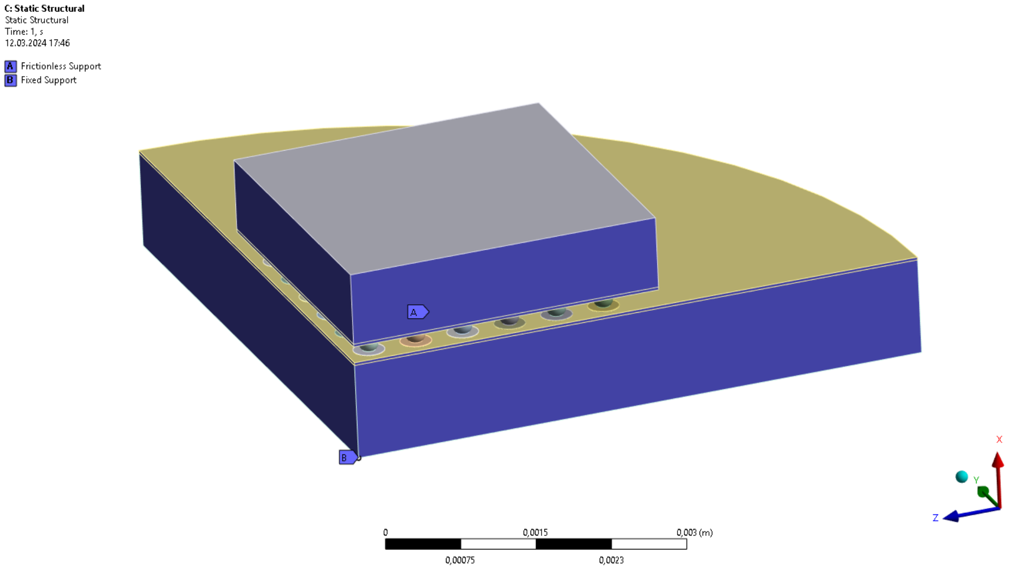

Figure 24. Boundary conditions of the global model

The global model was solved with the aforementioned setup. According to the result, the highest plastic strain values were found in the solder ball furthest from the center

(Fig. 25) through the temperature cycles. That is possibly because of the high displacement difference between upper and lower interfaces of the solder bump. Because at the location of the critical solder ball displacement difference between Die and Ceramic bodies are maximized due to different CTE's bodies have.

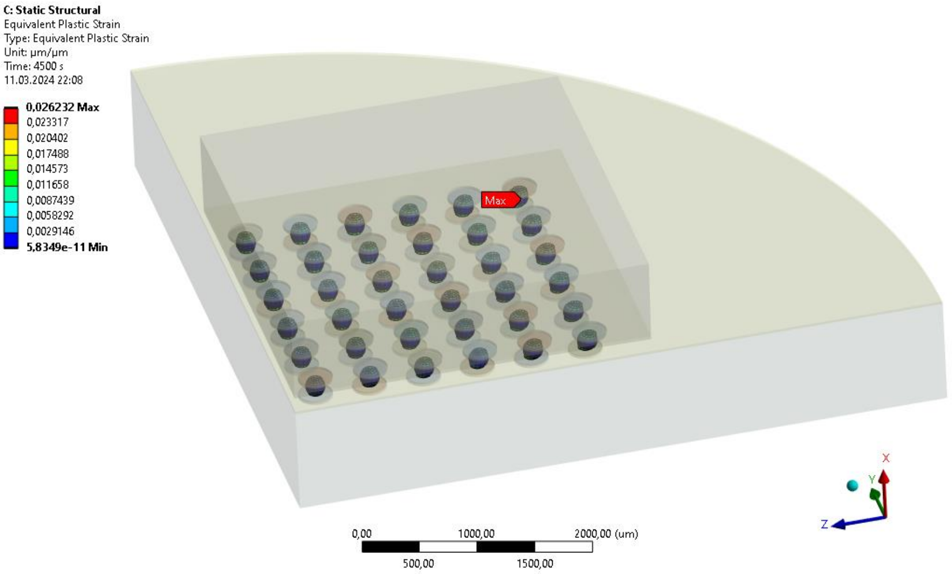

Figure 25. Critical solder ball in the global model during the temperature cycles

4.2 Local Model Preparation

After finding the most critical solder ball in the global model, a local model of this critical ball was created. When creating the local model, the cutting surfaces were chosen to be 0.25 mm away from the center of the critical solder ball [27]. This value is half of the pitch value of 0.5 mm. Fig. 26a and Fig. 26b shows the location of the cutting surfaces in the top view of global model and the generated local model of critical solder ball, respectively.

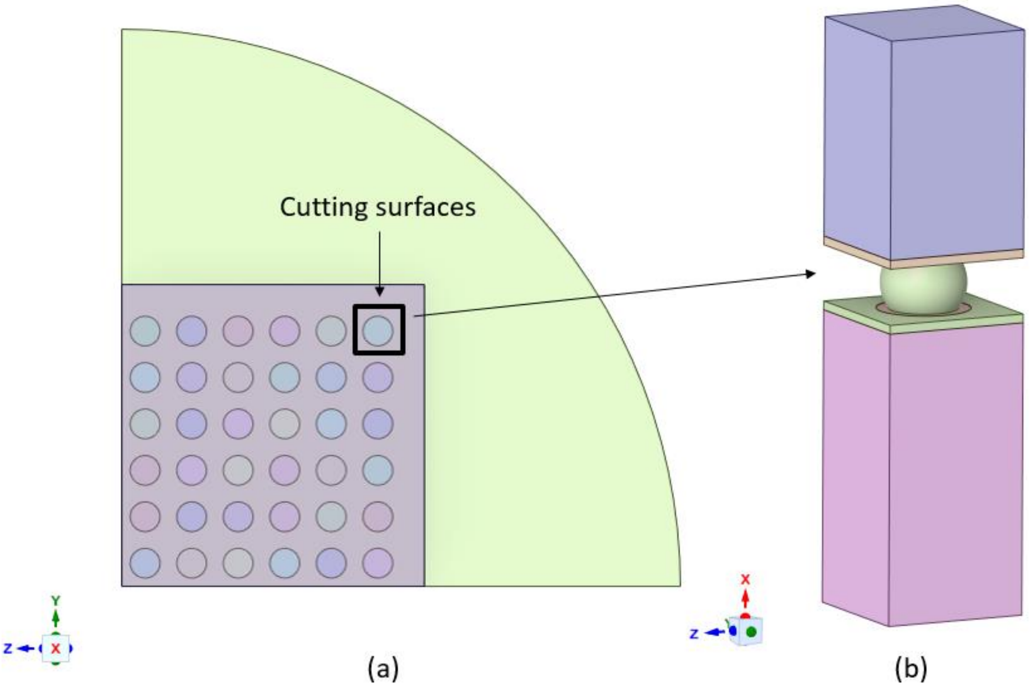

Figure 26. (a) Locations of cutting surfaces in the top view of global model (Die is transparent to show solder balls), (b) local model in isometric view

The displacement results in the global model are mapped to the cutting surfaces of the local model as boundary conditions. Therefore, no additional boundary condition is needed to be defined in the local model.

Also, the temperature load condition (Fig. 11) are defined to be consistent with the mapped displacement boundary conditions. For example, mapped displacement and temperature data at 5400 seconds of the local model are shown in Fig. 27a and Fig. 27b, respectively. In other words, for each second of the local model simulation, consistent boundary and load condition are applied which are originally applied in the global model.

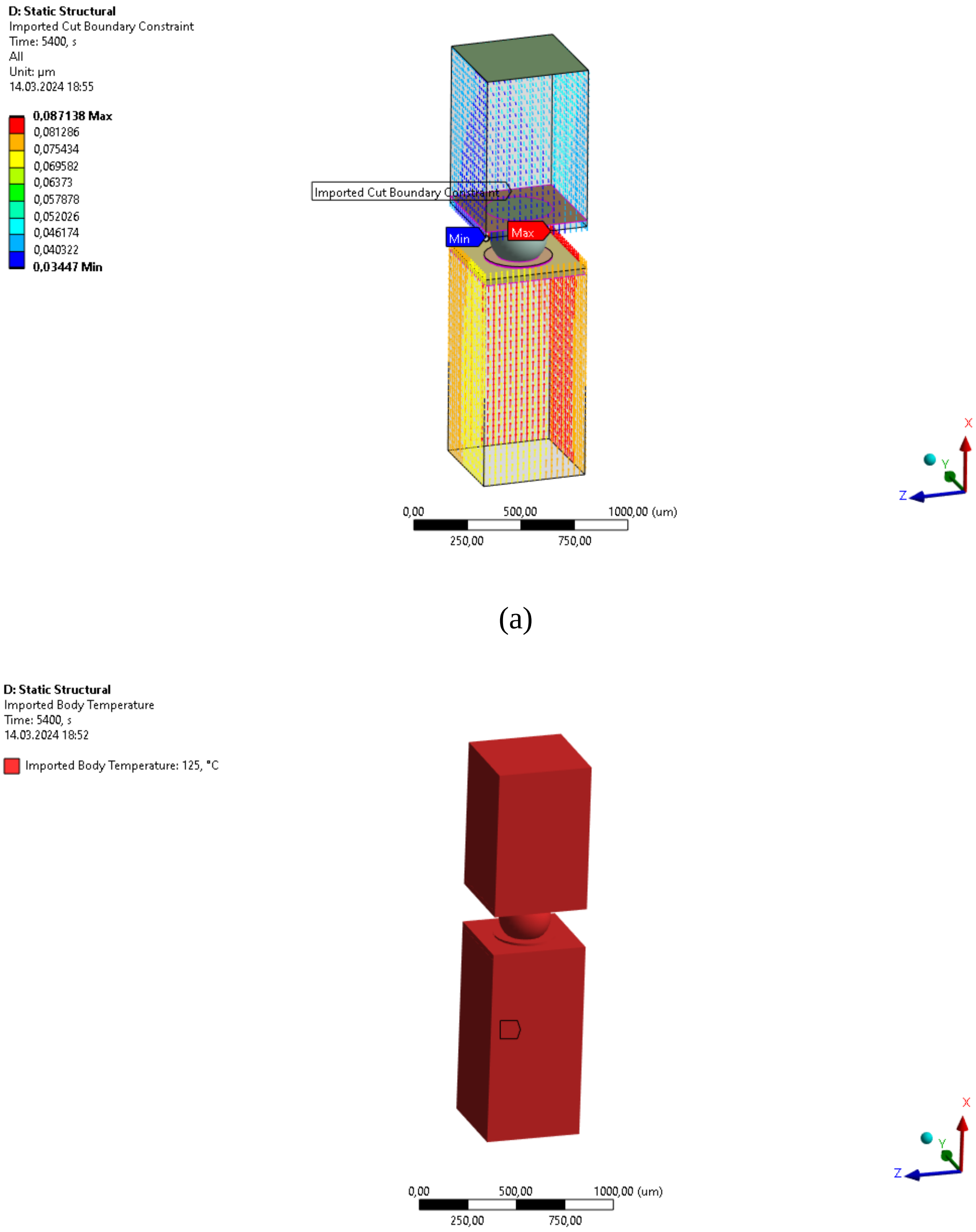

(a)

(b)

Figure 27. At 5400 seconds of the simulation, defined (a) displacement boundary condition and (b) temperature load condition

4.2.1 Mesh Dependency

Before proceeding to the optimization study, a mesh dependency study was performed in the local model. The maximum strain range value observed in the solder ball in the third cycle was taken as the control output [7,17,20,21].

In this study, it is aimed to avoid not only inaccurate results due to low element numbers but long computation times with unnecessarily high element numbers during optimization as well. Fig. 28 shows the variation of strain range value and solution time in seconds according to the total number of elements in the mesh.

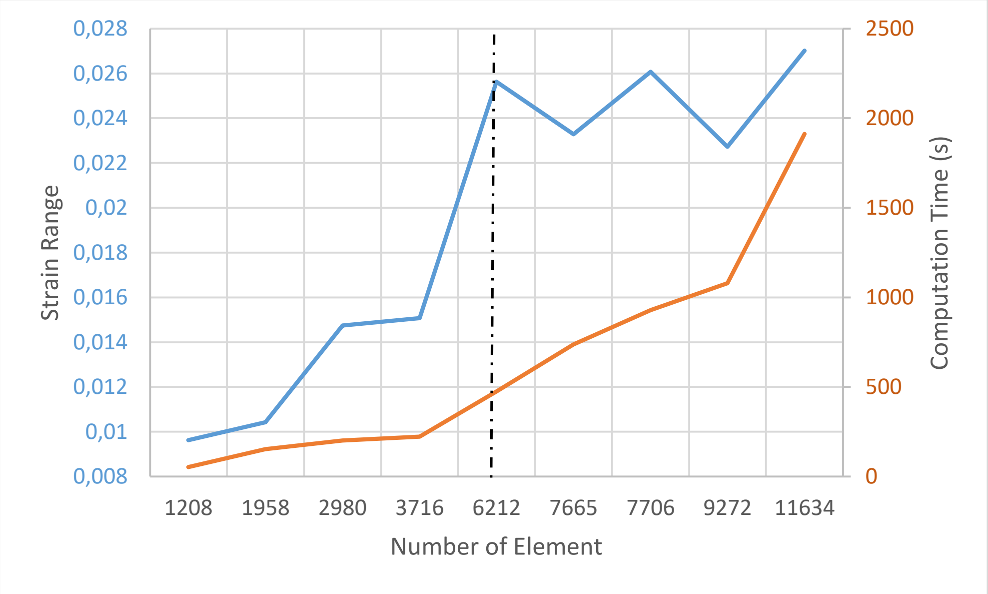

Figure 28. Variation of strain range and computation time values with respect to total number of elements of the local model mesh

When the graphs are examined, the strain range value increases with the number of elements in the model, but there is no significant increase after a certain value. This value corresponds to approximately 6200 elements. On the other hand, the solution time increases significantly with the number of elements and there seems exponential relationship between them.

In the light of this information, the elements in the local model was chosen as 6212. Thus, the optimum point was found by considering the strain range value and solution time. SOLID186 element type is used and in Fig. 29a and Fig. 29b mesh structure of the local model with 6212 elements can be seen.

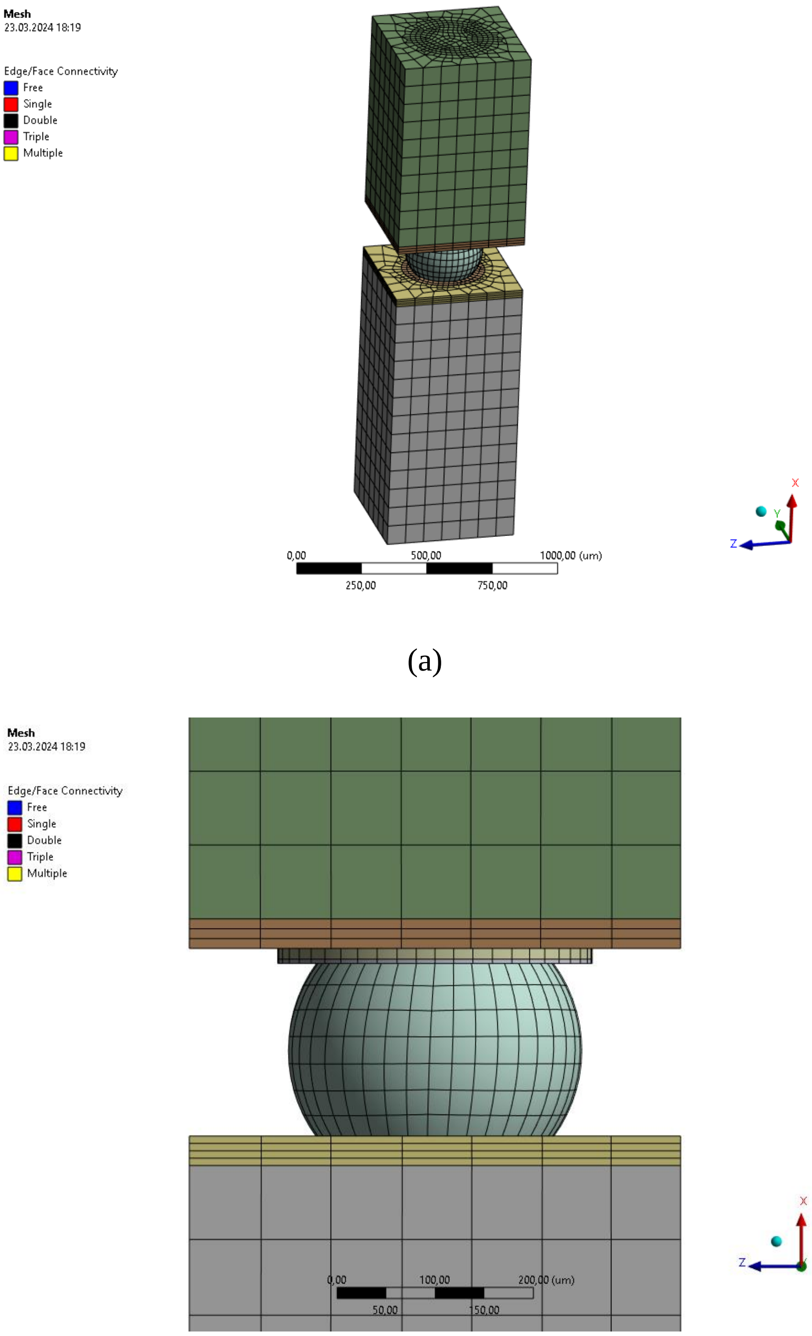

(a)

(b)

Figure 29. Mesh structure of the local model, (a) in isometric view, (b) in close-up view

4.3 Design of Experiment

Design of Experiment with Response Surface approach was used in the optimization study. In Fig. 30, visual summary of response surface optimization sequence in ANSYS can be seen. Also, ANSYS WB project schematic of the applied study can be seen in Appendix A.

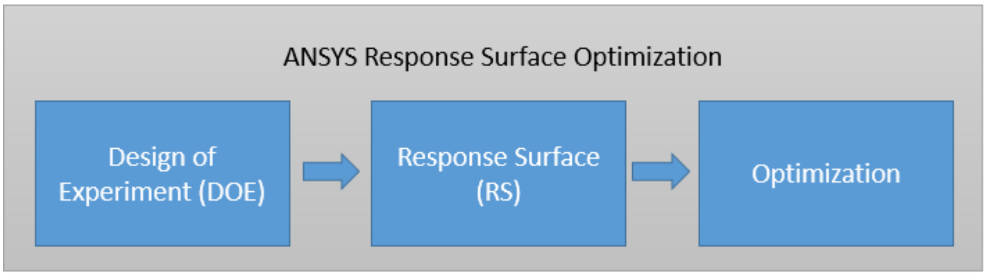

Figure 30. Workflow of response surface optimization study in ANSYS

DOE method is a tool used to define the relationship between design variables (input variable) and objectives (output variable) in processes or simulations where there is more than one design variable. With the DOE method, the design space is effectively scanned, and a statistical model can be established between design variables and objectives.

The DOE method is useful in situations where limited simulations or tests can be performed. The main idea is to minimize the number of points in the design space where solutions and results are obtained and generating a statistical model with low uncertainty. Then this model can be used to generate results at different design points.

The DOE method is embedded in the ANSYS Workbench program. Design points were generated using the ANSYS WB DOE tool. When generating design points, the value ranges of each design variable must be supplied. The definition and value ranges of the input parameters are listed in Table 15.

Table 15. Dimension ranges of parameters used in DOE/optimization study

Parameter Name	**Definition**	**Range (µm)**
P1	Bond pad 1 thickness	10-15
P2	UBM 1 thickness	10-15
P3	UBM 2 thickness	3-5
P4	Solder ball radius	110-150
P5	Solder ball height	100-180
P6	UBM 3 thickness	3-5
P7	UBM 4 thickness	10-15
P8	UBM 5 thickness	5-15
P9	Bond pad 2 thickness	10-25

Another setting to be determined is how the design points will be distributed in the design space. For this, the Optimal Space Filling option was selected with 147 design points. OSF with central composite design creates 160 design points as a raw data however 13 points are the same design points in the design space. In real, physical experiments these points are necessary to account for experimental errors and uncertainties. In simulations however, since corresponding simulations would give the same result these points are not necessary. Thus these 13 points eliminated and rest is processed. The generated and solved design points can be seen in Appendix B. Also, as a design type ANSYS use Face-centered option and with that Alfa value becomes 1.

The OSF option enables the design points in the design space to be placed equally distant from each other. For example, Fig. 31 shows the distribution of design points in a design space with two parameters (P1 & P2). In this way, the design space is scanned in general and the probability of not capturing global maximum and minimum objective values is reduced. Another advantage of this method is that the same parameter value only occurs in one design point. Two different design points do not share the same parameter value.

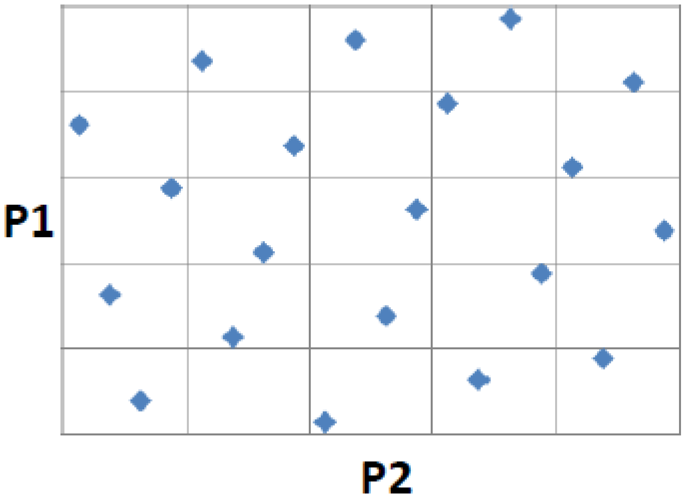

Figure 31. Two parameter design point distribution in design space with OSF method. Points are placed equally distant from each other [42]

4.4 Response Surface

After the results of design points were found by DOE, an RS was generated using these points. RS can basically be considered as a tool that covers the design space and construct a mathematical continuous model between design variables and objectives.

ANSYS Workbench includes a built-in RS generating tool. Non-parametric regression option was selected as the RS type to be created. This method creates a band with an error value of ±ε that contains the design points and generates the RS in the center of this band. Fig. 32 shows an example of the RS (redline) generated by the NPR method.

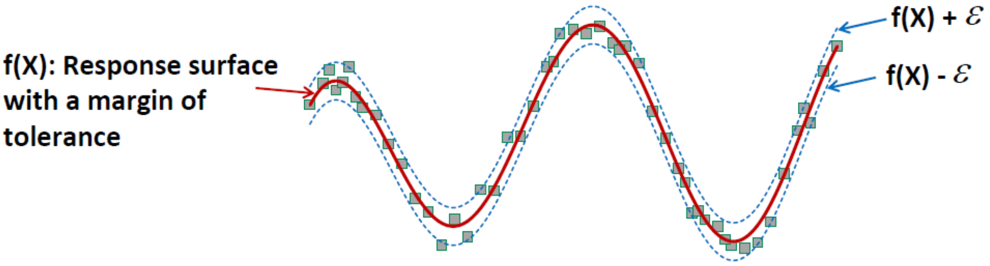

Figure 32. Generic figure to show how RS is generated with using NPR method [43]

The generated RS does not need to pass through each design point. For this reason, the generated RS should be checked for statistical accuracy. The goodness of fit values of the generated RS are shown in Fig. 33.

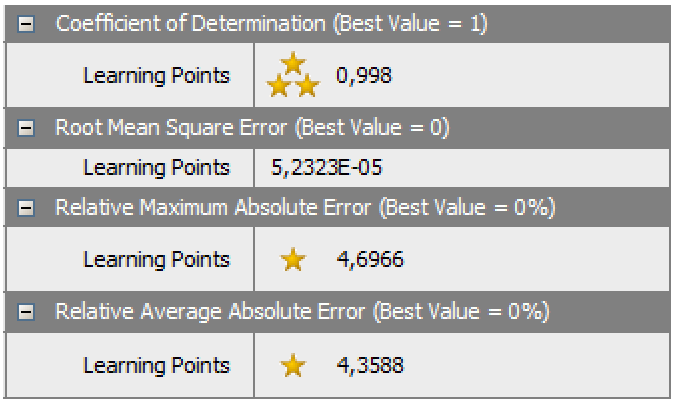

⊟ Coefficient of Determination (Best Value = 1)	
Learning Points	★★★ 0,998
⊟ Root Mean Square Error (Best Value = 0)	
Learning Points	5,2323E-05
⊟ Relative Maximum Absolute Error (Best Value = 0%)	
Learning Points	★ 4,6966
⊟ Relative Average Absolute Error (Best Value = 0%)	
Learning Points	★ 4,3588

Figure 33. Goodness of fit values of generated RS

When the metrics are analyzed, the following conclusions are obtained:

- Coefficient of determination value is close to 1 (Best value = 1).
- Root mean square error value is close to 0 (Best value = 0).
- Relative maximum absolute error value is close to 0 (Best value = 0).
- Relative average absolute error value is close to 0 (Best value = 0).

In addition, the real result values of the design points (see Appendix A) were compared with the result values obtained from RS using the same input parameters. Fig 34 shows the scatter plot generated by the comparison. The black solid curve with a slope value of 1 shows the ideal situation where the real solution value and the value found from RS are equal at each point. There seems distribution of green points is close to the ideal line.

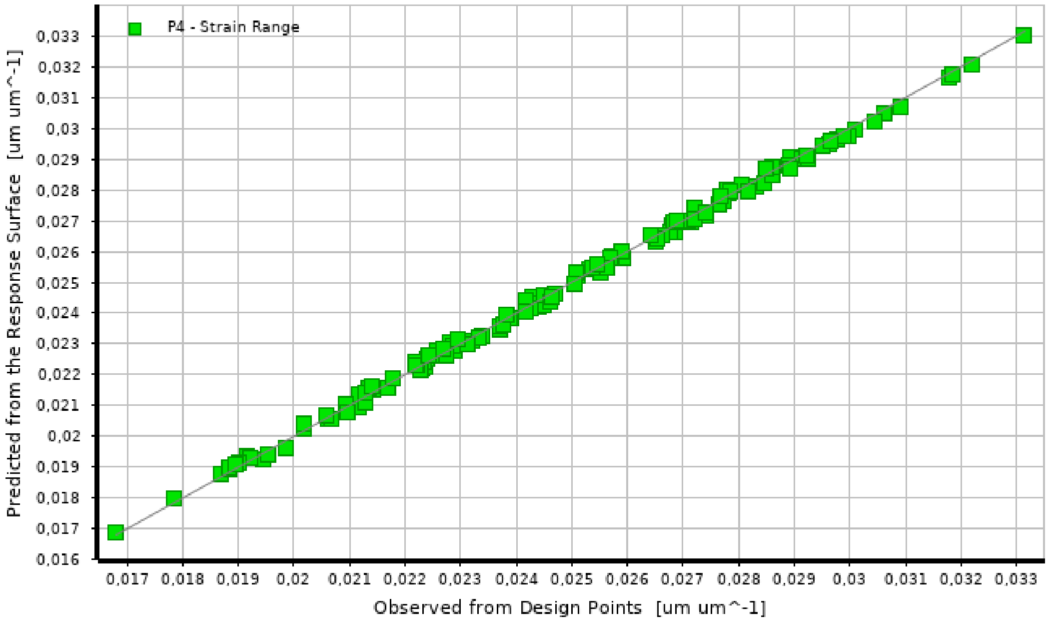

Figure 34. Distribution of the design points in the graph whose x axis shows the real solution values for the plastic strain range and y axis shows the values found from RS.

Another result that can be drawn is how much the change in each parameter affects the strain range output. Fig. 35 shows the sensitivity ratios of the parameters in the form of a pie chart. When the chart is analyzed, it is seen that the strain range output is most sensitive to solder ball height (P5).

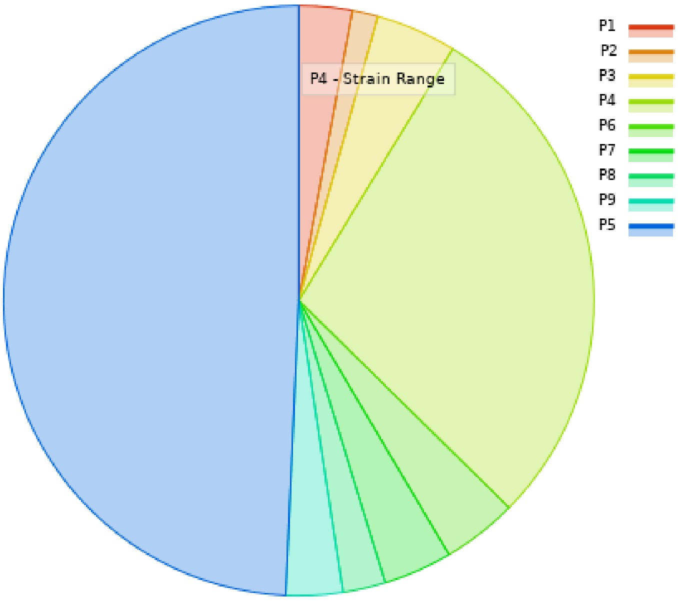

Figure 35. Pie chart that shows the sensitivity of the input parameters to strain range

After the statistical evaluation and having confidence in the generated RS the optimization part was started.

4.5 Optimization

The optimization tool is embedded in ANSYS WB. Multi-Objective Genetic Algorithm (MOGA) is chosen as the algorithm type. This method goes through many iterations trying to find the best result. In each iteration, it finds the best results and uses these results with the best ones from the previous iteration to determine where to go in the next iteration. In this way, it tries to achieve the best result repeatedly. This algorithm avoids focusing on local minimum and maximum, thus increases the chances of finding global minimum and maximum [44].

Also, to ensure the convenient manufacturability of the best configuration to be found, certain interval sizes are defined for parameter values in optimization. In Table 16 interval sizes can be seen for parameters. In other words, parameter values change with these defined values between optimization calculations.

Table 16. Specified interval sizes for parameter values changes accordingly between optimization calculations

Parameter Name	**Interval Size (µm)**
P1-3, P6-9	0.01
P4-5	0.1

After 20 iterations and 28413 evaluations, the geometric configuration with the lowest strain range value was obtained as a result of optimization. In Fig. 36, the relevant configuration appears as “Candidate Point 1”. According to the calculation, the resulting strain range value is 0.01516. In order to check the accuracy of the result, the analysis was run again at the relevant parameter values and the strain range value was found 0.016387. The difference between them is 7.7%. This difference was considered acceptable, and it was decided that the best configuration, considering the lowest strain range, was found.

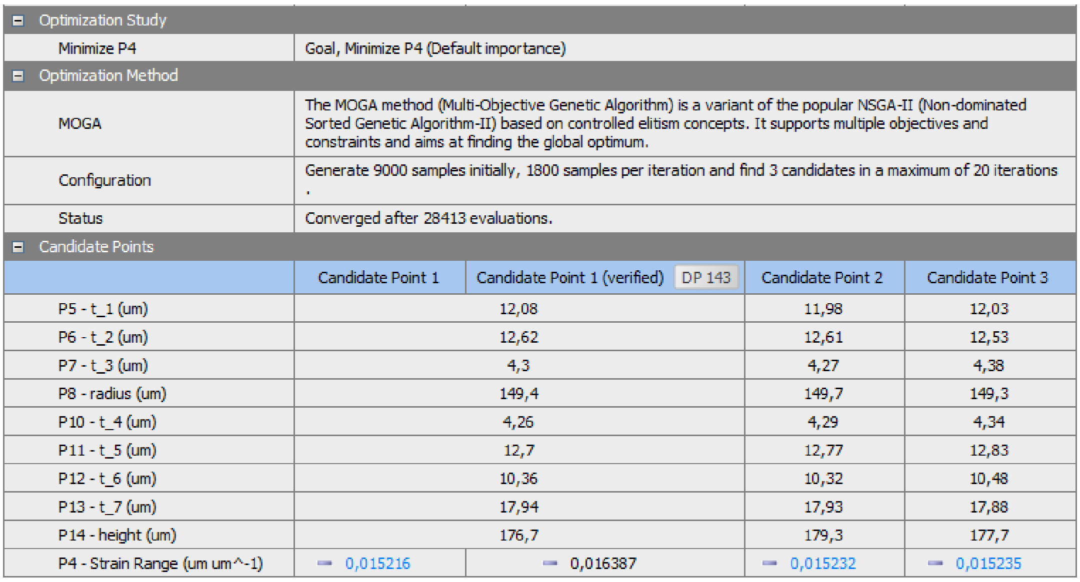

Optimization Study	
Minimize P4	Goal, Minimize P4 (Default importance)
Optimization Method	
MOGA	The MOGA method (Multi-Objective Genetic Algorithm) is a variant of the popular NSGA-II (Non-dominated Sorted Genetic Algorithm-II) based on controlled elitism concepts. It supports multiple objectives and constraints and aims at finding the global optimum.
Configuration	Generate 9000 samples initially, 1800 samples per iteration and find 3 candidates in a maximum of 20 iterations .
Status	Converged after 28413 evaluations.

Candidate Points

	Candidate Point 1	Candidate Point 1 (verified) DP 143	Candidate Point 2	Candidate Point 3
P5 - t_1 (um)	12,08		11,98	12,03
P6 - t_2 (um)	12,62		12,61	12,53
P7 - t_3 (um)	4,3		4,27	4,38
P8 - radius (um)	149,4		149,7	149,3
P10 - t_4 (um)	4,26		4,29	4,34
P11 - t_5 (um)	12,7		12,77	12,83
P12 - t_6 (um)	10,36		10,32	10,48
P13 - t_7 (um)	17,94		17,93	17,88
P14 - height (um)	176,7		179,3	177,7
P4 - Strain Range (um um^-1)	0,015216	0,016387	0,015232	0,015235

Figure 36. ANSYS optimization result showing the best geometric configuration with name “Candidate Point 1”

The values of the parameters in the best configuration are shown in Table 17.

Table 17. Parameter values of the best configuration

Parameter Name	**Definition**	**Value (µm)**
P1	Bond pad 1 thickness	12.08
P2	UBM 1 thickness	12.62
P3	UBM 2 thickness	4.3
P4	Solder ball radius	149.4
P5	Solder ball height	4.26
P6	UBM 3 thickness	12.7
P7	UBM 4 thickness	10.36
P8	UBM 5 thickness	17.94
P9	Bond pad 2 thickness	176.7

Fig. 37 shows the change of strain range values during iterations.

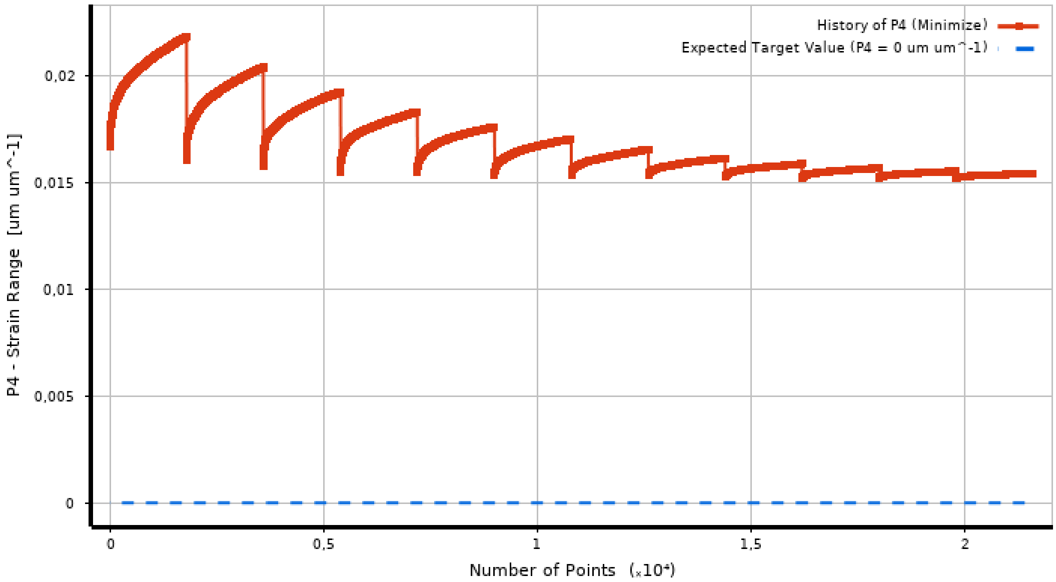

Figure 37. Change of strain range value during the optimization iterations

In addition, the change of each parameter value over the iterations is shown in Fig. 38a-i.

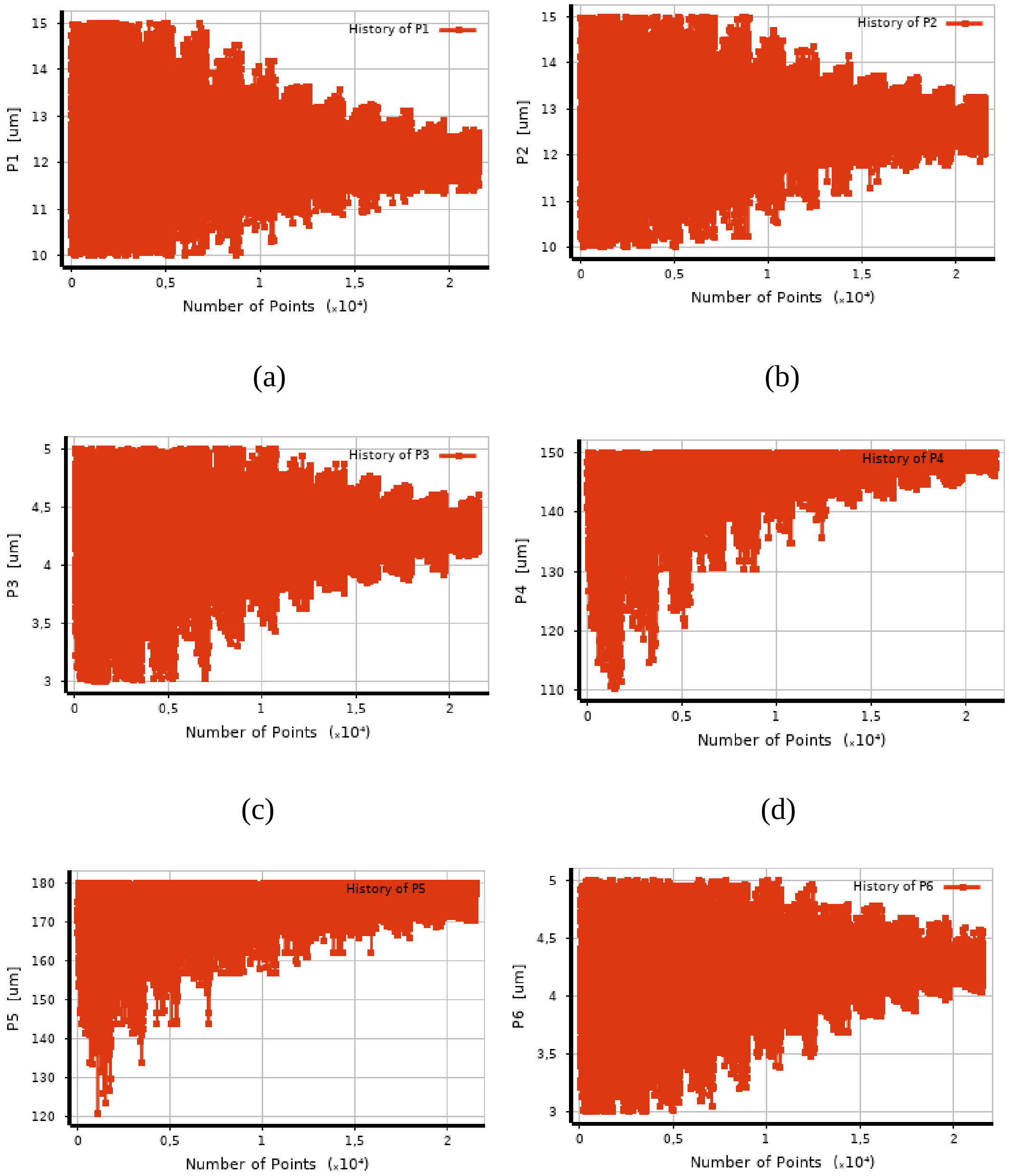

(a)

(b)

(c)

(d)

(e)

(f)

Figure 38. Change of each parameter value over the optimization iterations; (a) P1, (b) P2, (c) P3, (d) P4, (e) P5, (f) P6, (g) P7, (h) P8, (i) P9

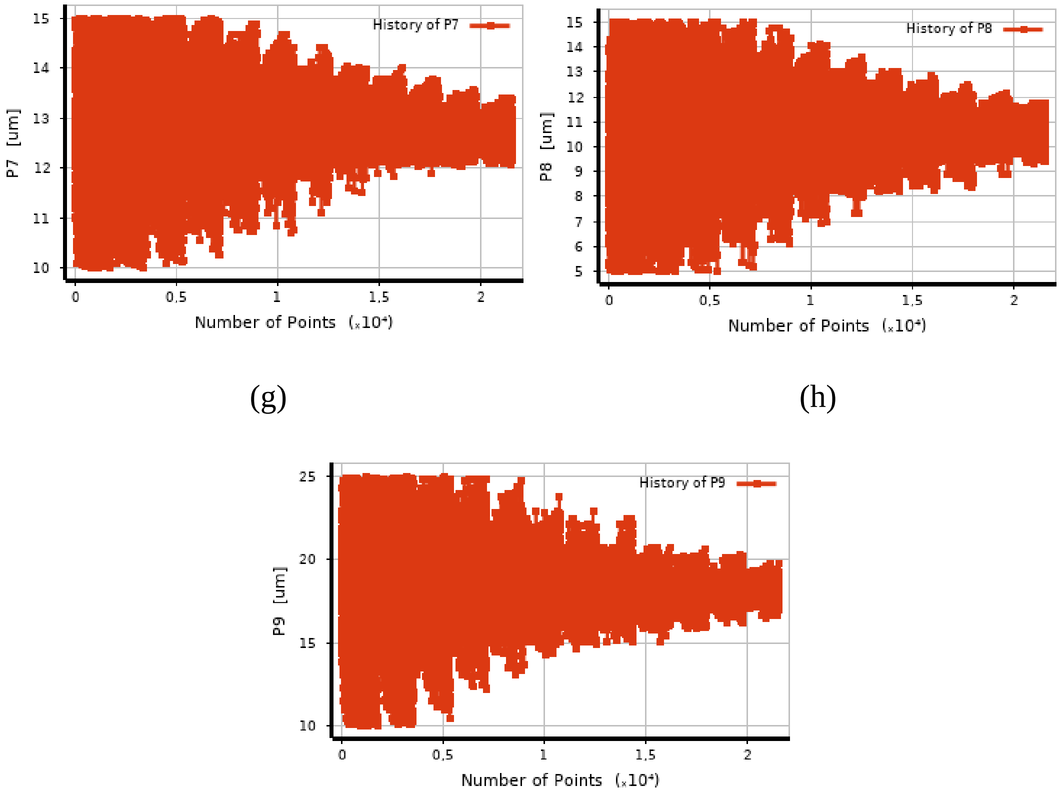

(g) (h)

(i)

Figure 38 (continued). Change of each parameter value over the optimization iterations; (a) P1, (b) P2, (c) P3, (d) P4, (e) P5, (f) P6, (g) P7, (h) P8, (i) P9

4.6 LifeTime Result of Solder Ball in the best Geometric Configuration

According to the results obtained with parameters in Table 17, it was seen that the most critical point on the solder ball is the outermost diameter of the surface where the ball comes into contact with UBM 3 (Gold) (Fig. 39).

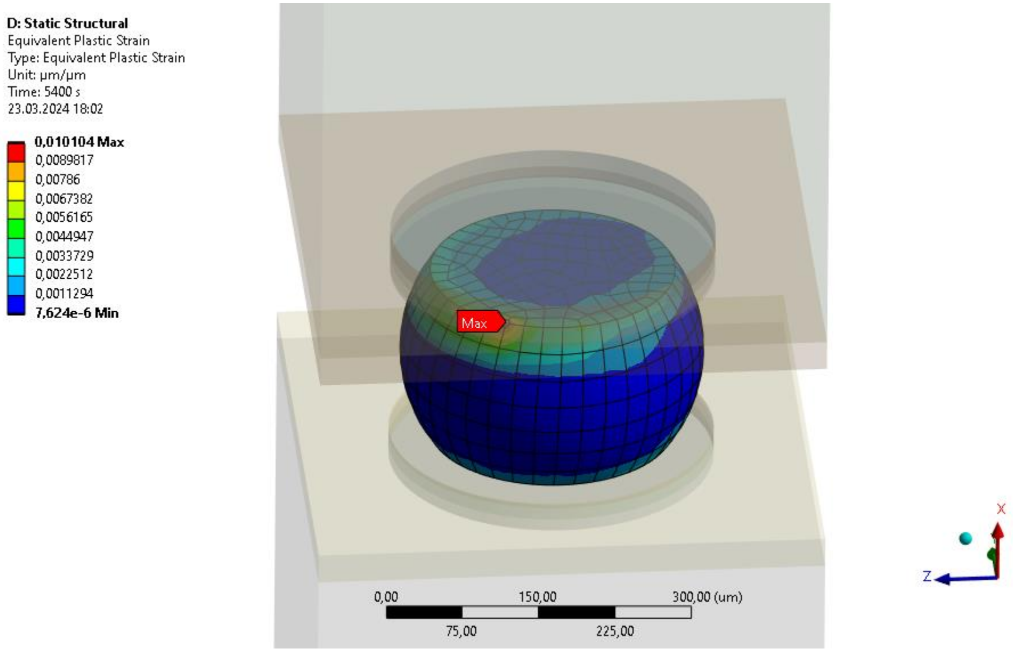

Figure 39. Most critical point appears in the upper contact surface and at the outermost diameter

Fig. 39a shows the equivalent stress vs equivalent strain curve of critical point for 3 cycles in ANSYS WB environment. Fig. 40b shows the values in the third cycle plotted in isolation and the strain range value is shown.

This strain range value was then used for lifetime prediction. ECM was used as the lifetime prediction model (Eq. 2.4.1)

$$N_f = \frac{1}{2}\left(\frac{\Delta\gamma}{2\epsilon'_f}\right)^{\frac{1}{c}} \tag{2.4.1}$$

Equivalent strain range value was converted to equivalent shear strain range using Eq. 2.4.2.

$$\Delta\gamma = \sqrt{3}\Delta\varepsilon = \sqrt{3} * 1.6387 * 10^{-2} = 2.8383 * 10^{-2} \tag{4.6.1}$$

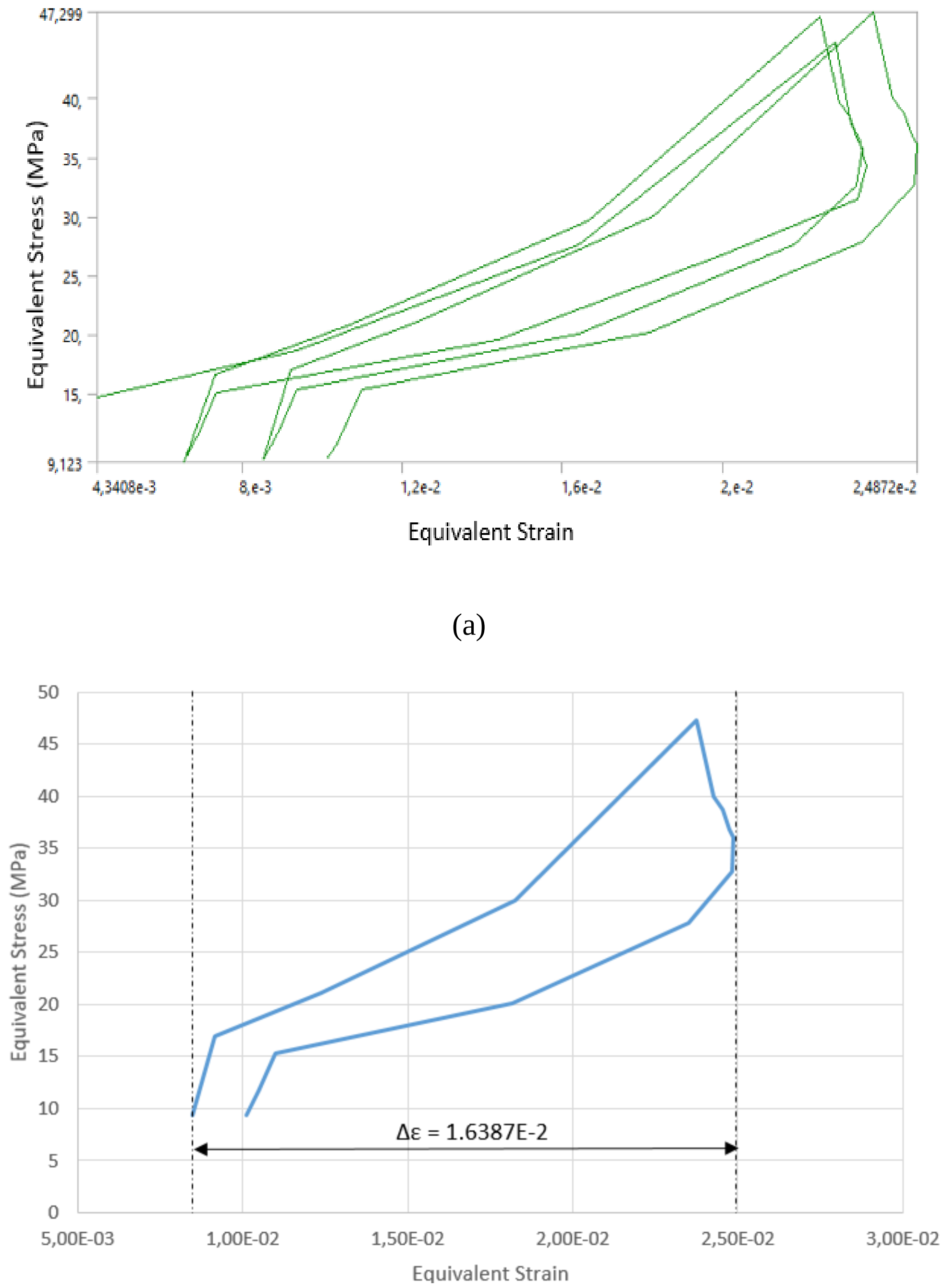

(a)

(b)

Figure 40. Equivalent stress vs equivalent strain curves; (a) generated in ANSYS WB to show behavior of the 3 cycles, (b) third cycle isolated to show equivalent strain range

And with Eq. 2.4.3 value c can be found.

$$c = -0.442 - 6 \times 10^{-4} T_m + 1.74 \times 10^{-2} \ln(1 + f) \tag{2.4.3}$$

$$T_m = \frac{T_{max} + T_{min}}{2} \tag{4.6.2}$$

$$T_m = \frac{125 - 55}{2} = 35 \tag{4.6.3}$$

Where T_m is the average of the temperature profile extreme values and f is the frequency of the temperature profile, $f = 48$ $(\frac{cycles}{day})$, thus $c = -0.395$.

And finally substituting all the generated and found ($2\epsilon'_f = 0.48$ [12]) values into Eq. 2.4.1.

$$N_f = \frac{1}{2}\left(\frac{\Delta\gamma}{2\epsilon'_f}\right)^{\frac{1}{c}} = \frac{1}{2}\left(\frac{2.8383 * 10^{-2}}{0.48}\right)^{\frac{1}{-0.395}} \cong 643\ cycles \tag{4.6.4}$$

As a result, it was concluded that in the best geometrical configuration, the solder ball has a lifetime of 643 cycles.

CHAPTER 5

FINITE ELEMENT SIMULATION AND OPTIMIZATION WITH EP MATERIAL MODEL

In Chapter 4, AV material model was defined for SAC305 material and optimization study was performed. In this chapter of the thesis, the EP material model for SAC305 material is defined and the optimization study is repeated.

The material test data of the SAC305 solder ball was obtained from the literature [45]. Fig. 41 shows the true stress-strain curve of SAC305 and other solder material types in compressive test.

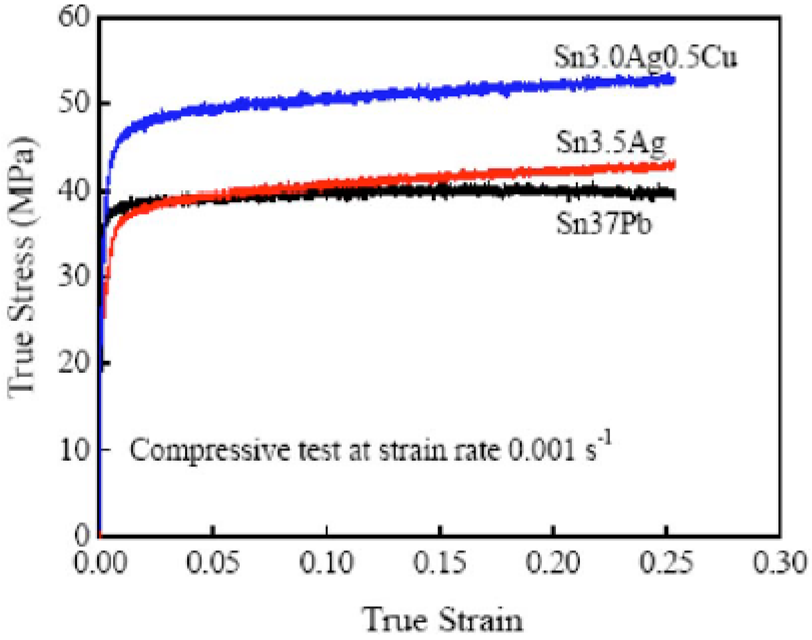

Figure 41. Curves of SAC305 and other solder material types in compressive test [45]

The EP material model is embedded in ANSYS WB. It is sufficient to provide parameter values for the relevant material. Multilinear kinematic hardening was selected as hardening type [28]. Table 18 shows the multilinear kinematic hardening values specified for SAC305 material. The values in Table 10 were used for elastic linear properties of SAC305.

Table 18. Multilinear kinematic hardening material model properties of SAC305

Plastic Strain	**Stress (MPa)**
0	41.2
8.32E-03	45.1
1.64E-02	47.6
2.91E-02	49.4
4.44E-02	50.4
5.83E-02	51.0
7.28E-02	51.1

In order to compare the results of the study with both material models with maintaining consistency, no changes were made in the settings of loading, global-local approach, mesh, parameter and optimization. The procedure followed in this chapter are listed and explained below.

1. The same material properties were used for all other materials except SAC305 (Table 10).
2. Temperature loading profile is kept the same (Fig. 11).
3. The same mesh models are used in the global and local model (Fig. 23,29, Table 14).
4. The analysis of the global model shows that the most critical solder ball is the outermost one (Fig. 43). For this reason, the cutting surfaces and data transfers in the global local transitions were made to be the same as in the previous chapter.
5. Same WB project schematic is used (Appendix C)

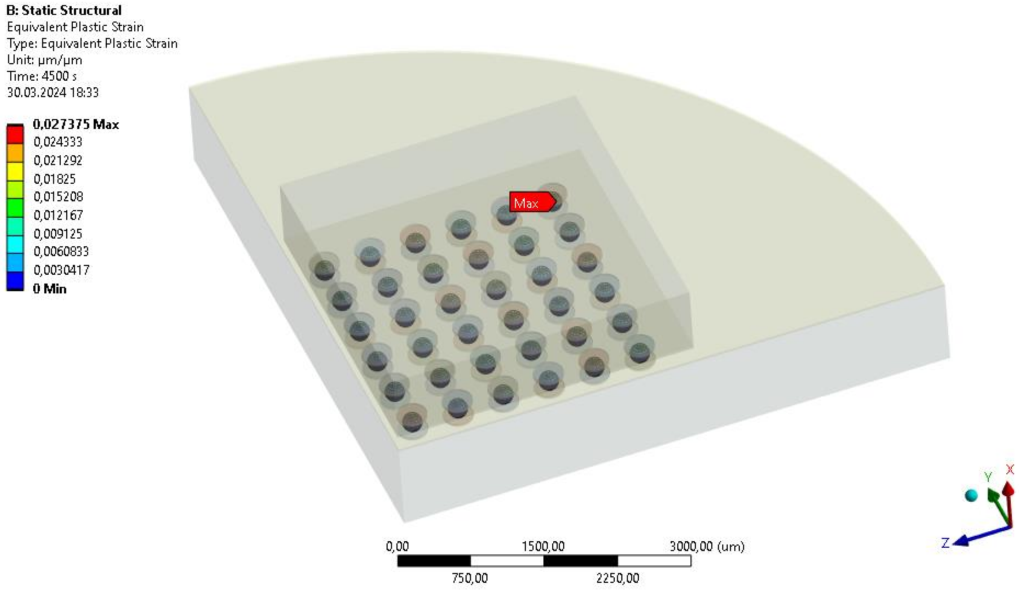

Figure 42. Critical solder joint in the simulation of the global model

5.1 Design of Experiment

After finding the most critical solder ball in the global model and creating a local model accordingly, a DOE study was performed. In the DOE study, the settings were kept the same as in Chapter 4.

- The value ranges of 9 different input parameters are given in Table 15.
- 147 design points were created with OSF method (Appendix C).

5.2 Response Surface

The design point results obtained with DOE were used to generate the RS. The NPR method was used, and the accuracy of the generated RS was checked with statistical metrics (Fig. 43, 44).

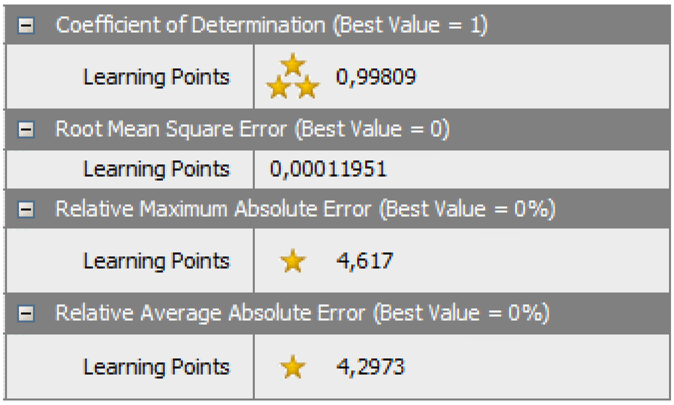

Coefficient of Determination (Best Value = 1)	
Learning Points	★★★ 0,99809
Root Mean Square Error (Best Value = 0)	
Learning Points	0,00011951
Relative Maximum Absolute Error (Best Value = 0%)	
Learning Points	★ 4,617
Relative Average Absolute Error (Best Value = 0%)	
Learning Points	★ 4,2973

Figure 43. Goodness of fit values of generated RS

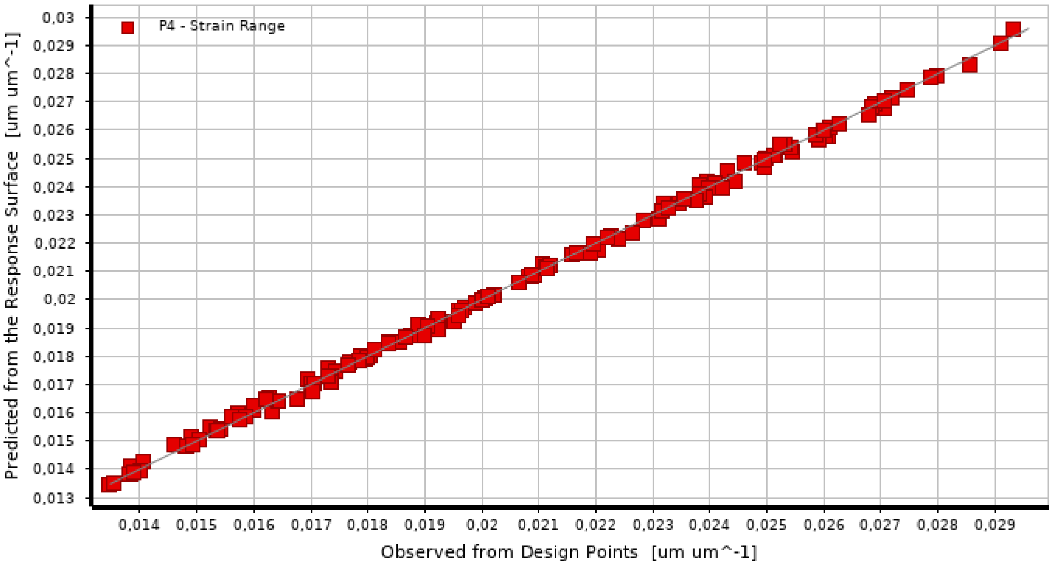

Figure 44. Distribution of the design points in the graph whose x axis shows the real solution values for the plastic strain range and y axis shows the values found from RS.

Another result that can be drawn is how much the change in each parameter affects the strain range output. Fig. 45 shows the sensitivity ratios of the parameters in the form of a pie chart. When the chart is analyzed, it is seen that the strain range output is most sensitive to solder ball height (P5).

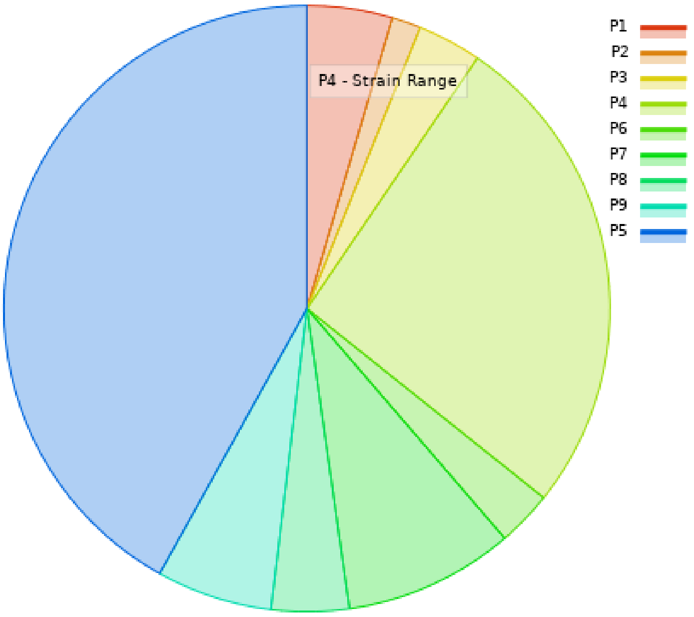

Figure 45. Pie chart that shows the sensitivity of the input parameters to strain range

After the statistical evaluation, confidence in the generated RS was ensured and the optimization part was started.

5.3 Optimization

After the RS was created, an optimization study was performed and the geometric configuration with the lowest strain range value was tried to be found. MOGA was selected as the optimization method. The values in Table 16 were selected as the interval sizes of the parameters in the optimization.

Fig. 46 shows the optimization result "Candidate Point 1". As a result of the calculation with RS, the strain range value was found to be 0.012316. The model was run again with the same parameter values and the actual value appeared as 0.01339. The difference between them is 8.7%. This difference was considered acceptable, and it was decided that the best configuration, considering the lowest strain range, was found.

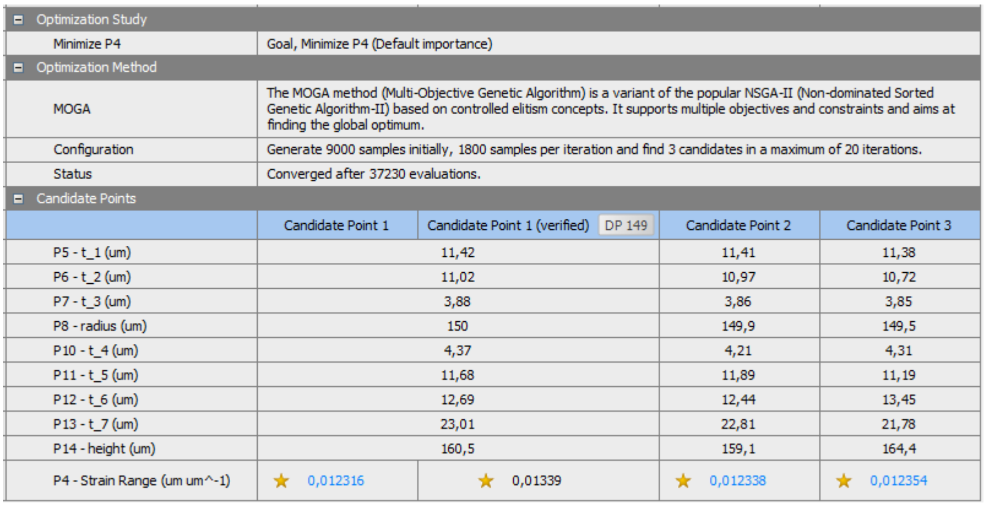

⊟ Optimization Study

Minimize P4	Goal, Minimize P4 (Default importance)

⊟ Optimization Method

MOGA	The MOGA method (Multi-Objective Genetic Algorithm) is a variant of the popular NSGA-II (Non-dominated Sorted Genetic Algorithm-II) based on controlled elitism concepts. It supports multiple objectives and constraints and aims at finding the global optimum.
Configuration	Generate 9000 samples initially, 1800 samples per iteration and find 3 candidates in a maximum of 20 iterations.
Status	Converged after 37230 evaluations.

⊟ Candidate Points

	Candidate Point 1	Candidate Point 1 (verified) DP 149	Candidate Point 2	Candidate Point 3
P5 - t_1 (um)	11,42		11,41	11,38
P6 - t_2 (um)	11,02		10,97	10,72
P7 - t_3 (um)	3,88		3,86	3,85
P8 - radius (um)	150		149,9	149,5
P10 - t_4 (um)	4,37		4,21	4,31
P11 - t_5 (um)	11,68		11,89	11,19
P12 - t_6 (um)	12,69		12,44	13,45
P13 - t_7 (um)	23,01		22,81	21,78
P14 - height (um)	160,5		159,1	164,4
P4 - Strain Range (um um^-1)	★ 0,012316	★ 0,01339	★ 0,012338	★ 0,012354

Figure 46 ANSYS optimization result showing the best geometric configuration with name “Candidate Point 1”

Table 19 shows the parameter values in the best configuration found.

Table 19. Parameter values of the best configuration

Parameter Name	**Definition**	**Value (µm)**
P1	Bond pad 1 thickness	11.42
P2	UBM 1 thickness	11.02
P3	UBM 2 thickness	3.88
P4	Solder ball radius	150
P5	Solder ball height	4.37
P6	UBM 3 thickness	11.68
P7	UBM 4 thickness	12.69
P8	UBM 5 thickness	23.01
P9	Bond pad 2 thickness	160.5

Fig. 47 shows the change of strain range values during iterations.

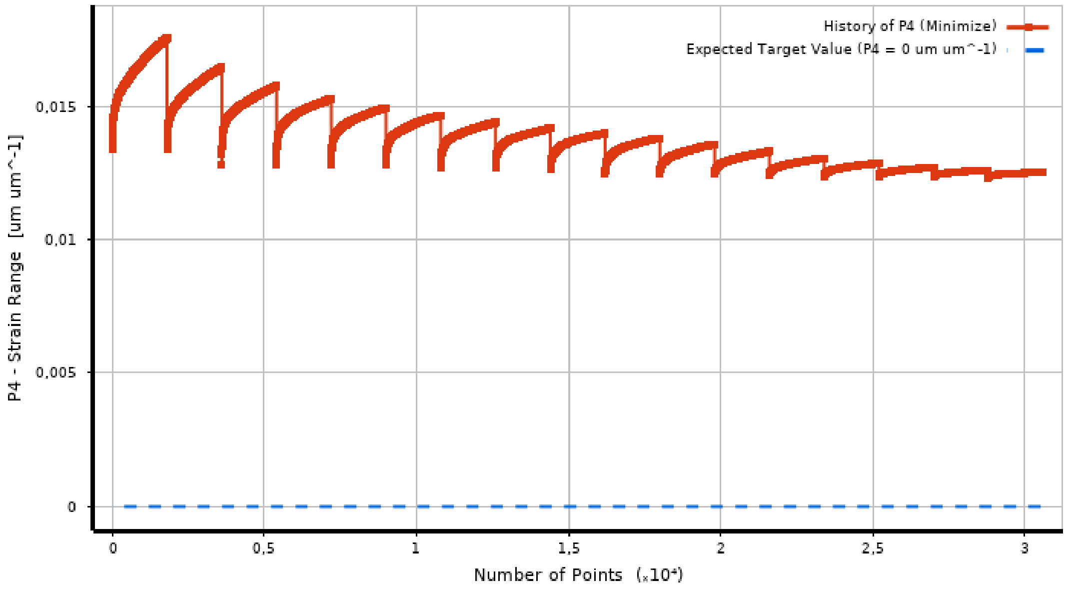

Figure 47. Change of strain range value during the optimization iterations

In addition, the variation of each parameter value over the iterations is shown in Fig. 47a-i.

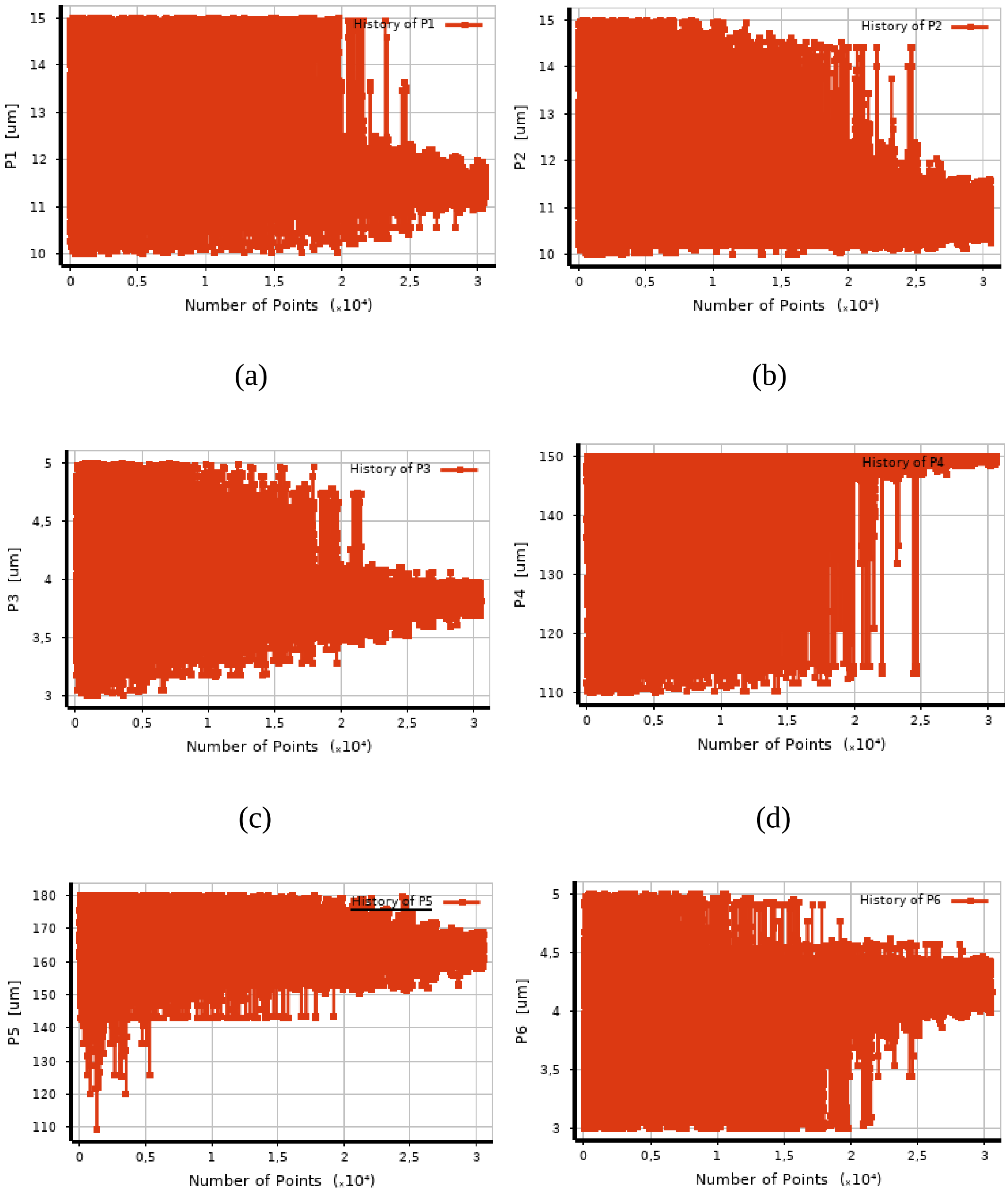

(a) (b)

(c) (d)

(e) (f)

Figure 48. Change of each parameter value over the optimization iterations; (a) P1, (b) P2, (c) P3, (d) P4, (e) P5, (f) P6, (g) P7, (h) P8, (i) P9

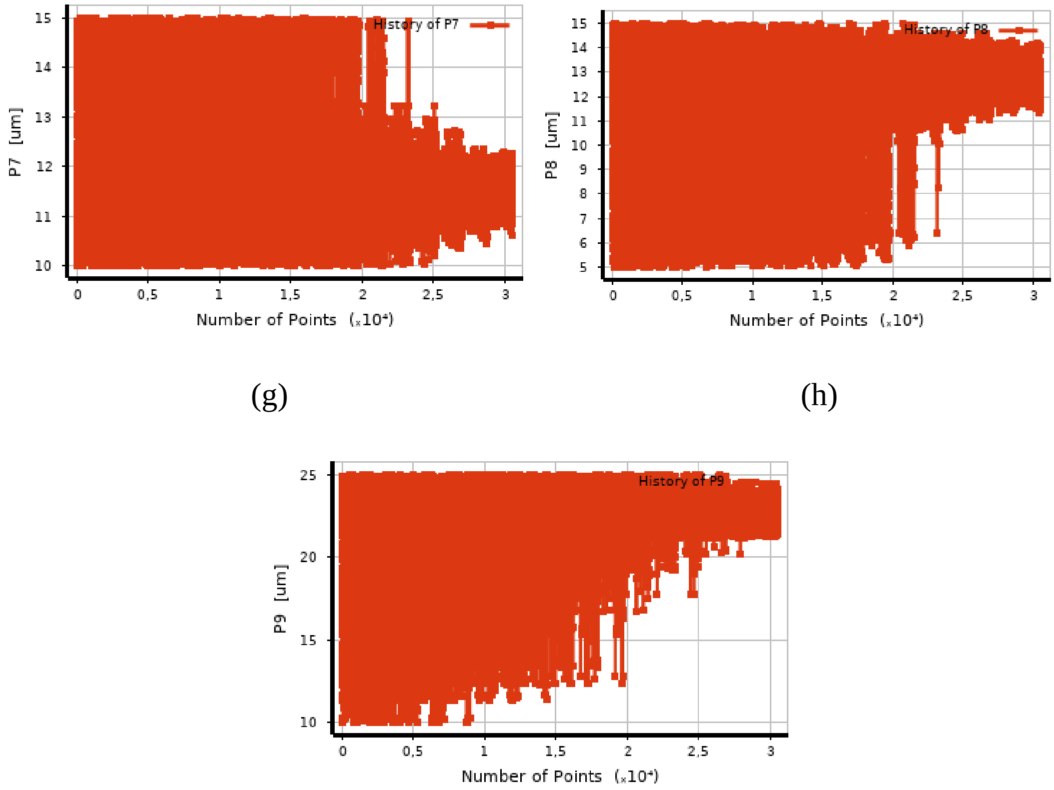

(g) (h)

(i)

Figure 48 (continued). Change of each parameter value over the optimization iterations; (a) P1, (b) P2, (c) P3, (d) P4, (e) P5, (f) P6, (g) P7, (h) P8, (i) P9

5.4 Lifetime Result of Solder Ball the best Geometric Configuration

According to the results obtained with parameters in Table 19, it was seen that the most critical point on the solder ball is the outermost diameter of the surface where the ball contacts UBM 3 (Gold) (Fig. 49).

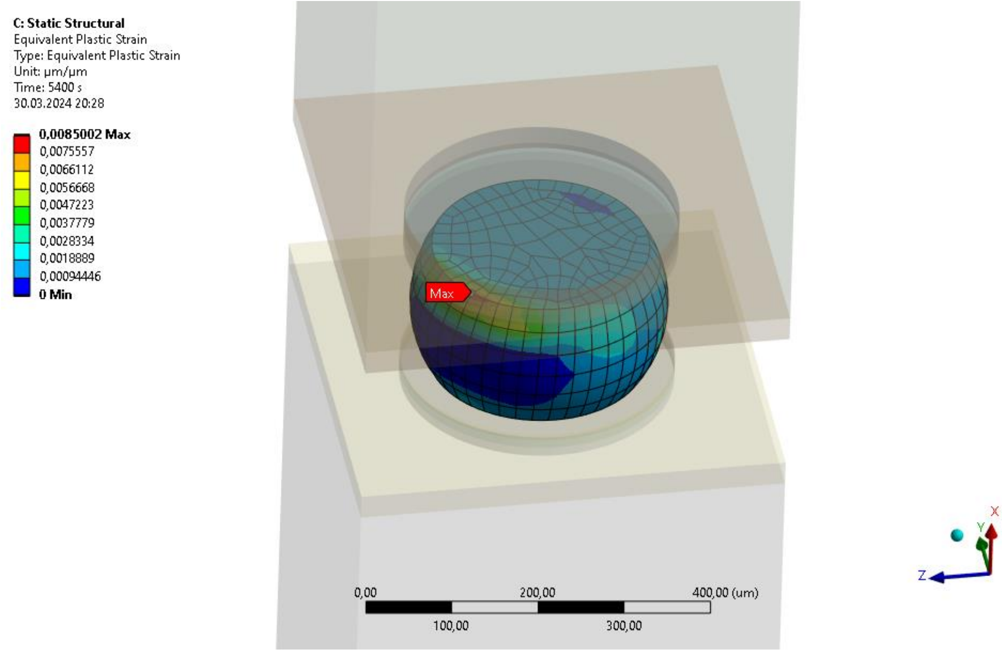

Figure 49. Most critical point appears in the upper contact surface and at the outermost diameter

Fig. 50a shows the equivalent stress vs equivalent strain curve of critical point for 3 cycles in ANSYS WB environment. Fig. 50b shows the values in the third cycle plotted in isolation and the strain range value is shown.

This strain range value was then used for lifetime prediction. ECM was used as the lifetime prediction model (Eq. 2.4.1)

$$N_f = \frac{1}{2}\left(\frac{\Delta\gamma}{2\epsilon'_f}\right)^{\frac{1}{c}} \tag{2.4.1}$$

Equivalent strain range value was converted to equivalent shear strain range using Eq. 2.4.2.

$$\Delta\gamma = \sqrt{3}\Delta\varepsilon = \sqrt{3} * 1.339 * 10^{-2} = 2.3192 * 10^{-2} \tag{5.1}$$

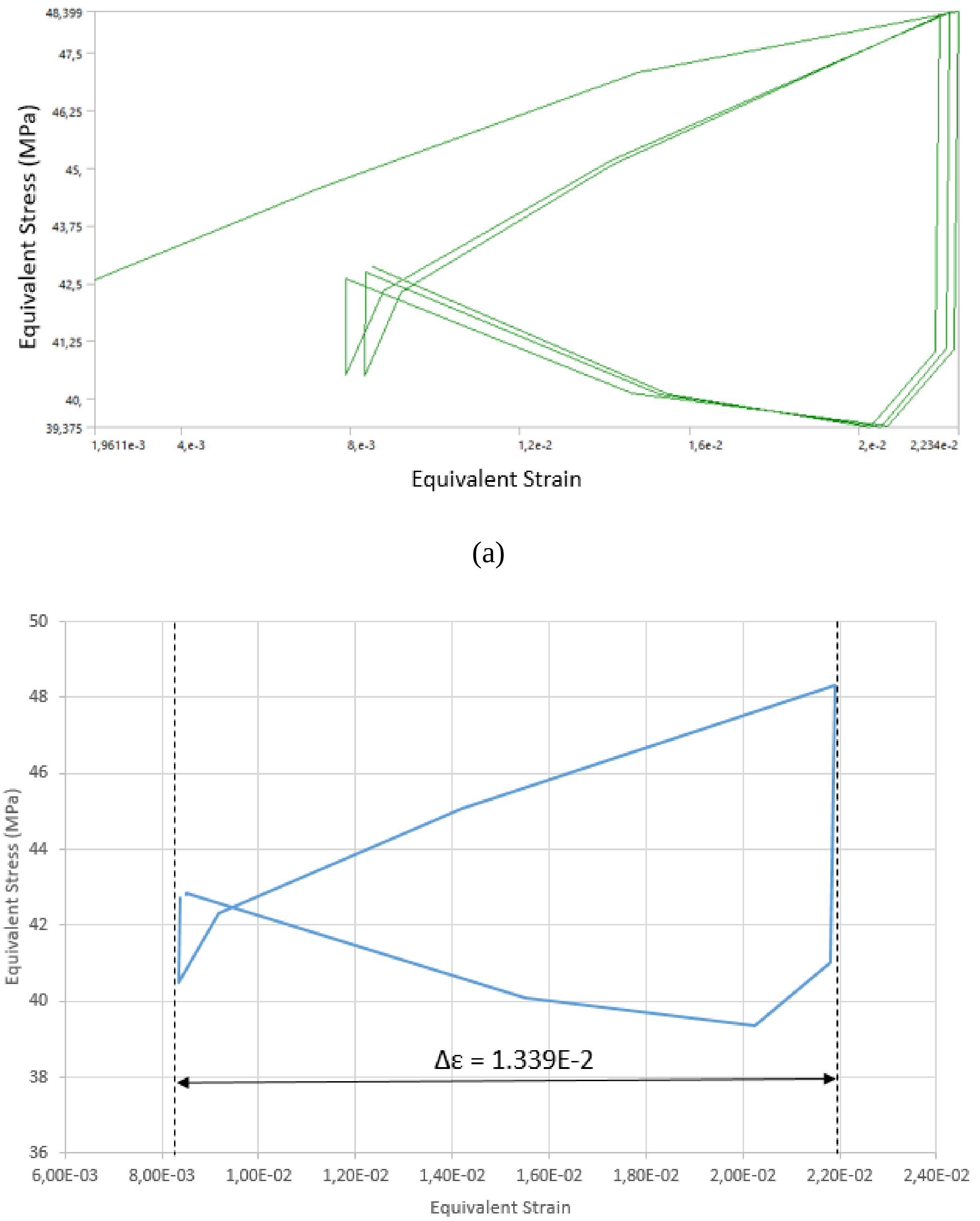

(a)

(b)

Figure 50. Equivalent stress vs equivalent strain curves; (a) generated in ANSYS WB to show behavior of the 3 cycles, (b) third cycle isolated to show equivalent strain range

And with Eq. 2.4.3 value c can be found.

$$c = -0.442 - 6 \times 10^{-4} T_m + 1.74 \times 10^{-2} \ln(1 + f) \qquad (2.4.3)$$

$$T_m = \frac{T_{max} + T_{min}}{2} \qquad (4.6.2)$$

$$T_m = \frac{125 - 55}{2} = 35 \qquad (4.6.3)$$

Where T_m is the average of the temperature profile extreme values and f is the frequency of the temperature profile, $f = 48$ ($\frac{cycles}{day}$), thus $c = -0.395$.

And finally substituting all the generated and found ($2\epsilon_f' = 0.48$ [12]) values into Eq. 2.4.1.

$$N_f = \frac{1}{2}\left(\frac{\Delta\gamma}{2\epsilon_f'}\right)^{\frac{1}{c}} = \frac{1}{2}\left(\frac{2.3192 * 10^{-2}}{0.48}\right)^{\frac{1}{-0.395}} \cong 1072 \; cycles \qquad (4.6.4)$$

As a result, it was concluded that in the best geometrical configuration, the solder ball has a lifetime of 1072 cycles according to EP material model.

CHAPTER 6

CONCLUSION

After optimization studies using AV and EP material models for SAC305 material, the geometric configurations with the highest lifetime were found. Table 20 shows the values of the parameters in the best result found with both material models.

Table 20. Comparison of optimized parameter values and life cycle obtained using two different material models

Parameter Name	**Definition**	**AV Model**	**EP Model**	**Percent Difference with Respect to AV Model (%)**
		Value (µm)	**Value (µm)**	
P1	Bond pad 1 thickness	12.08	11.42	-5.46
P2	UBM 1 thickness	12.62	11.02	-12.67
P3	UBM 2 thickness	4.3	3.88	-9.76
P4	Solder ball radius	149.4	150	0.4
P5	Solder ball height	4.26	4.37	2.58
P6	UBM 3 thickness	12.7	11.68	-8.03
P7	UBM 4 thickness	10.36	12.69	22.49
P8	UBM 5 thickness	17.94	23.01	28.26
P9	Bond pad 2 thickness	176.7	160.5	-9.16
Life cycle		643	1072	66.71

According to the simulation and optimization results in the same condition, it is concluded that the AV model leads to higher strain range values and therefore calculates lower life values. There is approximately 66.71% difference between the lifetime results of the best geometric configurations found using both material models. According to these results, it is seen that the AV model is more conservative.

In addition, from Table 20 it can be concluded that values of parameters P4 and P5 are close to each other for both material models. And for the other parameters, it shows that values are not close to each other and there are percentage differences.

6.1 Lifetime Improvements of the Optimized Configurations

After the optimization results were obtained, it was desired to find out how much improvement in lifetime was achieved compared to the original structure geometry for both material models separately. Table 13 shows the values of the parameters in the original structure.

6.1.1 AV Material Model

In this section, the original structure given in Table 13 is simulated with the AV model and the life of the most critical solder ball in the original structure is calculated. Fig. 51 shows that the most critical region is again at the largest diameter of the surface in contact with UBM 3.

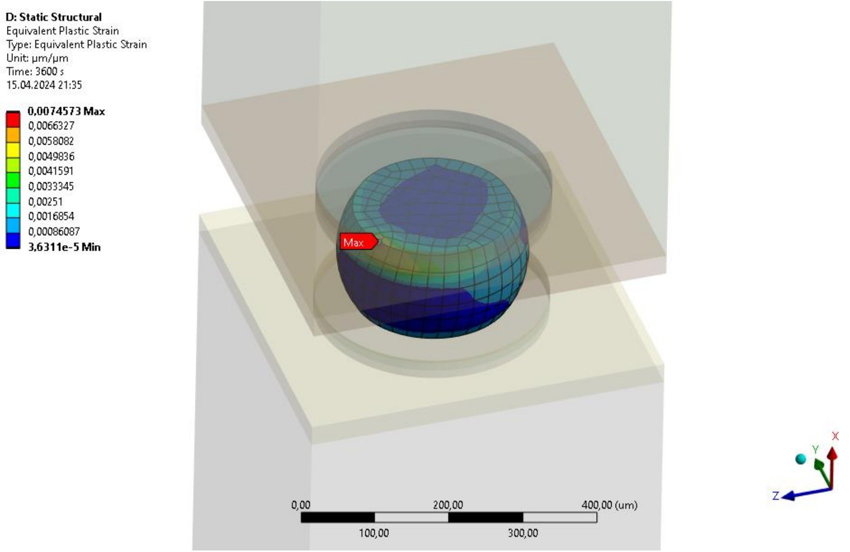

Figure 51. Most critical point appears in the upper contact surface and at the outermost diameter

The strain range value of the most critical solder ball in the original structure is 0.02317 (Fig. 52b). Using this value and Eq. 2.4.1, the lifetime of the original structure was found to be 267 cycles. Compared to the optimized structure (643 cycles), there is a 140% improvement in the lifetime of the critical solder ball.

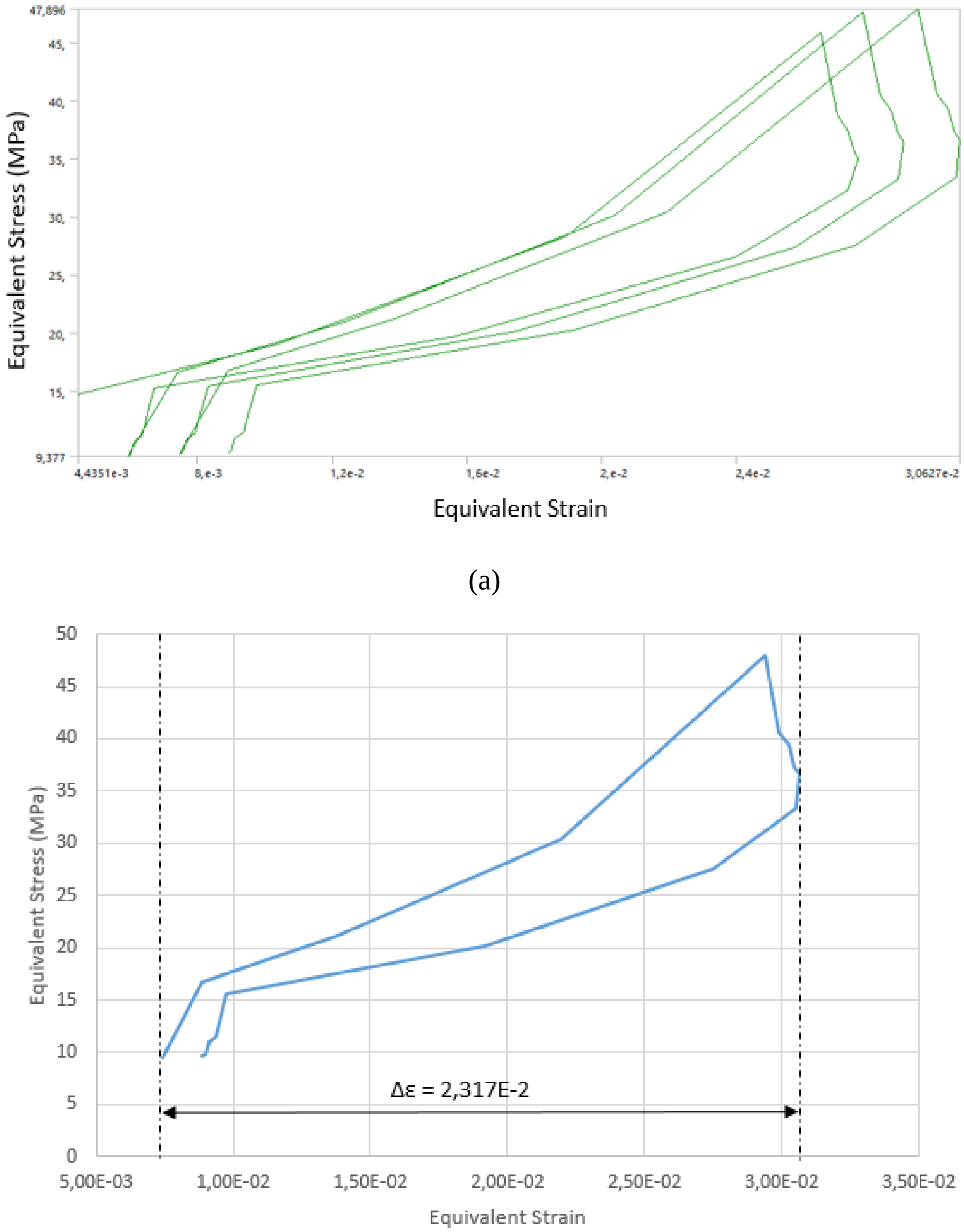

(a)

(b)

Figure 52. Equivalent stress vs equivalent strain curves of original structure with AV model; (a) generated in ANSYS WB to show behavior of the 3 cycles, (b) third cycle isolated to show equivalent strain range

6.1.2 EP Material Model

In this section, the original structure given in Table 13 is simulated with the EP model and the life of the most critical solder ball in the original structure is calculated. Fig. 53 shows that the most critical region is again at the largest diameter of the surface in contact with UBM 3.

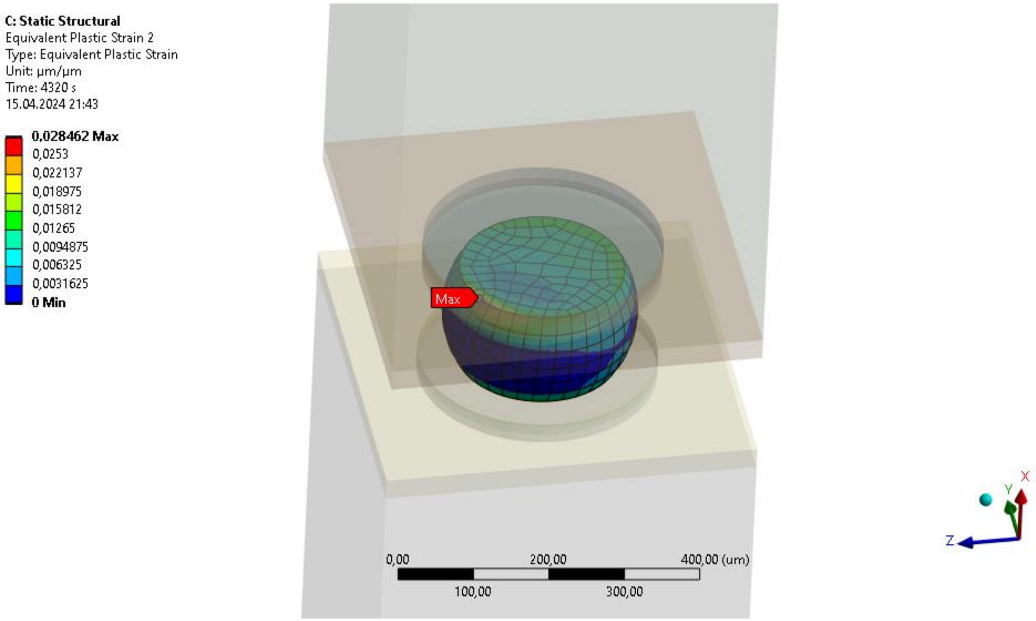

Figure 53. Most critical point appears in the upper contact surface and at the outermost diameter

The strain range value of the most critical solder ball in the original structure is 0.019632 (Fig. 54b). Using this value and Eq. 2.4.1, the lifetime of the original structure was found to be 407 cycles. Compared to the optimized structure (1072 cycles), there is a 163% improvement in the lifetime of the critical solder ball.

These results show that substantial improvement in lifetimes of solder balls could be achieved by optimizing the geometric parameters of the structure.

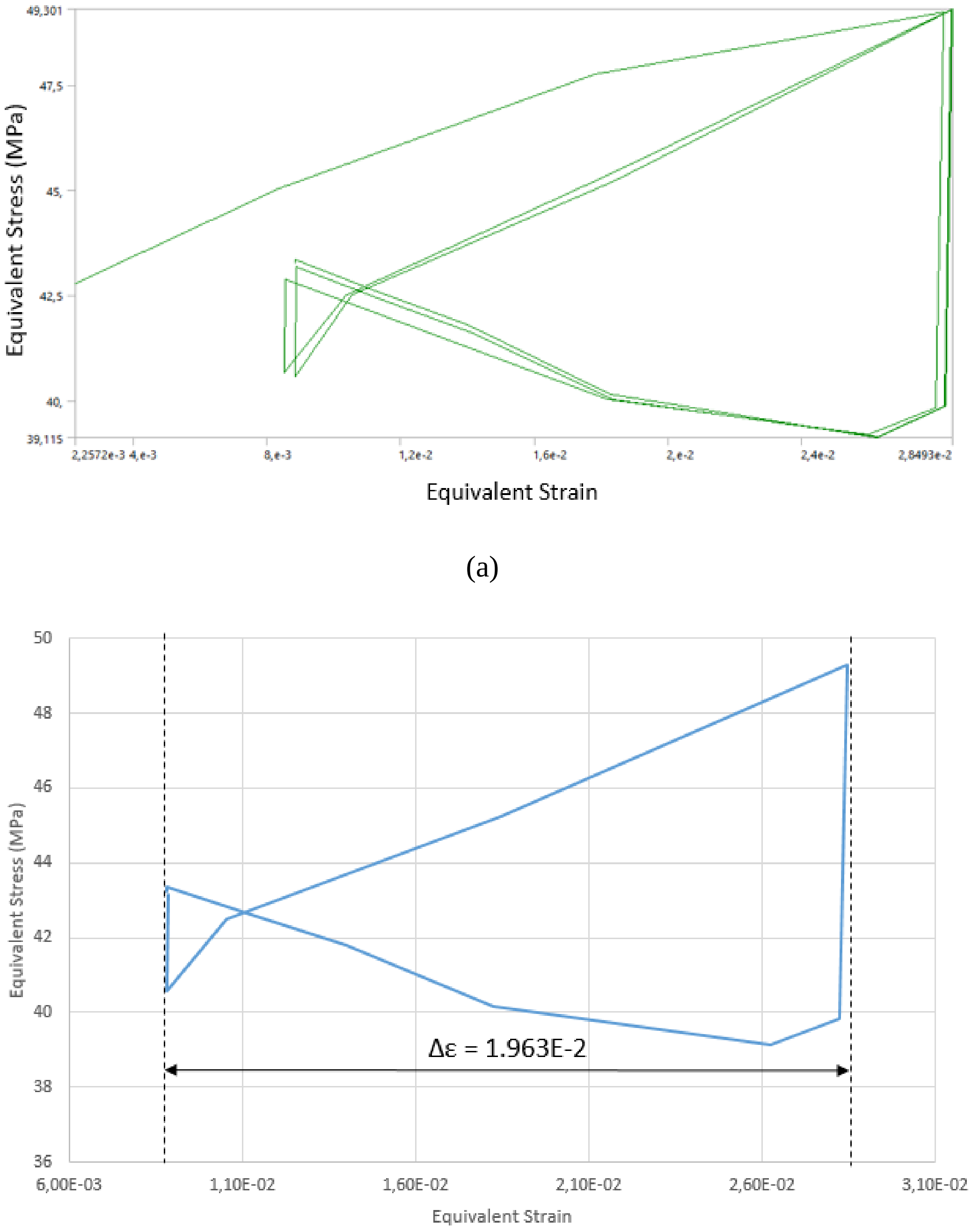

(a)

(b)

Figure 54. Equivalent stress vs equivalent strain curves of original structure with EP model; (a) generated in ANSYS WB to show behavior of the 3 cycles, (b) third cycle isolated to show equivalent strain range

6.1.3 Discussion

In this study, main desired motivation is to find the best geometric configuration whose have highest thermal fatigue life. Thus any other trade-off output parameter (weight, shape difference etc.) has not been taken into account in the optimizations.

As a result of the optimization study with the AV material model, a geometric configuration with a 140% increase in lifetime compared to the structure in the original dimensions was obtained. Here, the original structure was also analyzed with the AV model.

As a result of the optimization study with the EP material model, a geometric configuration with a 163% increase in lifetime compared to the structure in the original dimensions was obtained. Here, the original structure was also analyzed with the EP model.

As a result of the optimizations, lifetime results of critical solder ball were significantly increased for both material models.

6.2 Contribution to the Literature

In this study, the effect of thermomechanical loading due to temperature cycling on solder ball life in an electronic package with multiple UBM materials was investigated.

Results from this study shows that life values are similar to the values found in the literature [10] (Table 2).

9 different parameters were specified in the structure and an optimization study was carried out using these parameters. Optimization was performed separately using AV and EP material models for the solder balls.

The study carried out within the scope of this thesis is novel and contributes to the literature in terms of

- Unique and producible geometric dimensions of the working structure
- Optimization study with different material models
- And their comparison

6.3 Future Work

Response surface optimization method was used in the thesis using both material models (AV & EP). Instead of the OSF, NPR and MOGA methods used in this method, studies with different fit and optimization methods can be repeated using the same electronic package structure.

Within the scope of this thesis, physical samples of the resulting structures can be created for both material models and experimental cycle tests can be performed to see which material model gives results closer to simulations.

REFERENCES

[1] Pengli Z, Gang L, C P Wong, Encyclopedia of Packaging Materials, Processes, and Mechanics, World Scientific Publishing Company, Volume 1, Chapter 1, https://doi.org/10.1142/11303-vol1

[2] Joshua D, Mallik S, Harmanto D, Solder Joint Failures under Thermo-Mechanical Loading Conditions -A Review, Volume 7, Doi: 10.1080/2374068X.2020.1751514, Advances in Materials and Processing Technologies

[3] Puttlitz, K.J. and P. Totta, Area Array Interconnection Handbook. 2001: Kluwer Academic Publishers.

[4] Jintao He, Yun Ling, Dong Lei, Mechanical properties of Sn–Pb based solder joints and fatigue life prediction of PBGA package structure, Ceramics International, Volume 49, Issue 16, 2023, Pages 27445-27456, ISSN 0272-8842, https://doi.org/10.1016/j.ceramint.2023.06.017.

[5] M.P Rodriguez, N.Y.A Shammas, Finite element simulation of thermal fatigue in multilayer structures: thermal and mechanical approach, Microelectronics Reliability, Volume 41, Issue 4, 2001, Pages 517-523, ISSN 0026-2714, https://doi.org/10.1016/S0026-2714(00)00256-0.

[6] Qiang Guo, Mei Zhao, HongFang Wang, SMT solder joint's semi-experimental fatigue model, Mechanics Research Communications, Volume 32, Issue 3, 2005, Pages 351-358, ISSN 0093-6413, https://doi.org/10.1016/j.mechrescom.2004.03.011.

[7] H. Xiao, X.Y. Li, Y. Hu, F. Guo, Y.W. Shi, Damage behavior of SnAgCu/Cu solder joints subjected to thermomechanical cycling, Journal of Alloys and Compounds, Volume 578, 2013, Pages 110-117, ISSN 0925-8388, https://doi.org/10.1016/j.jallcom.2013.05.026.

[8] C. Huang, D. Yang, Daoguo, B. Wu, L. Liang, Y Yang, 2012/08/01, 1395, 1398, 978-1-4673-1682-8, Failure mode of SAC305 lead-free solder joint under thermal stress, doi: 10.1109/ICEPT-HDP.2012.6474866.

[9] F. X. Che and J. H. L. Pang, Fatigue Reliability Analysis of Sn–Ag–Cu Solder Joints Subject to Thermal Cycling, in IEEE Transactions on Device and Materials Reliability, vol. 13, no. 1, pp. 36-49, March 2013, doi: 10.1109/TDMR.2012.2195007.

[10] Hironori Tohmyoh, Shoho Ishikawa, Satoshi Watanabe, Motohisa Kuroha, Yoshikatsu Nakano, Estimation and visualization of the fatigue life of Pb-free SAC solder bump joints under thermal cycling, Microelectronics Reliability, Volume 53, Issue 2, 2013, Pages 314-320, ISSN 0026-2714, https://doi.org/10.1016/j.microrel.2012.08.012.

[11] G. Dong, X. Zhang, K. Ngo, G. Lu, 2010/04/13, SP-43, EP-48, Thermal fatigue behaviour of Al 2 O 3 -DBC substrates under high temperature cyclic loading, Volume 22, doi: 10.1108/09540911011036280, Journal Soldering & Surface Mount Technology

[12] Joshua A. Depiver, Sabuj Mallik, Emeka H. Amalu, Thermal fatigue life of ball grid array (BGA) solder joints made from different alloy compositions, Engineering Failure Analysis, Volume 125, 2021, 105447, ISSN 1350-6307, https://doi.org/10.1016/j.engfailanal.2021.105447.

[13] Jintao He, Yun Ling, Dong Lei, Mechanical properties of Sn–Pb based solder joints and fatigue life prediction of PBGA package structure, Ceramics International, Volume 49, Issue 16, 2023, Pages 27445-27456, ISSN 0272-8842, https://doi.org/10.1016/j.ceramint.2023.06.017.

[14] Rui W. Chang, F. Patrick McCluskey, Reliability assessment of indium solder for low temperature electronic packaging, Cryogenics, Volume 49, Issue 11, 2009, Pages 630-634, ISSN 0011-2275, https://doi.org/10.1016/j.cryogenics.2009.02.003.

[15] Ma, H., Suhling, J.C. A review of mechanical properties of lead-free solders for electronic packaging. J Mater Sci 44, 1141–1158 (2009). https://doi.org/10.1007/s10853-008-3125-9

[16] T. Hayashi, M. Takabe, Y. Ebihara, J. Shimura, Comparison between anand model and cassical decoupled creep and plasticity model, Tokyo Institute of Technology Research Report No. 46(1), 2014, https://www.jstage.jst.go.jp/article/tncttosho/46/1/46_14/_pdf/-char/ja

[17] J. -B. Libot, F. Dulondel, P. Milesi, J. Alexis, L. Arnaud and O. Dalverny, Experimental Strain Energy Density Dissipated in SAC305 Solder Joints During Different Thermal Cycling Conditions Using Strain Gages Measurement, 2018 IEEE 68th Electronic Components and Technology Conference (ECTC), San Diego, CA, USA, 2018, pp. 748-755, doi: 10.1109/ECTC.2018.00116.

[18] Wang, G. Z., Cheng, Z. N., Becker, K., and Wilde, J. (October 20, 1998). "Applying Anand Model to Represent the Viscoplastic Deformation Behavior of Solder Alloys ." ASME. J. Electron. Packag. September 2001; 123(3): 247–253. https://doi.org/10.1115/1.1371781

[19] Zhi-Hao Zhang, Xi-Shu Wang, Huai-Hui Ren, Su Jia, Hui-Hui Yang, Simulation study on thermo-fatigue failure behavior of solder joints in package-on-package structure, Microelectronics Reliability, Volume 75, 2017, Pages 127-134, ISSN 0026-2714, https://doi.org/10.1016/j.microrel.2017.06.033.

[20] X. Yan and G. Li, Study of thermal fatigue lifetime of fan-in package on package (FiPoP) by finite element analysis, 2009 International Conference on Electronic Packaging Technology & High Density Packaging, Beijing, China, 2009, pp. 1176-1180, doi: 10.1109/ICEPT.2009.5270614.

[21] Huang Chunyue, Thermal fatigue life analysis and forecast of PBGA solder joints on the flexible PCB based on finite element analysis, 2008 International Conference on Electronic Packaging Technology & High Density Packaging, Shanghai, China, 2008, pp. 1-4, doi: 10.1109/ICEPT.2008.4607162.

[22] Chen Ying, Hou Zebing and Kang Rui, Lifetime prediction and impact factors analysis of ball grid array solder joint based on FEA, 2010 11th International Conference on Electronic Packaging Technology & High Density Packaging, Xi'an, China, 2010, pp. 1142-1146, doi: 10.1109/ICEPT.2010.5582746.

[23] Xin Xu, Yang Liu, Yahui Su, Cong Sun, Yuxiong Xue, Lina Ju, Shuye Zhang, Fatigue behavior of 3D stacked packaging structures under extreme thermal cycling condition, Memories - Materials, Devices, Circuits and Systems, Volume 4, 2023, 100032, ISSN 2773-0646, https://doi.org/10.1016/j.memori.2023.100032.

[24] Kenny C. Otiaba, R.S. Bhatti, N.N. Ekere, S. Mallik, M. Ekpu, Finite element analysis of the effect of silver content for Sn–Ag–Cu alloy compositions on thermal cycling reliability of solder die attach, Engineering Failure Analysis, Volume 28, 2013, Pages 192-207, ISSN 1350-6307, https://doi.org/10.1016/j.engfailanal.2012.10.008.

[25] Mathias Ekpu, Raj Bhatti, Michael I. Okereke, Sabuj Mallik, Kenny Otiaba, Fatigue life of lead-free solder thermal interface materials at varying bond line thickness in microelectronics, Microelectronics Reliability, Volume 54, Issue 1, 2014, Pages 239-244, ISSN 0026-2714, https://doi.org/10.1016/j.microrel.2013.08.006.

[26] Sinda Ghenam, Abdelkhalak El Hami, Wajih Gafsi, Ali Akrout, Mohamed Haddar, Optimal performance and cost-effective design of BGA solder joints using a deterministic design optimization (DDO) under real operating conditions, Microelectronics Reliability, Volume 146, 2023, 115019, ISSN 0026-2714, https://doi.org/10.1016/j.microrel.2023.115019.

[27] C. Chen, J. C. Suhling and P. Lall, Improved Submodeling Finite Element Simulation Strategies for BGA Packages Subjected to Thermal Cycling, 2018 17th IEEE Intersociety Conference on Thermal and Thermomechanical Phenomena in Electronic Systems (ITherm), San Diego, CA, USA, 2018, pp. 1146-1154, doi: 10.1109/ITHERM.2018.8419533.

[28] Domen Šeruga, Marko Nagode, A new approach to finite element modelling of cyclic thermomechanical stress-strain responses, International Journal of Mechanical Sciences, Volume 164, 2019, 105139, ISSN 0020-7403, https://doi.org/10.1016/j.ijmecsci.2019.105139.

[29] Junzhou Huo, Debin Sun, Hanyang Wu, Weizheng Wang, lin Xue, Multi-axis low-cycle creep/fatigue life prediction of high-pressure turbine blades based on a new critical plane damage parameter, Engineering Failure Analysis, Volume 106, 2019, 104159, ISSN 1350-6307, https://doi.org/10.1016/j.engfailanal.2019.104159.

[30] M. Rassaian, W. Chang and Jung-Chan Lee, Multi-domain analysis of PBGA solder joints for structural design optimization, 1998 Proceedings. 48th Electronic Components and Technology Conference (Cat. No.98CH36206), Seattle, WA, USA, 1998, pp. 1332-1338, doi: 10.1109/ECTC.1998.678917.

[31] S. -C. Yang et al., Optimization of solder height and shape to improve the thermo-mechanical reliability of wafer-level chip scale packages, 2013 IEEE 63rd Electronic Components and Technology Conference, Las Vegas, NV, USA, 2013, pp. 1210-1218, doi: 10.1109/ECTC.2013.6575729.

[32] Lallit Anand, Constitutive equations for hot-working of metals, International Journal of Plasticity Volume 1, Issue 3, 1985, Pages 213-231, ISSN 0749-6419, https://doi.org/10.1016/0749-6419(85)90004-X.

[33] Mechanical Properties of Materials
https://mechanicalc.com/reference/mechanical-properties-of-materials

[34] Su, S., Akkara, F. J., Thaper, R., Alkhazali, A., Hamasha, M., and Hamasha, S. (May 17, 2019). "A State-of-the-Art Review of Fatigue Life Prediction Models for Solder Joint." ASME. J. Electron. Packag. December 2019; 141(4): 040802. https://doi.org/10.1115/1.4043405.

[35] W. Engelmaier, "Fatigue Life of Leadless Chip Carrier Solder Joints During Power Cycling," in IEEE Transactions on Components, Hybrids, and Manufacturing

Technology, vol. 6, no. 3, pp. 232-237, September 1983, doi: 10.1109/TCHMT.1983.1136183.

[36] A. A. Saad, Cyclic plasticity and creep of power plant materials, 2012/03/15

[37] A. Deshpande, H. Khan, F. Mirza and D. Agonafer, Global-local finite element optimization study to minimize BGA damage under thermal cycling, Fourteenth Intersociety Conference on Thermal and Thermomechanical Phenomena in Electronic Systems (ITherm), Orlando, FL, USA, 2014, pp. 483-487, doi: 10.1109/ITHERM.2014.6892321.

[38] P. Altieri-Weimar et al., Reliability model of LED package regarding the fatigue behavior of gold wires, 2016 17th International Conference on Thermal, Mechanical and Multi-Physics Simulation and Experiments in Microelectronics and Microsystems (EuroSimE), Montpellier, France, 2016, pp. 1-6, doi: 10.1109/EuroSimE.2016.7463326.

[39] Ross, R. B., and Sullivan, A. M. (October 1, 1981). Metallic Materials Specification Handbook, Third Edition. ASME. J. Eng. Mater. Technol. October 1981; 103(4): 347. https://doi.org/10.1115/1.3225027

[40] X. Gao, R. Chen, C. Li and S. Liu, "Dimension optimization of through silicon via(TSV) through simulation and design of experiment (DOE)," 2012 13th International Conference on Electronic Packaging Technology & High Density Packaging, Guilin, China, 2012, pp. 1185-1189, doi: 10.1109/ICEPT-HDP.2012.6474819.

[41] MIL-STD-883 Test Method Standard Microcircuits, Department of Defense, 1996.

[42] Introduction to ANSYS DesignXplorer, Module 03: Design of Experiments.

[43] Introduction to ANSYS DesignXplorer, Module 04: Response Surface.

[44] Introduction to ANSYS DesignXplorer, Module 05: Optimization.

[45] F Qin, T. An, N. Chen, Strain Rate Effects and Rate-Dependent Constitutive Models of Lead-Based and Lead-Free Solders, 2010/01/01, SP 1008, Volume 77, Journal of Applied Mechanics, doi: 10.1115/1.316860.

APPENDICES

A. ANSYS Workbench Project Schematic

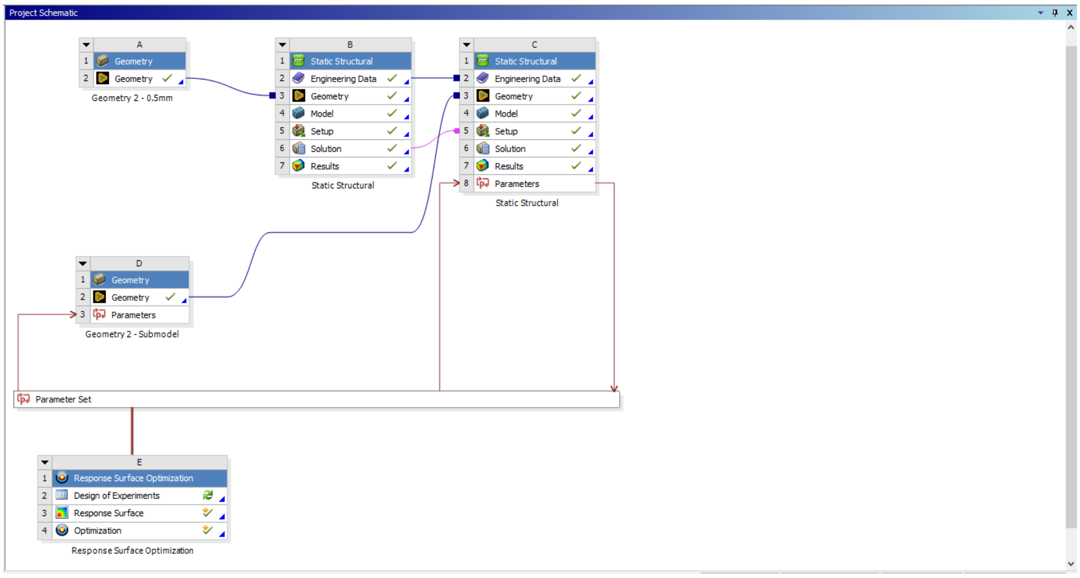

B. DOE Design Points with AV Material Model

Name	P1	P2	P3	P4	P5	P6	P7	P8	P9	Strain Range
1	12.56803	10.01701	4.435374	135.1701	139.4558	3.496599	14.40476	9.795918	10.05102	0.023934686
2	12.12585	12.60204	3.714286	124.5578	150.8844	4.857143	10.01701	14.7619	17.5	0.024306138
3	10.05102	12.7381	3.945578	122.381	144.898	3.020408	13.92857	12.72109	19.64286	0.025130488
4	11.78571	10.2551	4.612245	118.5714	134.0136	4.544218	13.21429	8.503401	24.94898	0.028336591
5	12.19388	11.27551	4.204082	128.3673	179.7279	3.891156	10.05102	7.006803	21.78571	0.022906264
6	14.71088	12.5	3.836735	144.4218	155.2381	3.673469	14.7449	12.92517	13.41837	0.02018047
7	10.15306	11.78571	4.884354	123.7415	124.2177	3.442177	11.10544	7.55102	20.05102	0.027175163
8	13.35034	11.03741	3.020408	121.2925	171.0204	4.489796	12.12585	6.870748	15.86735	0.021435717
9	10.59524	10.52721	4.353741	115.3061	132.381	4.816327	11.27551	7.959184	13.82653	0.028072337
10	11.92177	12.39796	4	114.2177	153.6054	4.952381	11.9898	5.442177	22.70408	0.026797383
11	10.79932	10.83333	3.768707	111.4966	137.2789	3.605442	11.71769	13.80952	22.09184	0.029785829
12	14.81293	13.45238	4.176871	121.0204	108.4354	4.040816	10.66327	6.190476	19.7449	0.028462381
13	10.96939	10.73129	3.591837	110.4082	134.5578	4.258503	14.43878	10.13605	13.0102	0.027828502
14	13.18027	11.88776	4.639456	126.1905	165.5782	3.265306	11.41156	14.4898	23.52041	0.02230716
15	13.72449	10.66327	4.92517	120.7483	160.6803	3.537415	11.95578	8.29932	22.90816	0.024428276
16	13.04422	13.72449	4.340136	112.0408	163.4014	3.646259	13.52041	5.306122	19.84694	0.023902785
17	12.29592	10.05102	4.217687	118.0272	119.3197	3.659864	14.54082	6.802721	18.52041	0.027752712
18	10.22109	11.81973	3.537415	116.1224	166.1224	4.666667	13.62245	10.95238	21.47959	0.022591236
19	14.94898	10.32313	4.721088	130.2721	156.3265	4.326531	14.13265	9.387755	17.70408	0.025530644
20	10.69728	13.55442	4.870748	132.1769	102.449	4.653061	13.65646	10	16.37755	0.025318276

21	14.47279	11.10544	4.857143	132.7211	147.619	3.102041	10.83333	10.7483	14.7449	0.022258289
22	13.65646	13.28231	3.510204	135.9864	130.2041	4.761905	11.37755	14.21769	24.13265	0.026874155
23	10.35714	13.9966	3.70068	115.8503	106.8027	3.578231	13.72449	8.77551	15.45918	0.031800501
24	13.52041	12.32993	3.115646	115.034	141.6327	3.238095	13.48639	7.346939	23.11224	0.025947188
25	11.54762	13.96259	3.918367	139.2517	153.0612	3.360544	14.91497	13.87755	14.13265	0.02265119
26	11.58163	11.37755	4.272109	140.3401	179.1837	3.034014	11.85374	11.97279	14.43878	0.022333371
27	13.0102	14.67687	3.891156	116.6667	171.5646	3.823129	10.4932	12.38095	20.45918	0.0213688
28	14.84694	12.2619	4.598639	124.2857	114.966	4.843537	13.2483	6.530612	18.72449	0.027814731
29	10.56122	11.92177	4.29932	144.1497	162.3129	4.639456	10.52721	12.2449	21.37755	0.019465442
30	14.06463	12.56803	4.027211	146.5986	173.1973	3.85034	10.73129	13.94558	19.03061	0.0191619
31	13.11224	11.44558	3.156463	133.8095	161.7687	3.714286	10.28912	11.56463	11.17347	0.023730022
32	13.86054	14.77891	4.530612	149.3197	141.0884	4.217687	12.46599	11.29252	22.19388	0.0223749
33	11.7517	10.28912	4.911565	141.7007	154.6939	3.387755	13.45238	6.666667	19.94898	0.01870519
34	10.83333	11.41156	3.401361	130.8163	166.6667	3.836735	13.55442	13.40136	10.56122	0.023728832
35	14.20068	10.39116	4.040816	129.1837	142.1769	4.693878	10.42517	6.734694	13.11224	0.024507956
36	14.26871	13.04422	3.346939	119.6599	152.517	3.428571	14.16667	14.08163	20.86735	0.021714581
37	14.67687	11.2415	3.795918	146.3265	100.2721	4.176871	13.31633	8.095238	16.07143	0.028632974
38	13.55442	13.82653	4.653061	148.5034	155.7823	3.768707	12.7381	5.034014	18.41837	0.021175765
39	11.64966	14.57483	3.292517	120.4762	119.8639	3.687075	11.92177	13.06122	11.37755	0.027210031
40	14.16667	13.58844	3.07483	116.9388	110.6122	3.619048	13.58844	9.659864	13.31633	0.029628786
41	10.66327	11.68367	3.687075	125.6463	108.9796	4.408163	10.79932	13.12925	12.29592	0.03063563
42	13.21429	12.36395	4.666667	132.9932	111.7007	4.108844	13.9966	14.42177	24.33673	0.029536228
43	14.7449	12.80612	4.408163	119.1156	146.5306	4.503401	11.81973	14.62585	11.9898	0.025535979

44	13.14626	12.70408	4.585034	140.6122	125.3061	3.877551	10.69728	6.462585	24.84694	0.022403943
45	14.03061	13.38435	4.571429	112.585	121.4966	4.163265	14.98299	9.115646	20.2551	0.028631211
46	10.32313	13.86054	3.183673	133.5374	138.3673	3.55102	10.32313	11.36054	20.15306	0.025087
47	12.02381	14.98299	3.306122	144.6939	172.1088	4.394558	12.05782	8.231293	20.35714	0.020621352
48	13.41837	10.86735	3.578231	124.0136	122.0408	4.870748	13.38435	14.89796	17.90816	0.027858898
49	14.23469	13.14626	3.85034	125.3741	145.9864	4.829932	14.77891	10.20408	11.27551	0.026778456
50	12.60204	12.12585	4.095238	118.2993	116.5986	3.564626	14.64286	14.14966	11.78571	0.028940095
51	14.60884	10.15306	3.741497	139.7959	150.3401	3.37415	13.41837	11.63265	22.5	0.02117562
52	11.10544	11.51361	3.55102	124.8299	118.7755	4.136054	14.84694	11.90476	24.64286	0.025388606
53	14.37075	10.90136	3.959184	133.2653	175.9184	4.557823	12.2619	11.70068	23.82653	0.023386722
54	13.31633	10.4932	3.564626	132.449	129.6599	4.802721	14.88095	8.843537	20.56122	0.027117224
55	11.41156	14.20068	3.414966	111.2245	123.6735	4.598639	12.87415	13.53741	18.11224	0.030932833
56	13.79252	14.26871	3.37415	130.5442	169.3878	3.156463	11.88776	10.27211	23.0102	0.021306335
57	13.38435	10.35714	4.054422	149.5918	107.3469	3.414966	11.44558	10.68027	20.76531	0.030461282
58	12.80612	10.11905	4.285714	148.7755	151.4286	4.612245	13.04422	13.19728	15.66327	0.018860779
59	13.48639	12.84014	3.333333	116.3946	104.6259	4.530612	11.64966	10.47619	23.62245	0.033148913
60	12.22789	11.7517	3.142857	142.2449	177.551	3.931973	12.94218	5.986395	21.07143	0.019877091
61	10.4932	13.69048	4.503401	147.9592	113.3333	3.755102	11.58163	12.51701	15.76531	0.024242086
62	11.81973	11.54762	4.993197	128.6395	165.034	4.312925	14.60884	12.78912	20.66327	0.023224826
63	12.70408	11.61565	4.979592	114.4898	167.2109	4.77551	11.68367	11.4966	16.88776	0.022824493
64	11.88776	11.0034	3.170068	128.9116	116.0544	3.863946	10.62925	5.578231	15.56122	0.026836366
65	14.64286	12.94218	4.748299	138.7075	129.1156	3.945578	11.03741	7.142857	11.07143	0.022335175
66	13.2483	14.16667	3.52381	135.7143	147.0748	3.129252	14.57483	6.326531	16.17347	0.022207303

67	11.07143	10.22109	4.14966	134.898	120.4082	3.741497	10.56122	12.9932	23.31633	0.025738361
68	12.87415	14.09864	3.319728	140.8844	110.068	3.727891	14.20068	6.938776	22.39796	0.02915917
69	12.39796	11.34354	3.809524	129.7279	176.4626	4.435374	14.94898	5.646259	15.05102	0.021295394
70	10.39116	12.29592	4.231293	137.8912	127.483	3.115646	10.86735	8.163265	11.88776	0.0228654
71	10.01701	11.85374	4.394558	134.3537	140	4.884354	14.26871	12.10884	12.90816	0.02427736
72	11.2415	10.59524	3.972789	142.7891	113.8776	3.455782	12.53401	14.69388	14.64286	0.02764398
73	11.03741	11.20748	3.129252	134.0816	128.5714	4.462585	11.2415	9.047619	24.43878	0.027418496
74	11.61565	12.46599	4.163265	118.8435	112.7891	4.204082	12.5	5.170068	10.15306	0.028915035
75	13.82653	12.09184	3.387755	123.1973	109.5238	3.047619	11.07143	12.85714	18.0102	0.02786836
76	14.40476	14.30272	3.238095	129.4558	143.8095	4.013605	10.11905	9.591837	12.60204	0.022531299
77	13.96259	12.22789	4.136054	127.8231	169.932	3.170068	11.17347	6.258503	12.09184	0.020188475
78	12.90816	13.2483	3.605442	144.966	103.5374	3.482993	10.08503	8.367347	18.31633	0.03185717
79	13.9966	14.7449	4.816327	110.6803	137.8231	3.959184	12.32993	8.707483	14.94898	0.027208521
80	10.86735	13.92857	4.544218	113.9456	160.1361	4.707483	13.7585	12.17687	14.54082	0.02419418
81	11.85374	13.11224	3.061224	138.4354	135.6463	4.353741	14.71088	7.687075	10.96939	0.024501951
82	10.2551	13.21429	4.380952	149.8639	149.7959	3.346939	13.79252	9.183673	16.58163	0.019540447
83	14.54082	14.03061	3.755102	131.3605	174.2857	4.734694	11.61565	7.210884	14.23469	0.02230345
84	12.15986	14.71088	4.122449	125.9184	102.9932	3.52381	12.36395	10.81633	24.7449	0.032214475
85	14.57483	10.69728	3.102041	143.3333	148.1633	4.272109	12.02381	12.44898	16.47959	0.022236476
86	14.30272	13.65646	3.047619	117.483	159.0476	4.62585	13.18027	11.02041	21.68367	0.021415881
87	11.47959	14.84694	4.068027	131.9048	177.0068	4.244898	14.67687	7.619048	15.96939	0.020683235
88	12.97619	10.08503	3.428571	115.5782	128.0272	3.401361	11.47959	11.42857	12.70408	0.028930869
89	10.90136	12.05782	4.421769	117.2109	144.3537	3.306122	10.18707	13.67347	14.84694	0.025899966

90	13.28231	14.47279	4.734694	119.932	154.1497	4.380952	10.76531	9.727891	24.23469	0.02652312
91	12.5	14.40476	4.680272	137.619	131.8367	3.22449	13.96259	7.891156	11.68367	0.02462138
92	12.67007	12.67007	4.952381	147.1429	135.102	4.190476	10.39116	11.76871	12.19388	0.023339651
93	12.46599	12.15986	4.761905	143.6054	114.4218	4.47619	13.86054	5.714286	13.52041	0.027419111
94	14.09864	10.56122	3.278912	111.7687	126.9388	3.918367	12.29592	6.598639	17.60204	0.02925963
95	10.73129	12.97619	3.442177	121.5646	178.6395	3.70068	12.77211	5.238095	13.72449	0.022743755
96	13.07823	11.17347	4.789116	119.3878	111.1565	4.517007	11.0034	11.83673	23.41837	0.030104704
97	11.27551	11.30952	4.312925	114.7619	162.8571	3.278912	13.0102	7.278912	11.58163	0.023127747
98	10.11905	11.71769	3.469388	138.1633	142.7211	4.367347	11.7517	6.122449	10.76531	0.023771053
99	11.44558	11.58163	3.034014	136.2585	117.1429	3.183673	13.82653	9.931973	12.5	0.02570008
100	11.68367	12.90816	4.938776	120.2041	104.0816	3.251701	14.5068	11.22449	17.80612	0.029983644
101	14.33673	14.54082	4.517007	141.9728	125.8503	4.081633	12.90816	13.33333	11.47959	0.024710205
102	12.36395	14.88095	3.986395	113.1293	133.4694	3.07483	11.20748	7.414966	19.13265	0.026902496
103	11.9898	13.52041	4.843537	147.6871	178.0952	4.285714	12.43197	9.251701	13.92857	0.0167998
104	13.58844	14.13265	4.44898	136.5306	157.9592	4.938776	14.30272	13.26531	18.62245	0.019222618
105	14.98299	14.06463	3.673469	125.102	122.585	4.027211	13.07823	7.07483	10.45918	0.023830509
106	11.30952	11.07143	3.455782	147.415	167.7551	3.591837	10.45918	9.455782	21.27551	0.017868586
107	14.13265	14.33673	4.707483	121.8367	140.5442	3.061224	12.56803	13.46939	17.39796	0.025063573
108	14.88095	13.48639	3.904762	136.8027	168.8435	3.972789	14.33673	8.571429	22.60204	0.019036363
109	13.62245	13.41837	4.489796	143.0612	151.9728	4.965986	10.35714	9.863946	19.43878	0.020940221
110	13.45238	12.19388	4.802721	122.9252	173.7415	3.510204	14.81293	10.61224	13.21429	0.018844668
111	12.84014	10.76531	4.47619	128.0952	100.8163	4.44898	12.63605	12.65306	10.86735	0.029901681
112	12.53401	13.35034	3.646259	146.0544	132.9252	3.088435	12.15986	14.55782	22.29592	0.025646542

113	10.08503	14.23469	4.367347	131.0884	159.5918	4.095238	11.13946	14.82993	13.62245	0.0242001
114	10.62925	14.43878	4.462585	122.6531	124.7619	4.979592	11.34354	8.435374	17.29592	0.02923254
115	10.93537	11.95578	3.088435	142.517	105.7143	4.571429	12.84014	12.04082	17.19388	0.02663889
116	11.51361	14.91497	4.897959	122.1088	143.2653	3.333333	10.96939	10.06803	14.03061	0.02268979
117	12.09184	13.79252	3.659864	110.9524	161.2245	4.122449	10.15306	8.911565	12.80612	0.02465569
118	10.42517	12.87415	4.829932	126.7347	138.9116	4.054422	12.39796	14.96599	23.21429	0.02656178
119	11.37755	10.62925	4.190476	127.551	174.8299	4.340136	10.93537	10.40816	10.2551	0.0218012
120	11.17347	10.79932	4.244898	145.7823	118.2313	4.911565	11.54762	7.823129	18.21429	0.02220044
121	13.69048	10.18707	3.823129	113.6735	168.2993	4.068027	13.11224	14.01361	15.35714	0.02296107
122	10.18707	13.07823	4.557823	137.3469	156.8707	4.748299	12.97619	5.85034	21.88776	0.0205961
123	14.91497	11.47959	3.931973	127.2789	117.6871	3.142857	14.06463	9.52381	21.58163	0.02547958
124	13.92857	10.96939	3.251701	145.2381	136.7347	3.319728	12.70408	6.394558	14.33673	0.02244718
125	10.52721	10.42517	4.081633	145.5102	149.2517	4.231293	14.23469	7.755102	20.96939	0.02097294
126	11.0034	12.43197	3.632653	146.8707	158.5034	4.421769	13.89456	12.31293	23.92857	0.0189785
127	13.89456	11.13946	3.782313	112.8571	130.7483	4.993197	10.90136	11.15646	16.68367	0.02851507
128	10.28912	14.94898	3.360544	134.6259	126.3946	4.680272	12.22789	7.482993	16.9898	0.02819233
129	14.43878	13.31633	4.326531	127.0068	107.8912	4	10.22109	14.28571	18.82653	0.02968306
130	12.77211	10.45918	4.77551	112.3129	112.2449	3.469388	11.51361	8.979592	15.15306	0.0276859
131	12.63605	13.18027	3.727891	139.5238	115.5102	4.721088	10.2551	9.319728	10.66327	0.0264460
132	11.34354	10.93537	3.197279	131.6327	172.6531	3.006803	13.28231	10.88435	19.23469	0.02327365
133	13.7585	11.64966	4.965986	141.1565	106.2585	3.292517	13.35034	11.08844	16.78571	0.02707664
134	11.20748	11.9898	4.108844	130	148.7075	3.210884	12.67007	5.102041	24.54082	0.02114532
135	14.5068	12.02381	3.496599	141.4286	131.2925	4.585034	11.30952	5.918367	21.9898	0.02422780

136	11.13946	12.53401	3.863946	117.7551	101.9048	3.986395	12.09184	5.782313	24.03061	0.020118442
137	10.76531	12.63605	4.258503	149.0476	101.3605	3.782313	13.14626	8.027211	22.80612	0.020651781
138	12.43197	12.77211	4.693878	123.4694	170.4762	4.789116	12.60204	6.054422	12.39796	0.025861365
139	10.45918	13.0102	3.006803	113.4014	157.415	3.809524	11.78571	8.639456	21.17347	0.023821607
140	12.7381	13.62245	3.877551	148.2313	105.1701	4.897959	14.03061	10.34014	17.09184	0.026000726
141	12.94218	13.7585	3.210884	126.4626	136.1905	4.92517	14.09864	5.510204	19.54082	0.0249794
142	12.2619	13.89456	4.62585	135.4422	175.3741	3.197279	13.69048	10.54422	23.72449	0.024979423
143	14.77891	14.37075	3.265306	143.8776	123.1293	3.904762	12.19388	13.7415	16.27551	0.025240437
144	12.05782	14.5068	4.013605	110.1361	164.4898	3.795918	14.47279	12.58503	19.33673	0.023557611
145	12.32993	14.60884	3.22449	137.0748	163.9456	4.14966	12.80612	13.60544	10.35714	0.024447436
146	11.71769	14.64286	3.619048	138.9796	145.4422	3.632653	10.59524	5.37415	15.2551	0.017887727
147	11.95578	14.81293	3.482993	140.068	120.9524	4.29932	14.37075	14.35374	18.92857	0.021135081

C. DOE Design Points with EP Material Model

Name	P1	P2	P3	P4	P5	P6	P7	P8	P9	Strain Range
1	12.56803	10.01701	4.435374	135.1701	139.4558	3.496599	14.40476	9.795918	10.05102	0.020074435
2	12.12585	12.60204	3.714286	124.5578	150.8844	4.857143	10.01701	14.7619	17.5	0.020837242
3	10.05102	12.7381	3.945578	122.381	144.898	3.020408	13.92857	12.72109	19.64286	0.022268571
4	11.78571	10.2551	4.612245	118.5714	134.0136	4.544218	13.21429	8.503401	24.94898	0.026075925
5	12.19388	11.27551	4.204082	128.3673	179.7279	3.891156	10.05102	7.006803	21.78571	0.017952817
6	14.71088	12.5	3.836735	144.4218	155.2381	3.673469	14.7449	12.92517	13.41837	0.015242203
7	10.15306	11.78571	4.884354	123.7415	124.2177	3.442177	11.10544	7.55102	20.05102	0.024233647
8	13.35034	11.03741	3.020408	121.2925	171.0204	4.489796	12.12585	6.870748	15.86735	0.017315517
9	10.59524	10.52721	4.353741	115.3061	132.381	4.816327	11.27551	7.959184	13.82653	0.026022075
10	11.92177	12.39796	4	114.2177	153.6054	4.952381	11.9898	5.442177	22.70408	0.023126874
11	10.79932	10.83333	3.768707	111.4966	137.2789	3.605442	11.71769	13.80952	22.09184	0.027981976
12	14.81293	13.45238	4.176871	121.0204	108.4354	4.040816	10.66327	6.190476	19.7449	0.025927385
13	10.96939	10.73129	3.591837	110.4082	134.5578	4.258503	14.43878	10.13605	13.0102	0.025461458
14	13.18027	11.88776	4.639456	126.1905	165.5782	3.265306	11.41156	14.4898	23.52041	0.017451553
15	13.72449	10.66327	4.92517	120.7483	160.6803	3.537415	11.95578	8.29932	22.90816	0.020887711
16	13.04422	13.72449	4.340136	112.0408	163.4014	3.646259	13.52041	5.306122	19.84694	0.016953865
17	12.29592	10.05102	4.217687	118.0272	119.3197	3.659864	14.54082	6.802721	18.52041	0.02394953
18	10.22109	11.81973	3.537415	116.1224	166.1224	4.666667	13.62245	10.95238	21.47959	0.016282878
19	14.94898	10.32313	4.721088	130.2721	156.3265	4.326531	14.13265	9.387755	17.70408	0.022043155
20	10.69728	13.55442	4.870748	132.1769	102.449	4.653061	13.65646	10	16.37755	0.021599832

21	14.47279	11.10544	4.857143	132.7211	147.619	3.102041	10.83333	10.7483	14.7449	0.019232647
22	13.65646	13.28231	3.510204	135.9864	130.2041	4.761905	11.37755	14.21769	24.13265	0.022838621
23	10.35714	13.9966	3.70068	115.8503	106.8027	3.578231	13.72449	8.77551	15.45918	0.02911545
24	13.52041	12.32993	3.115646	115.034	141.6327	3.238095	13.48639	7.346939	23.11224	0.023108731
25	11.54762	13.96259	3.918367	139.2517	153.0612	3.360544	14.91497	13.87755	14.13265	0.019531402
26	11.58163	11.37755	4.272109	140.3401	179.1837	3.034014	11.85374	11.97279	14.43878	0.018058758
27	13.0102	14.67687	3.891156	116.6667	171.5646	3.823129	10.4932	12.38095	20.45918	0.013864829
28	14.84694	12.2619	4.598639	124.2857	114.966	4.843537	13.2483	6.530612	18.72449	0.024328581
29	10.56122	11.92177	4.29932	144.1497	162.3129	4.639456	10.52721	12.2449	21.37755	0.015355979
30	14.06463	12.56803	4.027211	146.5986	173.1973	3.85034	10.73129	13.94558	19.03061	0.014060046
31	13.11224	11.44558	3.156463	133.8095	161.7687	3.714286	10.28912	11.56463	11.17347	0.020924381
32	13.86054	14.77891	4.530612	149.3197	141.0884	4.217687	12.46599	11.29252	22.19388	0.01736165
33	11.7517	10.28912	4.911565	141.7007	154.6939	3.387755	13.45238	6.666667	19.94898	0.014810327
34	10.83333	11.41156	3.401361	130.8163	166.6667	3.836735	13.55442	13.40136	10.56122	0.019712772
35	14.20068	10.39116	4.040816	129.1837	142.1769	4.693878	10.42517	6.734694	13.11224	0.022410209
36	14.26871	13.04422	3.346939	119.6599	152.517	3.428571	14.16667	14.08163	20.86735	0.017016158
37	14.67687	11.2415	3.795918	146.3265	100.2721	4.176871	13.31633	8.095238	16.07143	0.023194053
38	13.55442	13.82653	4.653061	148.5034	155.7823	3.768707	12.7381	5.034014	18.41837	0.017364646
39	11.64966	14.57483	3.292517	120.4762	119.8639	3.687075	11.92177	13.06122	11.37755	0.023830327
40	14.16667	13.58844	3.07483	116.9388	110.6122	3.619048	13.58844	9.659864	13.31633	0.027196752
41	10.66327	11.68367	3.687075	125.6463	108.9796	4.408163	10.79932	13.12925	12.29592	0.02789073
42	13.21429	12.36395	4.666667	132.9932	111.7007	4.108844	13.9966	14.42177	24.33673	0.025158694
43	14.7449	12.80612	4.408163	119.1156	146.5306	4.503401	11.81973	14.62585	11.9898	0.022067437

44	13.14626	12.70408	4.585034	140.6122	125.3061	3.877551	10.69728	6.462585	24.84694	0.019251908
45	14.03061	13.38435	4.571429	112.585	121.4966	4.163265	14.98299	9.115646	20.2551	0.025004611
46	10.32313	13.86054	3.183673	133.5374	138.3673	3.55102	10.32313	11.36054	20.15306	0.021079392
47	12.02381	14.98299	3.306122	144.6939	172.1088	4.394558	12.05782	8.231293	20.35714	0.016009747
48	13.41837	10.86735	3.578231	124.0136	122.0408	4.870748	13.38435	14.89796	17.90816	0.024110576
49	14.23469	13.14626	3.85034	125.3741	145.9864	4.829932	14.77891	10.20408	11.27551	0.023991413
50	12.60204	12.12585	4.095238	118.2993	116.5986	3.564626	14.64286	14.14966	11.78571	0.025427082
51	14.60884	10.15306	3.741497	139.7959	150.3401	3.37415	13.41837	11.63265	22.5	0.015998891
52	11.10544	11.51361	3.55102	124.8299	118.7755	4.136054	14.84694	11.90476	24.64286	0.021664059
53	14.37075	10.90136	3.959184	133.2653	175.9184	4.557823	12.2619	11.70068	23.82653	0.018751429
54	13.31633	10.4932	3.564626	132.449	129.6599	4.802721	14.88095	8.843537	20.56122	0.023169691
55	11.41156	14.20068	3.414966	111.2245	123.6735	4.598639	12.87415	13.53741	18.11224	0.028579599
56	13.79252	14.26871	3.37415	130.5442	169.3878	3.156463	11.88776	10.27211	23.0102	0.016328349
57	13.38435	10.35714	4.054422	149.5918	107.3469	3.414966	11.44558	10.68027	20.76531	0.027077317
58	12.80612	10.11905	4.285714	148.7755	151.4286	4.612245	13.04422	13.19728	15.66327	0.014612331
59	13.48639	12.84014	3.333333	116.3946	104.6259	4.530612	11.64966	10.47619	23.62245	0.029330474
60	12.22789	11.7517	3.142857	142.2449	177.551	3.931973	12.94218	5.986395	21.07143	0.01544223
61	10.4932	13.69048	4.503401	147.9592	113.3333	3.755102	11.58163	12.51701	15.76531	0.019715677
62	11.81973	11.54762	4.993197	128.6395	165.034	4.312925	14.60884	12.78912	20.66327	0.019258354
63	12.70408	11.61565	4.979592	114.4898	167.2109	4.77551	11.68367	11.4966	16.88776	0.015622807
64	11.88776	11.0034	3.170068	128.9116	116.0544	3.863946	10.62925	5.578231	15.56122	0.024609003
65	14.64286	12.94218	4.748299	138.7075	129.1156	3.945578	11.03741	7.142857	11.07143	0.018880126
66	13.2483	14.16667	3.52381	135.7143	147.0748	3.129252	14.57483	6.326531	16.17347	0.019060004

67	11.07143	10.22109	4.14966	134.898	120.4082	3.741497	10.56122	12.9932	23.31633	0.022223589
68	12.87415	14.09864	3.319728	140.8844	110.068	3.727891	14.20068	6.938776	22.39796	0.024902644
69	12.39796	11.34354	3.809524	129.7279	176.4626	4.435374	14.94898	5.646259	15.05102	0.016448309
70	10.39116	12.29592	4.231293	137.8912	127.483	3.115646	10.86735	8.163265	11.88776	0.019901648
71	10.01701	11.85374	4.394558	134.3537	140	4.884354	14.26871	12.10884	12.90816	0.020219015
72	11.2415	10.59524	3.972789	142.7891	113.8776	3.455782	12.53401	14.69388	14.64286	0.023459539
73	11.03741	11.20748	3.129252	134.0816	128.5714	4.462585	11.2415	9.047619	24.43878	0.023938608
74	11.61565	12.46599	4.163265	118.8435	112.7891	4.204082	12.5	5.170068	10.15306	0.026127897
75	13.82653	12.09184	3.387755	123.1973	109.5238	3.047619	11.07143	12.85714	18.0102	0.025330912
76	14.40476	14.30272	3.238095	129.4558	143.8095	4.013605	10.11905	9.591837	12.60204	0.019611211
77	13.96259	12.22789	4.136054	127.8231	169.932	3.170068	11.17347	6.258503	12.09184	0.015366174
78	12.90816	13.2483	3.605442	144.966	103.5374	3.482993	10.08503	8.367347	18.31633	0.027477153
79	13.9966	14.7449	4.816327	110.6803	137.8231	3.959184	12.32993	8.707483	14.94898	0.024447436
80	10.86735	13.92857	4.544218	113.9456	160.1361	4.707483	13.7585	12.17687	14.54082	0.017887727
81	11.85374	13.11224	3.061224	138.4354	135.6463	4.353741	14.71088	7.687075	10.96939	0.021135081
82	10.2551	13.21429	4.380952	149.8639	149.7959	3.346939	13.79252	9.183673	16.58163	0.014907504
83	14.54082	14.03061	3.755102	131.3605	174.2857	4.734694	11.61565	7.210884	14.23469	0.017980509
84	12.15986	14.71088	4.122449	125.9184	102.9932	3.52381	12.36395	10.81633	24.7449	0.02691661
85	14.57483	10.69728	3.102041	143.3333	148.1633	4.272109	12.02381	12.44898	16.47959	0.020002239
86	14.30272	13.65646	3.047619	117.483	159.0476	4.62585	13.18027	11.02041	21.68367	0.017688423
87	11.47959	14.84694	4.068027	131.9048	177.0068	4.244898	14.67687	7.619048	15.96939	0.015733819
88	12.97619	10.08503	3.428571	115.5782	128.0272	3.401361	11.47959	11.42857	12.70408	0.026838425
89	10.90136	12.05782	4.421769	117.2109	144.3537	3.306122	10.18707	13.67347	14.84694	0.021206824

90	13.28231	14.47279	4.734694	119.932	154.1497	4.380952	10.76531	9.727891	24.23469	0.022656139
91	12.5	14.40476	4.680272	137.619	131.8367	3.22449	13.96259	7.891156	11.68367	0.021910029
92	12.67007	12.67007	4.952381	147.1429	135.102	4.190476	10.39116	11.76871	12.19388	0.019648714
93	12.46599	12.15986	4.761905	143.6054	114.4218	4.47619	13.86054	5.714286	13.52041	0.025138917
94	14.09864	10.56122	3.278912	111.7687	126.9388	3.918367	12.29592	6.598639	17.60204	0.026806751
95	10.73129	12.97619	3.442177	121.5646	178.6395	3.70068	12.77211	5.238095	13.72449	0.017866927
96	13.07823	11.17347	4.789116	119.3878	111.1565	4.517007	11.0034	11.83673	23.41837	0.02628188
97	11.27551	11.30952	4.312925	114.7619	162.8571	3.278912	13.0102	7.278912	11.58163	0.017317328
98	10.11905	11.71769	3.469388	138.1633	142.7211	4.367347	11.7517	6.122449	10.76531	0.018571103
99	11.44558	11.58163	3.034014	136.2585	117.1429	3.183673	13.82653	9.931973	12.5	0.023273651
100	11.68367	12.90816	4.938776	120.2041	104.0816	3.251701	14.5068	11.22449	17.80612	0.027076635
101	14.33673	14.54082	4.517007	141.9728	125.8503	4.081633	12.90816	13.33333	11.47959	0.021145319
102	12.36395	14.88095	3.986395	113.1293	133.4694	3.07483	11.20748	7.414966	19.13265	0.024227801
103	11.9898	13.52041	4.843537	147.6871	178.0952	4.285714	12.43197	9.251701	13.92857	0.013883937
104	13.58844	14.13265	4.44898	136.5306	157.9592	4.938776	14.30272	13.26531	18.62245	0.015061437
105	14.98299	14.06463	3.673469	125.102	122.585	4.027211	13.07823	7.07483	10.45918	0.02089191
106	11.30952	11.07143	3.455782	147.415	167.7551	3.591837	10.45918	9.455782	21.27551	0.013839452
107	14.13265	14.33673	4.707483	121.8367	140.5442	3.061224	12.56803	13.46939	17.39796	0.020226115
108	14.88095	13.48639	3.904762	136.8027	168.8435	3.972789	14.33673	8.571429	22.60204	0.013478746
109	13.62245	13.41837	4.489796	143.0612	151.9728	4.965986	10.35714	9.863946	19.43878	0.016219002
110	13.45238	12.19388	4.802721	122.9252	173.7415	3.510204	14.81293	10.61224	13.21429	0.013827852
111	12.53401	13.35034	3.646259	146.0544	132.9252	3.088435	12.15986	14.55782	22.29592	0.020118442
112	10.08503	14.23469	4.367347	131.0884	159.5918	4.095238	11.13946	14.82993	13.62245	0.020651781

113	10.62925	14.43878	4.462585	122.6531	124.7619	4.979592	11.34354	8.435374	17.29592	0.025861365
114	10.93537	11.95578	3.088435	142.517	105.7143	4.571429	12.84014	12.04082	17.19388	0.023821607
115	11.51361	14.91497	4.897959	122.1088	143.2653	3.333333	10.96939	10.06803	14.03061	0.018380899
116	12.09184	13.79252	3.659864	110.9524	161.2245	4.122449	10.15306	8.911565	12.80612	0.018386065
117	10.42517	12.87415	4.829932	126.7347	138.9116	4.054422	12.39796	14.96599	23.21429	0.023783643
118	11.37755	10.62925	4.190476	127.551	174.8299	4.340136	10.93537	10.40816	10.2551	0.017053803
119	11.17347	10.79932	4.244898	145.7823	118.2313	4.911565	11.54762	7.823129	18.21429	0.018139159
120	13.69048	10.18707	3.823129	113.6735	168.2993	4.068027	13.11224	14.01361	15.35714	0.015620676
121	10.18707	13.07823	4.557823	137.3469	156.8707	4.748299	12.97619	5.85034	21.88776	0.017676285
122	14.91497	11.47959	3.931973	127.2789	117.6871	3.142857	14.06463	9.52381	21.58163	0.021980566
123	13.92857	10.96939	3.251701	145.2381	136.7347	3.319728	12.70408	6.394558	14.33673	0.018687831
124	10.52721	10.42517	4.081633	145.5102	149.2517	4.231293	14.23469	7.755102	20.96939	0.016780294
125	11.0034	12.43197	3.632653	146.8707	158.5034	4.421769	13.89456	12.31293	23.92857	0.013908584
126	13.89456	11.13946	3.782313	112.8571	130.7483	4.993197	10.90136	11.15646	16.68367	0.026000726
127	10.28912	14.94898	3.360544	134.6259	126.3946	4.680272	12.22789	7.482993	16.9898	0.0249794
128	14.43878	13.31633	4.326531	127.0068	107.8912	4	10.22109	14.28571	18.82653	0.024979423
129	12.77211	10.45918	4.77551	112.3129	112.2449	3.469388	11.51361	8.979592	15.15306	0.025240437
130	12.63605	13.18027	3.727891	139.5238	115.5102	4.721088	10.2551	9.319728	10.66327	0.023557611
131	12.84014	10.76531	4.47619	128.0952	100.8163	4.44898	12.63605	12.65306	10.86735	0.017035068
132	11.34354	10.93537	3.197279	131.6327	172.6531	3.006803	13.28231	10.88435	19.23469	0.015871617
133	13.7585	11.64966	4.965986	141.1565	106.2585	3.292517	13.35034	11.08844	16.78571	0.01483236
134	11.20748	11.9898	4.108844	130	148.7075	3.210884	12.67007	5.102041	24.54082	0.015768878
135	14.5068	12.02381	3.496599	141.4286	131.2925	4.585034	11.30952	5.918367	21.9898	0.014005776

136	11.13946	12.53401	3.863946	117.7551	101.9048	3.986395	12.09184	5.782313	24.03061	0.019003309
137	10.76531	12.63605	4.258503	149.0476	101.3605	3.782313	13.14626	8.027211	22.80612	0.014933294
138	12.43197	12.77211	4.693878	123.4694	170.4762	4.789116	12.60204	6.054422	12.39796	0.013903989
139	10.45918	13.0102	3.006803	113.4014	157.415	3.809524	11.78571	8.639456	21.17347	0.019608033
140	12.7381	13.62245	3.877551	148.2313	105.1701	4.897959	14.03061	10.34014	17.09184	0.0135503
141	12.94218	13.7585	3.210884	126.4626	136.1905	4.92517	14.09864	5.510204	19.54082	0.014390179
142	12.2619	13.89456	4.62585	135.4422	175.3741	3.197279	13.69048	10.54422	23.72449	0.015305212
143	14.77891	14.37075	3.265306	143.8776	123.1293	3.904762	12.19388	13.7415	16.27551	0.0168016
144	12.05782	14.5068	4.013605	110.1361	164.4898	3.795918	14.47279	12.58503	19.33673	0.015245085
145	12.32993	14.60884	3.22449	137.0748	163.9456	4.14966	12.80612	13.60544	10.35714	0.015894743
146	11.71769	14.64286	3.619048	138.9796	145.4422	3.632653	10.59524	5.37415	15.2551	0.014934279
147	11.95578	14.81293	3.482993	140.068	120.9524	4.29932	14.37075	14.35374	18.92857	0.013724683